Project Deliverable Report

DELIVERABLE 4.1

CALIBRATION OF MODEL

WORK PACKAGE NUMBER: WP4

WORK PACKAGE TITLE: MODELLING & DIGITAL TWINS

TYPE: REPORT

AUTHORS: CRISTINA CORNARO, MARCELLO PETITTA, GIANLUIGI BOVESECCHI, ALI SOHANI, FEDERICO ANDREOZZI, LUCA ROSATI, EMILIANO SERI

REGACE Action Information	
Action full title	Responsive Greenhouse Agrivoltaics System with CO2 Enrichment for Higher Yields
Action acronym	REGACE
Grant agreement number	101096056
Project coordinator	Prof. Ibrahim Yehia
Project start date and duration	1 February 2023, 36 months
Project website	https://regaceproject.com/

Funded by the European Union under Grant Agreement No 101096056. Views and opinions expressed are however those of the author(s) only and do not necessarily reflect those of the European Union or CINEA. Neither the European Union nor the granting authority can be held responsible for them.

Document Information

Deliverable Information	
Work package number	**4**
Work package title	**Modelling & Digital Twins**
Deliverable number	**4.1**
Deliverable title	**CALIBRATION OF MODEL**
Description	**Develop a predictive simulation model of the greenhouse system that includes energy modelling, PV system modelling and provides an estimation for crop growth with CO2 enrichment**
Lead beneficiary	**Tor Vergata University**
Lead Author(s)	**Tor Vergata University**
Contributor(s)	**Cristina Cornaro, Marcello Petitta, Gianluigi Bovesecchi, Ali Sohani, Federico Andreozzi, Luca Rosati, Emiliano Seri, Ibrahim Yehia, Papaioannou Chrysoula, Catherine Baxevanou, Dimitrios Fidaros, Uwe Schmidt, Thorsten Rocksch, Basma Majadley, Esther Magadley**
Revision number	**3**
Revision Date	**24/07/2024**
Status (Final (F), Draft (D), Revised Draft (RV))	**F**
Dissemination level (Public (PU), Restricted to other program participants (PP), Restricted to group speci-fied by consortium (RE), Confidential for consortium members only (CO))	**PU**

Funded by the European Union under Grant Agreement No 101096056. Views and opinions expressed are however those of the author(s) only and do not necessarily reflect those of the European Union or CINEA. Neither the European Union nor the granting authority can be held responsible for them.

Document History			
Revision	**Date**	**Modification**	**Author**
1	24/6/24	Initialization	M. Petitta
2	23/07/24	Comments from partners	M. Petitta
3	24/07/24	Finalization	R. Slaugther

Approvals				
	Name	**Organisation**	**Date**	**Signature (initials)**
Coordinator	Prof. Ibrahim Yehia	Alzahrawy Society	24/07/24	IY
WP Leaders	Cristina Cornaro	Tor Vergata University	24/07/24	CC

Table of Contents

Funded by the European Union under Grant Agreement No 101096056. Views and opinions expressed are however those of the author(s) only and do not necessarily reflect those of the European Union or CINEA. Neither the European Union nor the granting authority can be held responsible for them.

Executive Summary

The activities carried out in Work Package 4 (WP4) of our project have focused on developing advanced modeling techniques for a novel photovoltaic (PV) greenhouse system. This effort spans multiple tasks, each addressing a specific aspect of the system, from microclimate modeling to the integration of various models into a comprehensive Digital Twin. Below is a summary of the main activities and achievements to date:

Task 4.1: Dynamic Modelling of the Greenhouse Microclimate and Energy Demand

- Developed a dynamic model using advanced software for Dynamic Building Simulation (DBS) to simulate greenhouse microclimates.
- Integrated physical processes such as plant growth and water use into the model.
- Calibrated and validated the model with data from WP3, enhancing understanding of thermo-hygrometric behavior and energy demand.

Task 4.2: CFD Modelling of the Greenhouse Microclimate

- Structured CFD modeling at two levels: radiation transport and internal microclimate.
- Developed 2D models for radiation transport through greenhouse covers and validated them.
- Created 3D models for internal microclimate, incorporating heat exchange, plant interaction, and CO2 distribution.
- Conducted extensive parametric studies to feed data into the Digital Twin model.

Task 4.3: Modelling of the PV Modules Performance

- Reviewed available PV performance models for bifacial technologies and developed a semi-empirical performance model.
- Calibrated the model using PV module parameters and validated it with data from WP3.
- Accounted for temperature, irradiance, spectral effects, reflection, and rear-side contribution in the bifacial PV modules performance model.

Task 4.4 Water Efficiency

- Installed a closed recirculating irrigation system in the Berlin-Dahlem greenhouse and utilized detailed water meters to measure inflow and outflow.
- Developed and installed the BERMONIS-plant monitoring system with leaf transpiration and soil moisture sensors for precise irrigation control at the Watzkendorf site.
- Installed a closed recirculating irrigation system in the Berlin-Dahlem greenhouse and utilized detailed water meters to measure inflow and outflow.
- Developed and installed the BERMONIS-plant monitoring system with leaf transpiration and soil moisture sensors for precise irrigation control at the Watzkendorf site.

Funded by the European Union under Grant Agreement No 101096056. Views and opinions expressed are however those of the author(s) only and do not necessarily reflect those of the European Union or CINEA. Neither the European Union nor the granting authority can be held responsible for them.

Task 4.5: Digital Twins

- Integrated outputs from previous tasks into a comprehensive empirical model based on machine learning (ML).
- Utilized Recurrent Neural Networks (RNNs) for capturing temporal dependencies in microclimate data.
- Explored the potential of Graph Neural Networks (GNNs) to handle complex interactions within the PV greenhouse system.
- Developed models that predict the general behavior of the PV/greenhouse with appropriate uncertainty levels.

Main Results

- **Dynamic Modeling**: Successfully developed and validated a dynamic model for greenhouse microclimates, incorporating key physical processes and calibrated with real-world data.
- **CFD Modeling**:
  - Completed 2D and 3D CFD models for radiation transport and internal microclimate.
  - Conducted detailed parametric studies to improve model accuracy and feed into the Digital Twin.
- **PV Modules Performance**:
  - Developed a semi-empirical performance model for bifacial PV modules.
  - Achieved significant accuracy in predicting PV performance by accounting for multiple environmental factors.
- **Water Efficiency**
  - Preliminary results indicate significant water savings in the PV-integrated greenhouse at the Berlin-Dahlem site. The closed greenhouse maintains higher relative humidity, resulting in lower plant transpiration rates and reduced overall water consumption due to the efficient recycling of condensed water.
- **Digital Twins**:
  - Integrated various model outputs into a unified ML-based empirical model.
  - Demonstrated strong predictive capabilities using RNNs for greenhouse temperature and humidity.

Initiated exploration of GNNs to further enhance model capabilities and understanding of complex system interactions.

Funded by the European Union under Grant Agreement No 101096056. Views and opinions expressed are however those of the author(s) only and do not necessarily reflect those of the European Union or CINEA. Neither the European Union nor the granting authority can be held responsible for them.

Introduction

This deliverable presents the mid-term progress and achievements of Work Package 4 (WP4) in our ongoing project, which focuses on the development of advanced modeling techniques for photovoltaic (PV) greenhouse systems. WP4 is dedicated to creating comprehensive models that simulate various aspects of these systems, providing critical insights into their behavior and supporting their optimization.

Dynamic Modelling of the Greenhouse Microclimate and Energy Demand (Task 4.1)

Task 4.1 aims to build a dynamic model of greenhouse microclimates and energy demand using advanced Dynamic Building Simulation (DBS) software. This task addresses the complexities involved in simulating an enclosed greenhouse environment, which, unlike typical buildings, requires consideration of plant growth and water use. The model developed under Task 4.1 is calibrated and validated using data from the Volos greenhouse for the year 2020, focusing on understanding the thermo-hygrometric behaviour of the greenhouse system and accurately estimating its energy demand. The successful completion of these steps ensures that the model can simulate the environmental conditions within the greenhouse, providing a reliable tool for optimizing microclimate control and energy management.

CFD Modelling of the Greenhouse Microclimate (Task 4.2)

Task 4.2 focuses on Computational Fluid Dynamics (CFD) modeling to simulate the greenhouse microclimate at two levels: radiation transport and internal microclimate. The first level involves simulating the radiation transport inside the greenhouse, particularly through different types of covers with various geometries such as arched or gothic designs. This modeling provides essential information for the energy and PV performance models in Tasks 4.1 and 4.3, respectively. The second level involves simulating the internal microclimate, accounting for heat exchange among incident radiation, heat storage, and transport by plants, the structure, and the ground. These detailed simulations are crucial for understanding the microclimate dynamics and optimizing the greenhouse's internal environment. The progress in Task 4.2 includes the development and validation of 2D and 3D CFD models, extensive parametric studies, and integration with other models to form part of the Digital Twin.

Modelling of the PV Modules Performance (Task 4.3)

Task 4.3 is dedicated to developing a performance model for bifacial PV modules, which are a key component of the PV greenhouse system. Bifacial PV modules capture irradiance on both the front and rear sides, enhancing energy production. The performance of these modules is represented by the Performance Ratio (PR) parameter, which considers various factors such as temperature, irradiance, spectral effects, and reflection. This task involves a comprehensive review of existing performance models for bifacial technologies and the development of a semi-empirical model customized for the specific module architecture used in the project. The model is calibrated and validated using data from the Volos greenhouse for the period 2020, ensuring it accurately predicts PV performance under various environmental conditions. This task is critical for optimizing the energy production of PV greenhouses and integrating these results into the broader system model.

Funded by the European Union under Grant Agreement No 101096056. Views and opinions expressed are however those of the author(s) only and do not necessarily reflect those of the European Union or CINEA. Neither the European Union nor the granting authority can be held responsible for them.

Water Efficiency (Task 4.4)

Task 4.4 aims to optimize water use in PV greenhouses, leveraging advanced irrigation systems and detailed water balance analyses. At the Berlin-Dahlem site, a closed recirculating irrigation system has been implemented, allowing precise measurement of water inflow and outflow, and facilitating comprehensive water balance calculations. This system, along with comparative analysis with a reference greenhouse, provides insights into the impacts of PV integration on water efficiency. Preliminary results highlight significant water savings due to higher humidity and water recycling in the PV greenhouse. These findings are complemented by additional studies at other sites, contributing to a broader understanding of water use efficiency in diverse greenhouse environments.

Digital Twins (Task 4.5)

Task 4.5 focuses on integrating the outputs from the previous tasks into a comprehensive empirical model based on machine learning (ML). This task aims to develop Digital Twins that provide a generalized model of the entire PV greenhouse system, from solar radiation input to crop production, including internal environment control. The complexity of PV and crop production involves numerous physical and biological processes that require detailed modeling and extensive data. By leveraging the outputs of Tasks 4.1, 4.2, 4.3, and 4.4, Task 4.5 integrates these models into a unified framework. This integration is essential for predicting the general behavior of the PV/greenhouse system with an appropriate level of uncertainty, providing actionable insights for stakeholders.

The integration involves advanced deep learning methods, particularly Recurrent Neural Networks (RNNs) and Graph Neural Networks (GNNs). RNNs are employed to recognize patterns in time-series data, effectively capturing temporal dependencies crucial for predicting greenhouse conditions. The exploration of GNNs aims to model complex interactions within the PV greenhouse system, offering a more generalized and introspective approach to understanding energy fluxes and interconnected processes. The progress in Task 4.5 includes data collection and preprocessing, initial model development, and exploration of advanced neural network architectures.

The work carried out in WP4 so far demonstrates significant advancements in modeling and integrating various aspects of PV greenhouse systems. The dynamic models developed for microclimate and energy demand, the CFD simulations for radiation transport and internal microclimate, the performance modeling of bifacial PV modules, and the integration into comprehensive Digital Twins all contribute to a robust foundation for optimizing greenhouse design and operation. These models provide critical insights that support decision-making processes, enhance resource efficiency, and maximize crop yield, aligning with the project's overall objectives of promoting sustainable and innovative agricultural practices. Moving forward, continued refinement, validation, and integration of these models will ensure their applicability across different greenhouse designs and geographic locations, ultimately contributing to the successful implementation and operational efficiency of PV greenhouse systems.

Funded by the European Union under Grant Agreement No 101096056. Views and opinions expressed are however those of the author(s) only and do not necessarily reflect those of the European Union or CINEA. Neither the European Union nor the granting authority can be held responsible for them.

Pilot greenhouses

Pilot greenhouse survey

At the onset of the REGACE project, Tor Vergata University conducted a comprehensive survey of all greenhouses involved in the project. This survey gathered crucial information regarding the location, dimensions, and instrumentation of each greenhouse. These data points form the starting point for the project's modeling and analysis efforts, providing a detailed understanding of the existing conditions and capabilities of each site.

The survey's findings highlighted the diversity of greenhouse setups across different geographic locations, each with unique environmental conditions and technological implementations. By documenting these variations, the project team can tailor their approaches to each site's specific needs, ensuring that the models and strategies developed are both applicable and effective in various contexts.

The survey covered a range of parameters critical to the performance and optimization of PV greenhouses. These parameters include temperature, relative humidity, CO2 concentration, wind, precipitation, solar radiation, light intensity, and more. The detailed instrumentation installed in each greenhouse allows for precise monitoring and control of these variables, ensuring optimal conditions for crop growth and energy efficiency.

The tables in the next pages provide a comprehensive overview of the instrumentation deployed across the project's greenhouses. These instruments are designed to measure and record various environmental and operational parameters, such as:

Microclimate sensors:

- Temperature Sensors: Measure the internal and external temperature to ensure optimal growing conditions and energy management.
- Relative Humidity Sensors: Monitor the humidity levels to maintain the ideal microclimate for plant growth.
- CO2 Concentration Meters: Track CO2 levels to optimize photosynthesis and enhance crop yields.
- Wind Speed and Direction Sensors: Capture wind data to assess its impact on greenhouse conditions and energy efficiency.
- Precipitation Gauges: Measure rainfall to manage water use and irrigation needs effectively.
- Solar Radiation Sensors (Pyranometers): Record the amount of solar radiation received, which is crucial for both energy production and plant growth.
- Light Sensors: Monitor light intensity and distribution to ensure that plants receive adequate illumination.

Funded by the European Union under Grant Agreement No 101096056. Views and opinions expressed are however those of the author(s) only and do not necessarily reflect those of the European Union or CINEA. Neither the European Union nor the granting authority can be held responsible for them.

Microclimate

Variable	Type	Brand/Model	Accuracy	Scan Rate	Position	Location
Temperature	PT100	Hortimax-Systems (Ridder); Art.-No.21150910	c. 1°C	2 min?	h=1.4m; One sensor each is located centrally on the 6.3m-long wall (not in the centre of the room)	Austria - Cabin 3, 4, 5
Temperature	EE07 combined Temperatur and Humidity sensor	PTF30 Fa. Positronik Moosbach	0.1°C	30 s with 5 min average in the database	5 sensors in cube principle + 1 sensor in Roof zone h=1.7m, l=3m	Berlin - GH 1
Temperature	PT1000	-	0.1°C	30 s with 5 min average in the database	one sensor inside the phytomonitor (location flexible)	Berlin - GH 1
Temperature					indoor	Mecklenburg - GH 1
Temperature					outdoor	Mecklenburg - GH 1
Temperature	PT100	ROTRONIC/X200	0.1°C	10 min	h=1.8 , l=12.0 m	Volos - GH 1, 2, 3
Temperature	PT100	Sercom	0.1°C	10 min	outdoor	Volos - GH 1, 2, 3
Temperature	RS485	RS-WS-N01-XZ1	±0.5°C (25°C)	every minute, can be changed	A4 - Top above PV	Israel - GH 1
Temperature	RS485	RS-WS-N01-XZ2	±0.5°C (25°C)	every minute, can be changed	B7 - Middle below PV	Israel - GH 1
Temperature	RS485	RS-WS-N01-XZ3	±0.5°C (25°C)	every minute, can be changed	C11 - Bottom	Israel - GH 1
Relative Humidity	PT100	Hortimax-Systems (Ridder); Art.-No.21150910	c. 1°C	2 min?	h=1.4m; One sensor each is located centrally on the 6.3m-long wall (not in the centre of the room)	Austria - Cabin 3, 4, 5
Relative Humidity	https://www.epluse.com/de/produkte/feuchtemesstechnik/feuchte-module-und-messfuehler/ee07/	PTF30 Fa. Positronik Moosbach	2 % rH	30 s with 5 min average in the database	5 sensors in cube principle + 1 sensor in Roof zone h=1.7m, l=3m	Berlin - GH 1

Funded by the European Union under Grant Agreement No 101096056. Views and opinions expressed are however those of the author(s) only and do not necessarily reflect those of the European Union or CINEA. Neither the European Union nor the granting authority can be held responsible for them.

Relative Humidity	capacity sensor	Sercom	±3%	10 min	h=1.8 , l=12.0 m	Volos - GH 1, 2, 3
Relative Humidity	capacity sensor	Sercom	±3%	10 min	outdoor	Volos - GH 1, 2, 3
Relative Humidity	RS485	RS-WS-N01-XZ1	±3%RH (60%RH, 25°C)	every minute, can be changed	A4 - Top above PV	Israel - GH 1
Relative Humidity	RS485	RS-WS-N01-XZ2	±3%RH (60%RH, 25°C)	every minute, can be changed	B7 - Middle below PV	Israel - GH 1
Relative Humidity	RS485	RS-WS-N01-XZ3	±3%RH (60%RH, 25°C)	every minute, can be changed	C11 - Bottom	Israel - GH 1
CO2 concentration	-	NO (1 EGM from PP-Systems available)	< 20 ppm	manually once a day during the week	in the plant population	Austria - Cabin 3, 4, 5
CO2 concentration	GMP343	VAISALA	5 ppm (2000 ppm measurement range)	30 s with 5 min average in the database	one sensor inside the phytomonitor (location flexible)	Berlin - GH 1
CO2 concentration	4-20mA, CO2 measurement range: 0~5000ppm	RS-CO2-N01-XZ1	±(50ppm+ 3%F·S) (25°C)@400-5000ppm	every minute, can be changed	A5 - Top above PV	Israel - GH 1
CO2 concentration	4-20mA, CO2 measurement range: 0~5000ppm	RS-CO2-N01-XZ2	±(50ppm+ 3%F·S) (25°C)@400-5000ppm	every minute, can be changed	B8 - Middle upper below PV	Israel - GH 1
CO2 concentration	4-20mA, CO2 measurement range: 0~5000ppm	RS-CO2-N01-XZ3	±(50ppm+ 3%F·S) (25°C)@400-5000ppm	every minute, can be changed	C9 - Middle lower crop height	Israel - GH 1
CO2 concentration	4-20mA, CO2 measurement range: 0~5000ppm	RS-CO2-N01-XZ4	±(50ppm+ 3%F·S) (25°C)@400-5000ppm	every minute, can be changed	C12 - Bottom	Israel - GH 1

Funded by the European Union under Grant Agreement No 101096056. Views and opinions expressed are however those of the author(s) only and do not necessarily reflect those of the European Union or CINEA. Neither the European Union nor the granting authority can be held responsible for them.

wind speed		Sercom		10 min	outdoor	Volos - GH 1, 2, 3
wind direction		Sercom		10 min	outdoor	Volos - GH 1, 2, 3
rainfall		Sercom		10 min	outdoor	Volos - GH 1, 2, 3
Light sensor	RS485, 0-65535Lux; 0-200,000 Lux	RS-GZ-N01-2-XZ5; RS-GZ-N01-2-XZ4; RS-GZ-N01-2-XZ3; RS-GZ-N01-2-XZ2; RS-GZ-N01-2-XZ1; RS-GZ-N01-2-XZ2;Model :RS-GZ-N01-2-XZ1; RS-GZ-N01-2-XZ0	±7%(25°C)	every minute, can be changed	A3 - Top above PV	Israel - GH 1
Light sensor	RS485, 0-65535Lux; 0-200,000 Lux	RS-GZ-N01-2-XZ5; RS-GZ-N01-2-XZ4; RS-GZ-N01-2-XZ3; RS-GZ-N01-2-XZ2; RS-GZ-N01-2-XZ1; RS-GZ-N01-2-XZ2;Model :RS-GZ-N01-2-XZ1; RS-GZ-N01-2-XZ0	±7%(25°C)	every minute, can be changed	B6 - Middle below PV	Israel - GH 1
Light sensor	RS485, 0-65535Lux; 0-200,000 Lux	RS-GZ-N01-2-XZ5; RS-GZ-N01-2-XZ4; RS-GZ-N01-2-XZ3; RS-GZ-N01-2-XZ2; RS-GZ-N01-2-XZ1; RS-GZ-N01-2-XZ2;Model :RS-GZ-N01-2-XZ1; RS-GZ-N01-2-XZ0	±7%(25°C)	every minute, can be changed	C10 - Bottom	Israel - GH 1
Light sensor	RS485, 0-65535Lux; 0-200,000 Lux	RS-GZ-N01-2-XZ5; RS-GZ-N01-2-XZ4; RS-GZ-N01-2-XZ3; RS-GZ-N01-2-XZ2; RS-GZ-N01-2-XZ1; RS-GZ-N01-2-XZ2;Model :RS-GZ-N01-2-XZ1; RS-GZ-N01-2-XZ0	±7%(25°C)	every minute, can be changed	F17 - Above crops facing down	Israel - GH 1
Light sensor	RS485, 0-65535Lux; 0-200,000 Lux	RS-GZ-N01-2-XZ5; RS-GZ-N01-2-XZ4; RS-GZ-N01-2-XZ3; RS-GZ-N01-2-XZ2; RS-GZ-N01-2-XZ1; RS-GZ-N01-2-XZ2;Model :RS-GZ-N01-2-XZ1; RS-GZ-N01-2-XZ0	±7%(25°C)	every minute, can be changed	F13 - Above crops facing up	Israel - GH 1
Light sensor	RS485, 0-65535Lux; 0-200,000 Lux	RS-GZ-N01-2-XZ5; RS-GZ-N01-2-XZ4; RS-GZ-N01-2-XZ3; RS-GZ-N01-2-XZ2; RS-GZ-N01-2-XZ1; RS-GZ-N01-2-XZ2;Model :RS-GZ-N01-2-XZ1; RS-GZ-N01-2-XZ0	±7%(25°C)	every minute, can be changed	F14 - Above crops facing up	Israel - GH 1
Light sensor	RS485, 0-65535Lux; 0-200,000 Lux	RS-GZ-N01-2-XZ5; RS-GZ-N01-2-XZ4; RS-GZ-N01-2-XZ3; RS-GZ-N01-2-XZ2; RS-GZ-N01-2-XZ1; RS-GZ-N01-2-XZ2;Model :RS-GZ-N01-2-XZ1; RS-GZ-N01-2-XZ0	±7%(25°C)	every minute, can be changed	E15 - Above crops facing up	Israel - GH 1
Light sensor	RS485, 0-65535Lux; 0-200,000 Lux	RS-GZ-N01-2-XZ5; RS-GZ-N01-2-XZ4; RS-GZ-N01-2-XZ3; RS-GZ-N01-2-XZ2; RS-GZ-N01-2-XZ1; RS-GZ-N01-2-XZ2;Model :RS-GZ-N01-2-XZ1; RS-GZ-N01-2-XZ0	±7%(25°C)	every minute, can be changed	E16 - Above crops facing up	Israel - GH 1

Funded by the European Union under Grant Agreement No 101096056. Views and opinions expressed are however those of the author(s) only and do not necessarily reflect those of the European Union or CINEA. Neither the European Union nor the granting authority can be held responsible for them.

Solar radiation

Variable	Type	Brand/Model	Accuracy	Scan Rate	Position	Location
Pyranometer					outdoor	Austria - Cabin 3, 4, 5
Pyranometer	CMP6	Kipp&Zonen	individual calibration certificate	30 s with 5 min average in the database	outside weather station	Berlin - GH 1
PAR	LI-190	LI-COR Bioscience	individual calibration certificate	30 s with 5 min average in the database	outside weather station	Berlin - GH 1
PAR	LI-190	LI-COR Bioscience	individual calibration certificate	30 s with 5 min average in the database	inside -2 sensors in flexible position	Berlin - GH 1
Solar Radiation		Sercom	±10 W m-2	10 min	h=8,0 m	Volos - GH 1, 2, 3
Light intensity	-	-	5 Lx	30 s with 5 min average in the database	outside weather station	Berlin - GH 1
Light intensity	handheld lux meter	R&D Instruments/MT-30	±4%	ND	handheld device	Israel - GH 1
incident irradiance on the PV modues	ref cell (Si-mV-85)	Ingenieurbuero Mencke & Tegtmeyer GmbH	ND	currently every 1 min (can be changed)	top - next to PV module on tracker	Israel - GH 1
incident irradiance on the PV modues	ref cell (Si-mV-85)	Ingenieurbuero Mencke & Tegtmeyer GmbH	ND	currently every 1 min (can be changed)	below - next to PV module on tracker	Israel - GH 1
incident irradiance on the PV modues	silicon pyranometer, ISO 9060:2018 Class C	EKO/ML-01	Non-stability (change/year): ± 2 %, Non-linearity (100 to 1000W/m²): < 0.2 %, Directional Response (at 1000W/m² | 0 to 80°): < 10 W/m², Spectral Error: ± 3.07 %, Temperature Response (-20°C to 50°C): < 0.15 %	currently every 1 min (can be changed)	top - next to PV module on tracker	Israel - GH 3
incident irradiance on	silicon pyranometer, ISO 9060:2018 Class C	EKO/ML-00	Non-stability (change/year): ± 2 %, Non-linearity (100 to 1000W/m²): < 0.2 %, Directional Response (at 1000W/m² | 0 to 80°): < 10 W/m², Spectral Error: ± 3.07 %, Temperature Response (-20°C to 50°C): < 0.15 %	currently every 1 min	below - next to PV module on tracker	Israel - GH 3

Funded by the European Union under Grant Agreement No 101096056. Views and opinions expressed are however those of the author(s) only and do not necessarily reflect those of the European Union or CINEA. Neither the European Union nor the granting authority can be held responsible for them.

the PV modues				(can be changed)		
fixed horizontal position at tracker level	ref cell (Si-mV-85)	Ingenieurbuero Mencke & Tegtmeyer GmbH	ND	currently every 1 min (can be changed)	horizontal at tracker height (fixed)	Israel - GH 1
fixed horizontal position at tracker level	silicon pyranometer, ISO 9060:2018 Class C	EKO/ML-01	Non-stability (change/year): ± 2 %, Non-linearity (100 to 1000W/m²): < 0.2 %, Directional Response (at 1000W/m² | 0 to 80°): < 10 W/m², Spectral Error: ± 3.07 %, Temperature Response (-20°C to 50°C): < 0.15 %	currently every 1 min (can be changed)	horizontal at tracker height (fixed)	Israel - GH 3
fixed horizontal position outdoors	ref cell (Si-mV-85)	Ingenieurbuero Mencke & Tegtmeyer GmbH	ND	currently every 1 min (can be changed)	horizontal outdoor (fixed)	Israel - GH 1
outdoor Global irradiance	Pyranometer analog signal, / ISO 9060:2018 Class A	EKO/MS-80	ND	ND	ND	Israel - GH 1
DNI sensor	DNI sensor, ISO 9060:2018, Class C (DNI) + Class A (GHI, DHI), Output: DNI, GHI, DHI (MODBUS 485 RTU)	EKO/M-90 DNI Sensor	<5% uncertainty	currently every 1 min (can be changed)	horizontal outdoor (fixed)	Israel - GH 1

Funded by the European Union under Grant Agreement No 101096056. Views and opinions expressed are however those of the author(s) only and do not necessarily reflect those of the European Union or CINEA. Neither the European Union nor the granting authority can be held responsible for them.

Crop and Soil Sensors: Measure various aspects of crop health and soil conditions, including soil moisture and temperature, to optimize irrigation and nutrient delivery.

Variable	Type	Brand/Model	Accuracy	Scan Rate	Position	Location
net photosynthesis	- " -	BERMONIS Fa. Steinbeis GmbH	individual calibration certificate	30 s with 5 min average in the database	in the middle of the canopy (flexible)	Berlin - GH 1
transpiration	Phytomonitoring	- " -	- " -	-"-	- " -	Berlin - GH 1
stomatal conductivity	System	- " -	- " -	-"-	- " -	Berlin - GH 1
VPD	- " -	- " -	- " -	-"-	- " -	Berlin - GH 1
dew point	- " -	- " -	- " -	-"-	- " -	Berlin - GH 1
leaf/frut temperature	infrared thermometer	Optris	0.3 K	30 s with 5 min average in the database	in the middle of the canopy (flexible)	Berlin - GH 1

Crop Type

Location	Type	Watering type
Austria - Cabin 1, 2, 3	TBD	ebb and flow/drip irrigation
Berlin - GH 1	tomatoes	hydroponics on high gutter with drip irrigation
Macklenburg - GH 1	tomatoes, cucumber, lambs lattuce, radish	pipe with micro sprinkler
Volos - GH 1, 2, 3	cucumber	hydroponics (drip irrigation)
Israel - GH 1, 2, 3, 4	cucumber, bell pepper	drip irrigation

Funded by the European Union under Grant Agreement No 101096056. Views and opinions expressed are however those of the author(s) only and do not necessarily reflect those of the European Union or CINEA. Neither the European Union nor the granting authority can be held responsible for them.

Soil

Variable	Type	Brand/Model	Accuracy	Scan Rate	Position	Location
drain backflow	own construction	-	-	-	at the end of each gutter	Berlin - GH 1

Heating and Cooling Systems: Document the type and efficiency of systems used to maintain optimal temperature conditions within the greenhouses.

Heating

Location	Operational	Monitored	Type
Austria - Cabin 1, 2, 3			District heating
Berlin - GH 1			District heating
Macklenburg - GH 1			boiler/ biogas plant
Volos - GH 1, 2, 3			boiler
Israel - GH 1, 2, 3, 4			-

Cooling

Location	Operational	Monitored	Type
Austria - Cabin 1, 2, 3			Gable & side ventilation
Berlin - GH 1			heat pump with finned pipes under the roof
Macklenburg - GH 1			Evap. Cooling
Volos - GH 1, 2, 3			Evap. Cooling
Israel - GH 1, 2, 3, 4			-

Funded by the European Union under Grant Agreement No 101096056. Views and opinions expressed are however those of the author(s) only and do not necessarily reflect those of the European Union or CINEA. Neither the European Union nor the granting authority can be held responsible for them.

CO2 Enrichment

Location	Type
Austria - Cabin 3	CO2 bags (test)
Berlin - GH 1	2 CO2 bottle boundles
Macklenburg - GH 1	biomass uncontrolled
Volos - GH 1, 2, 3	CO2 tank
Israel - GH 3, 4	biomass

Materials

Location	Roof	Ext. Wall	Int. Wall
Austria - Cabin 1, 2, 3	polycarbonate Thermoclear 2UV 16mm	polycarbonate Thermoclear 2UV 16mm	polycarbonate Thermoclear 2UV 16mm
Berlin - GH 1	thick plain glass	double glass	-
Macklenburg - GH 1	glass	glass	none/glass
Volos - GH 1, 2, 3	HDPE	polycarbonate	polycarbonate
Israel - GH 1, 2, 3, 4	PE	PE	-

Funded by the European Union under Grant Agreement No 101096056. Views and opinions expressed are however those of the author(s) only and do not necessarily reflect those of the European Union or CINEA. Neither the European Union nor the granting authority can be held responsible for them.

Regace Project

Partners Greenhouses summary

Volos (Greece)
39°23'40"N; 22°45' 30"E

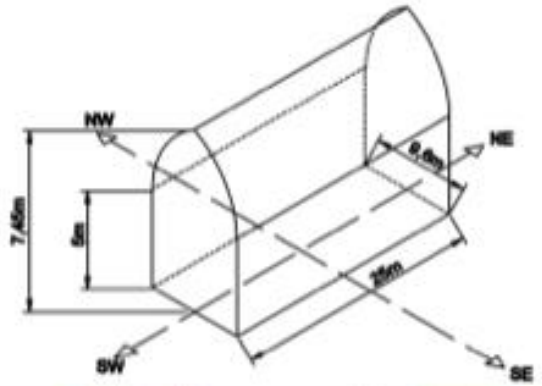

General Informations

Number of greenhouses: 6 (Only 3 are part of Regace project)
Type of coltivation: hydroponics (3/3 GHs)
Watering type: drip irrigation
Cover material: PC for walls and HDPE for roofs (3/3 GHs)
Crop: Cucumber (3/3 GHs)
Heating system: boiler (3/3 GHs)
Cooling system: evaporative cooling (3/3 GHs)
CO2 enrichment: CO2 tank (3/3 GHs)

Monitoring systems

Microclimate: Yes (3/3GHs)
Solar radiation: Yes (3/3 GHs)
Crop: No
Soil: No
Heating: No
Cooling: No

Kfar Qara (Israel)
32°30'21"N; 35°3'14"E

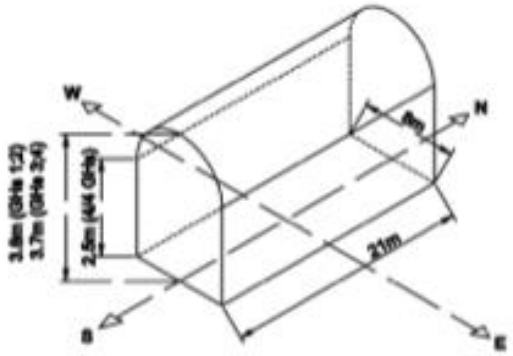

General Informations

Number of Greenhouses: 4
Type of coltivation: traditional (4/4 GHs)
Watering type: drip irrigation (4/4 GHs)
Cover material: polyethylene (PE) (4/4 GHs)
Crop: cucumber/bell pepper (4/4 GHs)
Heating system: No
Cooling system: No
CO2 enrichment: biomass (GHs 3;4)

Monitoring systems

Microclimate: Yes (GH 1)
Solar radiation: Yes (GHs 1;3)
Crop: No
Soil: No
Heating: No
Cooling: No

Mecklenburg-Vorpommern (Germany)
53°23'33"N; 13°19'11"E

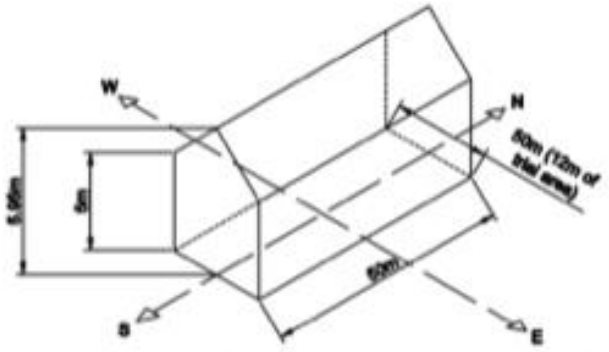

General Informations

Number of Greenhouses: 1
Type of coltivation: traditional
Watering type: pipe with micro sprinkler
Cover material: glass
Crop: tomatoes, cucumber, lambs lettuce, radish
Heating system: boiler (biogas)
Cooling system: evaporative cooling
CO2 enrichment: biomass

Monitoring Systems

Microclimate: Yes
Solar radiation: Yes
Crop: No
Soil: No
Heating: No
Cooling: No

Berlin (Germany)
52°31'12"N;13°23'17"E

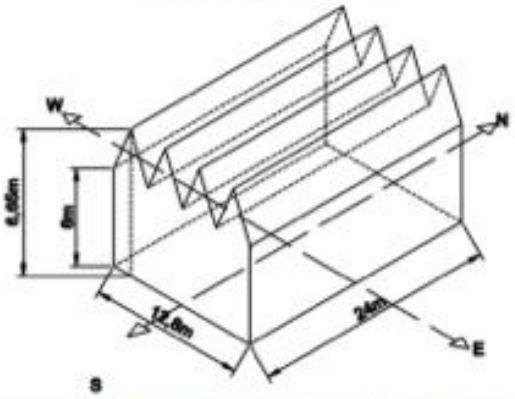

General Informations

Number of greenhouses: 2 (Only 1 is part of Regace project)
Type of coltivation: hydroponics
Watering type: drip irrigation
Cover material: glass
Crop: tomatoes
Heating system: district heating/ heat pump
Cooling system: heat pump
CO2 enrichment: CO2 bottles

Monitoring systems

Microclimate: Yes
Solar radiation: Yes
Crop: Yes
Soil: Yes
Heating: No
Cooling: No

Vienna (Austria)
48°12'30"N;16°22'21"E

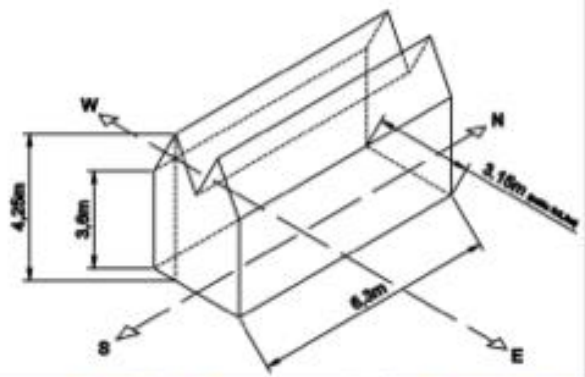

General Informations

Number of greenhouses: 6 (Only 3 are part of Regace project)
Type of coltivation: on tables
Watering type: ebb flow/drip irrigation
Cover material: polycarbonate (3/3 GHs)
Crop: to be determined (3/3 GHs)
Heating system: pipe heating (3/3 GHs)
Cooling system: gable and side ventilation (3/3 GHs)
CO2 enrichment: CO2 bags (GH 3)

Monitoring Systems

Microclimate: Yes (3/3 GHs)
Solar radiation: (3/3 GHs)
Crop: No
Soil: No
Heating: No
Cooling: No

Pontinia (Italy)
41°24'29"N; 13°02'39"E

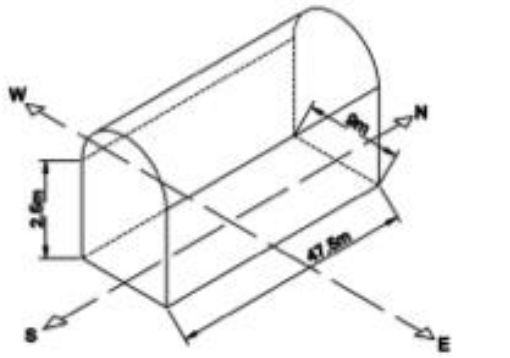

General Informations

Number of greenhouses: 2
Type of coltivation: traditional
Watering type:
Cover material:
Crop:
Heating System:
Cooling System:
CO2 enrichment:

Monitoring Systems

Microclimate:
Solar radiation:
Crop:
Soil:
Heating:
Cooling:

The figure presents the greenhouses in various locations, including Greece, Israel, Germany, Austria, and Italy. Each greenhouse is depicted with its dimensions, orientation, and key features. The survey covered several critical aspects:

General Information:

- Number of Greenhouses: Indicates the total number of greenhouses at each site.
- Type of Cultivation: Specifies whether traditional or hydroponic methods are used.
- Irrigation Systems: Details the type of irrigation system in place, such as drip irrigation.
- Cover Material: Identifies the material used for the greenhouse covering, which affects light transmission and insulation.
- Cooling and Heating Systems: Describes any cooling or heating mechanisms used to maintain optimal internal temperatures.
- CO2 Enrichment: Notes if CO2 enrichment is utilized to enhance plant growth.

Monitoring Systems:

- Microclimate Monitoring: Includes sensors for temperature, relative humidity, and other environmental conditions inside the greenhouse.
- Solar Radiation Sensors: Devices to measure the amount of solar energy received.
- CO2 Sensors: Tools for tracking CO2 levels to ensure optimal photosynthesis.
- Soil and Crop Sensors: Measure soil moisture and crop health parameters to optimize irrigation and nutrient management.
- Additional Instruments: Includes pyranometers, light sensors, and systems for monitoring wind speed, precipitation, and other external conditions.

Detailed Description of Each Site

1. Volos, Greece:
    - Coordinates: 39°23'40"N, 22°54'30"E
    - Features: one greenhouse consisted of 5 chambers and one control room (or engine room). The greenhouse has hydroponic cultivation, equipped with advanced drip irrigation, polycarbonate for the side walls and HDPE for the roof. Heating by pipe rail and cooling is achieved through the use of evaporative cooling systems. CO2 enrichment is managed via CO2 tank.

2. Kfar Qara, Israel:
    - Coordinates: 32°30'21"N, 35°3'14"E
    - Features: Four greenhouses with traditional cultivation and an open ventilation system. The greenhouse uses plastic film as cover material. There is no cooling and heating system, but CO2 enrichment is provided by biomass sources.

3. Mecklenburg-Vorpommern, Germany:
    - Coordinates: 53°23'38"N, 13°19'11"E

Funded by the European Union under Grant Agreement No 101096056. Views and opinions expressed are however those of the author(s) only and do not necessarily reflect those of the European Union or CINEA. Neither the European Union nor the granting authority can be held responsible for them.

- Features: One glass greenhouse with traditional cultivation. Heating by pipe rail, cooling by evaporative cooling. Monitoring systems include sensors for various climatic parameters, CO2 enrichment with biomass.

4. Berlin, Germany:
    - Coordinates: 52°31'12"N, 13°23'17"E
    - Features: One glass greenhouse with hydroponic systems, utilizing a heat pump for heating and cooling. Advanced monitoring includes a full set of environmental sensors and CO2 bottles for enrichment.

5. Vienna, Austria:
    - Coordinates: 48°12'30"N, 16°22'21"E
    - Features: Three greenhouses featuring traditional cultivation methods on tables and policarbonate cover material. The greenhouse is equipped with pipe rail heating and cooling with gable and side ventilation and CO2 gas bags for enrichment.

6. Pontinia, Italy:
    - Coordinates: 41°24'29"N, 13°02'39"E
    - Features: Two greenhouses has been recently built for the purposes of the project. At the moment they are equipped with two responsive PV tracking systems and UR is providing a design of the microclimate monitoring system that will be built in the near future. The greenhouses are not provided with heating and cooling systems, as most of the greenhouses in Italy and CO2 enrichment is not specified, at present.

The detailed survey and subsequent instrumentation of the greenhouses provide a comprehensive understanding of the conditions and capabilities at each site. The monitoring systems installed enable precise control and data collection, which are essential for developing accurate models and strategies to enhance greenhouse performance across diverse locations.

Funded by the European Union under Grant Agreement No 101096056. Views and opinions expressed are however those of the author(s) only and do not necessarily reflect those of the European Union or CINEA. Neither the European Union nor the granting authority can be held responsible for them.

Installation and System Setup Overview for REGACE Project Sites

Introduction

There are many ongoing studies for increasing the efficiency of PV modules. One way to increase the energy yield of the PV modules using tracking system and the other one to use bifacial solar panels by capturing the rear side illumination as well.

This technology enables us to increase the yield and to compensate for the lost radiation caused by the reflected light on the greenhouse cover. Energy production of bifacial panels provides a bit more of a challenge versus mono facial one, this is because the energy production of bifacial solar panels depends not only on the absorption of direct sunlight on the front side, but also on the less straightforward influx of reflected or diffuse light on the rear side. The general formula for determining the total energy production of a bifacial solar panel is the sum of the energy output on the front side and the energy output on the rear side. However, as the energy output on the rear side is calculated by the power generation on a bifacial panel's rear side in terms of the "bifacial gain," as a fraction of the energy produced by the front side of the module. Since the light reaching the module's rear side behaves differently than the light reaching the front side (partially diffuse), bifacial modules must be understood in terms of "bifacial ratio" (i.e., the ratio of irradiance on the rear to that on the front) and "module bifaciality" (i.e., the ratio of the front and rear sides' energy conversion efficiency). Rear side irradiation also depends upon factors like sunlight reflected from the ground and sunlight diffused through the atmosphere caused by the type of the plastic cover of the greenhouse. When trying to understand the level of irradiation reflected from earth surface (Combined with crops light reflection), its required to take into account the surface reflection coefficient, which is known as an "albedo." factors include shading, module height, and the distance between different module rows (pitch). To measure the direct and the rear side irradiance we used a series of light sensors at different heights (0.5, 1.5, 2.5 and 3.5 m) enabling us to differentiate the type of the albedo (reflected by ground and by crops). In addition, we installed light sensors on the panels level to measure the real received illuminance on both panel sides. Outside the greenhouse we installed a tracking panel with both front and rear illumination sensors and one fixed bifacial panel to compare the performance In and outside the greenhouse.

To measure the power output in relation to the bifacial gain and module operating temperature for front, rear and combined irradiance, we stuck temperature sensor on the back side of two panels inside the greenhouse and on one panel outside the greenhouse. Lamers et al. found that the effect heat input for bifacial glass-glass module (our case) is increasingly larger with increasing rear irradiance compared to mono facial modules. He found that the effective heat transfer coefficient of glass-glass panel is higher than that of white back sheet panel. The combined effect of heat input and heat transfer is that only at rear irradiance fraction beyond 15% the additional heat input can cause the bifacial panel to be hotter that their mono facial counterpart, but the energy yield is still much higher due to the large bifacial gain

Funded by the European Union under Grant Agreement No 101096056. Views and opinions expressed are however those of the author(s) only and do not necessarily reflect those of the European Union or CINEA. Neither the European Union nor the granting authority can be held responsible for them.

(solar energy material and solar cells, vol. 185, 2018, p. 192-197). Using a small (5Wp) mono-facial panel mounted on the tracking system inside and outside the greenhouse we will measure differences on performance between the two types of technologies in relation to the heat effect.

At the current stage of experimentation (started two weeks ago) we cannot 'present reliable data on solar panel level and we hope within the next two month be able to send a comprehensive report that refer to all above mentioned parameters.

The current report refers to general data collected from eight solar systems in five locations. It includes energy output for the PV-system and internal microclimate parameters.

The report gives a general overview about the current situation in all sites.

AZ - Israel

The installation at AZ is fully operational, featuring four greenhouses—two equipped with PV tracking systems and two without. These greenhouses are uniformly planted with cucumber crops. Advanced microclimate sensors have been installed to monitor temperature, humidity, and CO2 levels, along with crop response sensors to track the growth and health of the cucumber plants. An integrated software system facilitates real-time data collection and analysis. Continuous recording of microclimate conditions and crop responses is in place, and data on PV system performance, including energy production and system efficiency, is stored on a centralized server accessible to all project participants for analysis and optimization. Currently, all systems are fully functional, providing valuable data on the interaction between PV systems and greenhouse conditions. Future steps include ongoing monitoring and analysis to optimize system performance and explore the potential for expanding the installation to other crops or additional greenhouses.

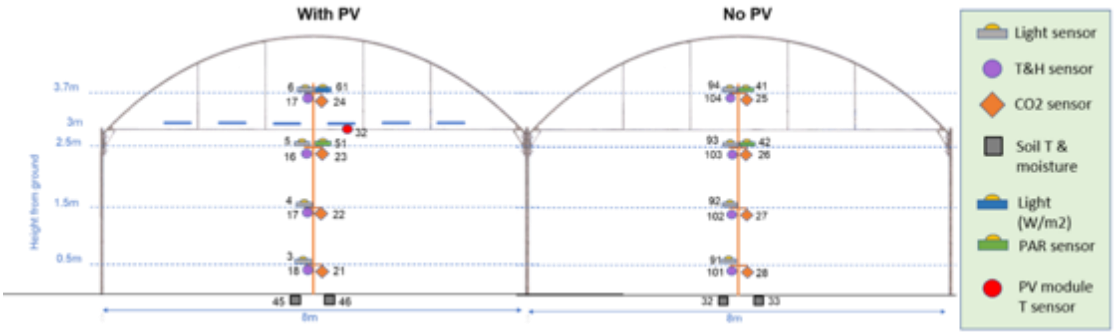

Figure 1. AZ site microclimate data collection map for the presented data bellow.

Funded by the European Union under Grant Agreement No 101096056. Views and opinions expressed are however those of the author(s) only and do not necessarily reflect those of the European Union or CINEA. Neither the European Union nor the granting authority can be held responsible for them.

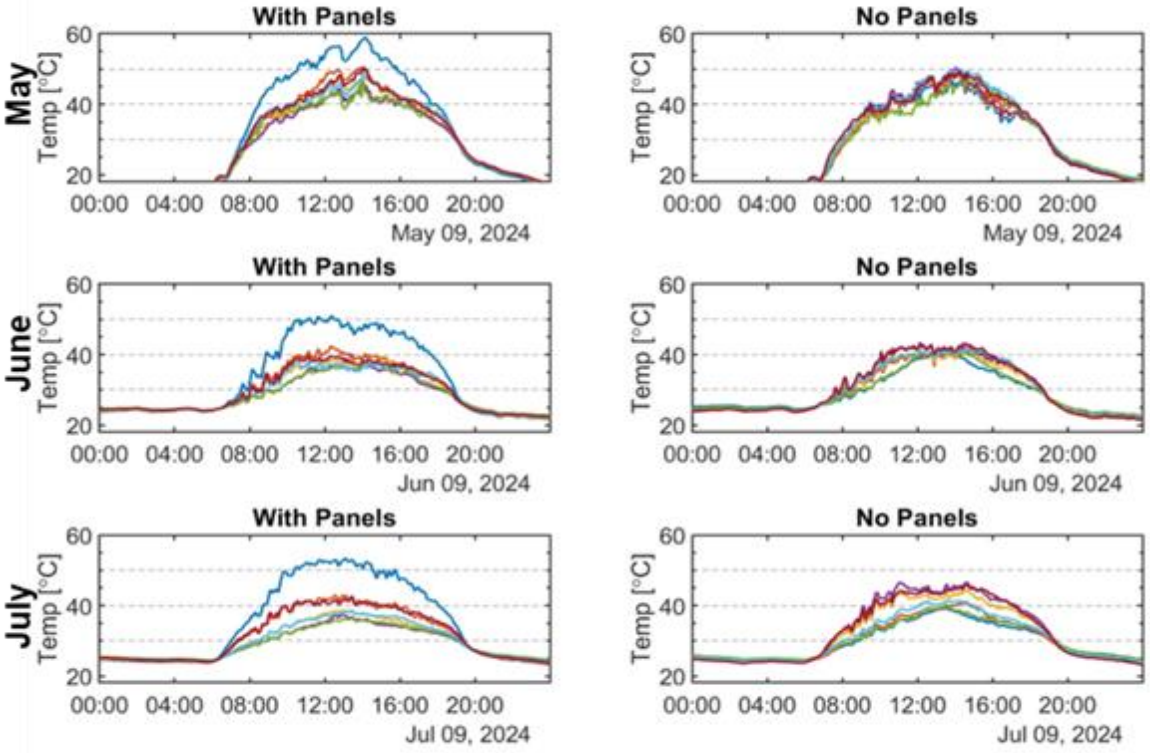

Figure 2. Temperature at four different level in GH with PV and without. The data collection date is indicated below, and the heights are 0.5, 1.5, 2.5, 3.5 meters above the ground.

The analysis of temperature data over three different days in various months reveals distinct differences in temperature distribution between greenhouses equipped with PV panels and those without. In the greenhouse with PV panels, the light distribution was more uniform, resulting in higher temperatures at the top above the panels. However, near the plants and the ground, temperatures were significantly lower. The temperature gradient in this greenhouse reached up to 20 degrees Celsius, indicating a pronounced difference between the top regions and the areas near the plants and ground.

In contrast, the greenhouse without PV panels exhibited a noticeable temperature gradient from the beginning of the observation period, which increased as the plants grew. The temperature differences in this greenhouse were below 10 degrees Celsius initially. Overall, the presence of PV panels created a more pronounced temperature gradient, with higher temperatures at the top and cooler temperatures near the plants and ground, compared to the greenhouse without PV panels. This highlights the impact of PV panels on temperature distribution within greenhouses, emphasizing their role in maintaining cooler conditions near the plant level. This thing is seen in figure 2 and will be elaborated later.

Funded by the European Union under Grant Agreement No 101096056. Views and opinions expressed are however those of the author(s) only and do not necessarily reflect those of the European Union or CINEA. Neither the European Union nor the granting authority can be held responsible for them.

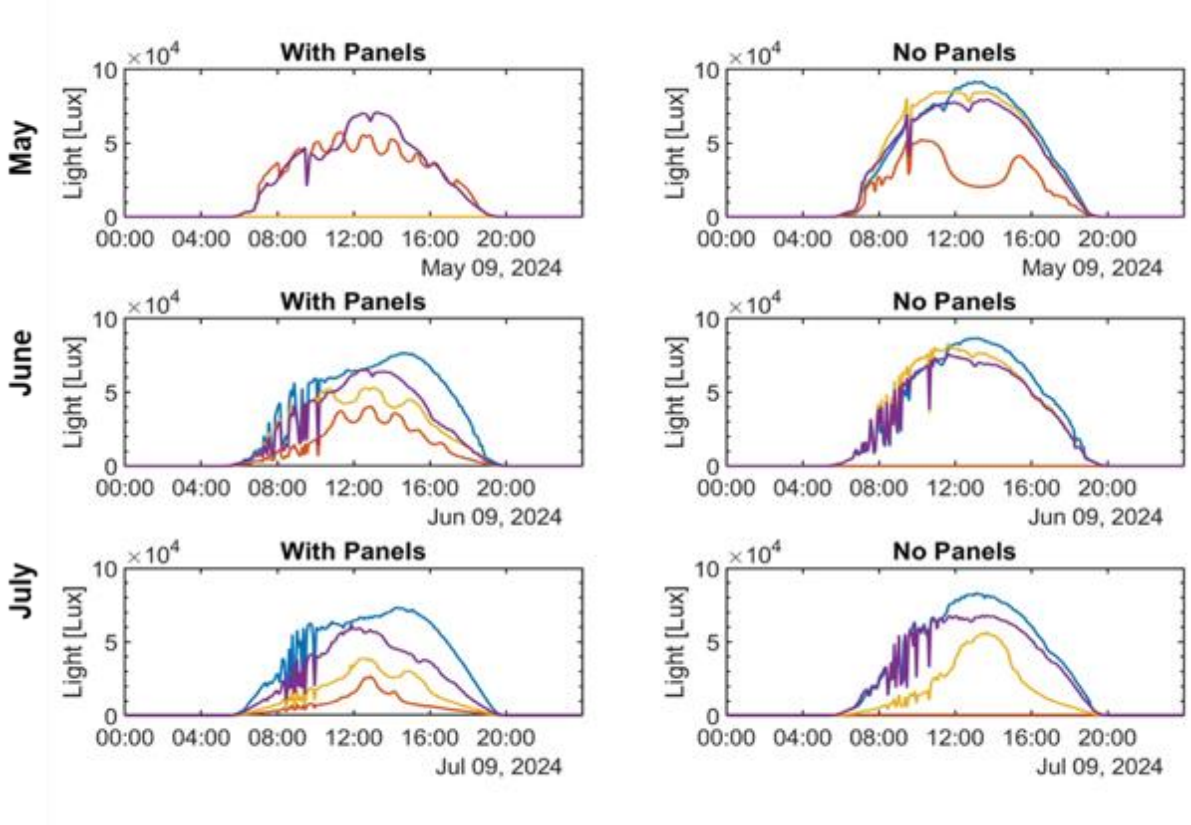

Figure 3. Light Intensity at four different level in GH with PV and without. The data collection date is indicated below, and the heights are 0.5, 1.5, 2.5, 3.5 meters above the ground.

The analysis of light distribution in greenhouses equipped with PV panels versus those without reveals significant differences from the outset. In the greenhouse with PV panels, a distinct pattern of shading was observed from the beginning, characterized by shallow dips in light intensity. This shading pattern remained relatively consistent, with uniform light distribution being maintained across the greenhouse. Despite the shading from the panels, the light levels were adequate for plant growth and were evenly spread throughout the space.

In contrast, the greenhouse without PV panels exhibited a more straightforward light distribution pattern with less pronounced shading. The light intensity was more consistent, without the shallow dips observed in the greenhouse with PV panels. This difference emphasizes the impact of PV panels on light distribution, where the presence of panels creates a pattern of shading that, while causing dips in light intensity, still allows for uniform and sufficient light for plant growth. These observations will be further elaborated in the following sections, providing a detailed analysis of how PV panels affect light conditions within greenhouses.

Funded by the European Union under Grant Agreement No 101096056. Views and opinions expressed are however those of the author(s) only and do not necessarily reflect those of the European Union or CINEA. Neither the European Union nor the granting authority can be held responsible for them.

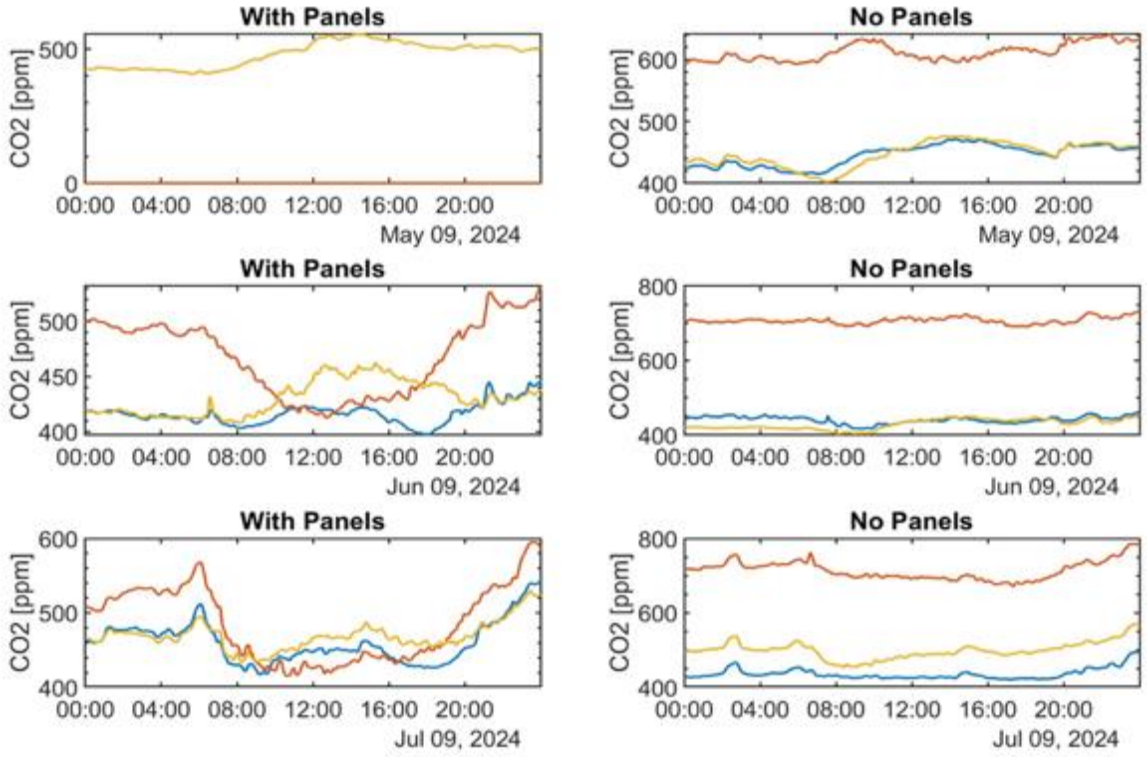

Figure 4. CO2 levels in ppm at four different level in GH with PV and without. The data collection date is indicated below, and the heights are 0.5, 1.5, 2.5, 3.5 meters above the ground.

The analysis of CO2 levels in greenhouses with and without PV panels reveals notable patterns. In both types of greenhouses, CO2 levels rise during the night and decrease throughout the day, with a local maxima occurring around midday. This pattern is consistent, but the fluctuations in CO2 levels are more pronounced in the greenhouse equipped with PV panels. The presence of the panels appears to accentuate the variations, making the rising and falling trends more distinct.

In contrast, the greenhouse without PV panels exhibits a similar daily cycle of CO2 level changes, but the fluctuations are less pronounced. The overall pattern of CO2 levels rising at night and dropping during the day is still evident, but the peaks and troughs are less marked compared to the greenhouse with PV panels. These observations suggest that the presence of PV panels may influence the microclimate dynamics more significantly, leading to clearer patterns of CO2 level changes. These trends will be analyzed in greater detail in subsequent studies to understand the underlying mechanisms and their implications for greenhouse management.

Funded by the European Union under Grant Agreement No 101096056. Views and opinions expressed are however those of the author(s) only and do not necessarily reflect those of the European Union or CINEA. Neither the European Union nor the granting authority can be held responsible for them.

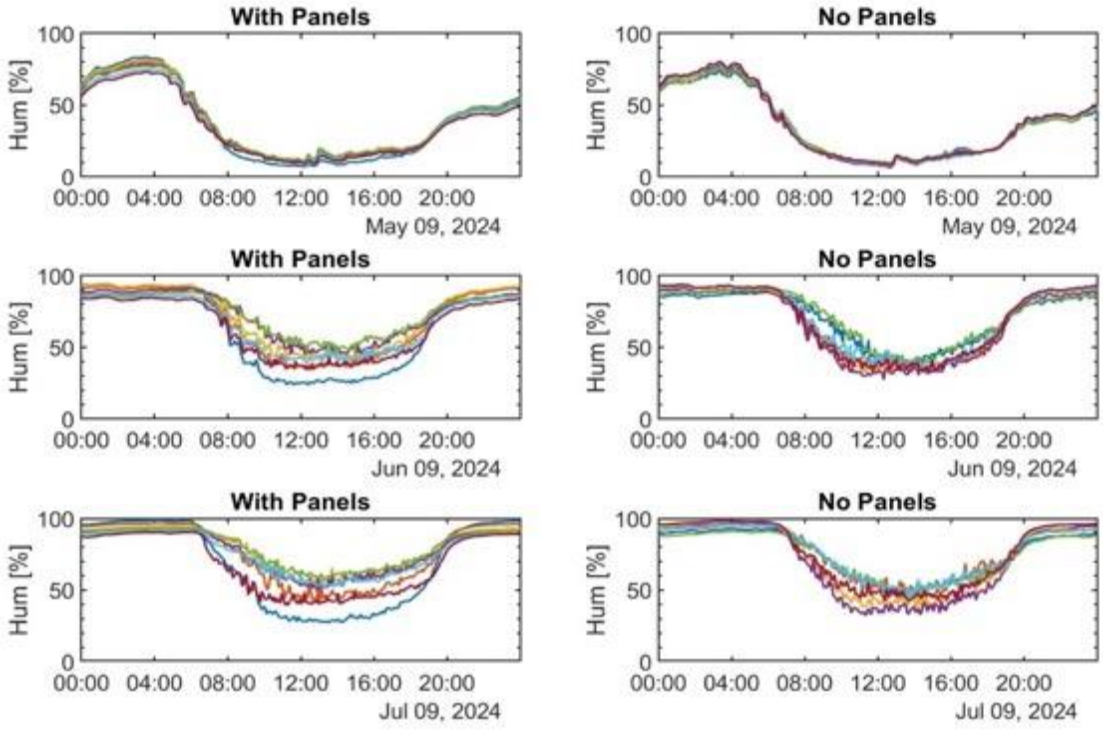

Figure 5. Humidity levels in % at four different level in GH with PV and without. The data collection date is indicated below, and the heights are 0.5, 1.5, 2.5, 3.5 meters above the ground.

The analysis of humidity levels in greenhouses with and without PV panels shows notable differences, particularly as the plants grow. Initially, when the plants are small, humidity levels near the ground are similar in both greenhouses. However, as the plants grow, humidity levels increase in both greenhouses. In the greenhouse with PV panels, this increase is more pronounced, resulting in higher humidity levels near the ground compared to the greenhouse without PV panels. As the plants continue to grow, the humidity gradient becomes more significant in the greenhouse with PV panels.

In contrast, while the greenhouse without PV panels also experiences an increase in humidity as the plants grow, the overall levels remain lower than those in the greenhouse with PV panels. The increase in humidity is more gradual, and the gradient is less pronounced. This indicates that the presence of PV panels influences the microclimate, leading to higher humidity levels and a steeper gradient as the plants grow. These trends will be analyzed further in later sections to understand the impact of PV panels on humidity dynamics within greenhouses.

Circeo-Italy

In Italy, the installation is complete and fully operational. The setup mirrors that of AZ, with greenhouses uniformly planted with cucumber crops. PV tracking systems and microclimate sensors are installed and functional. The Cornaro group is responsible for managing the microclimate systems. Continuous data collection ensures the monitoring of microclimate conditions, crop responses, and PV system performance. Current efforts are focused on installing and operationalization of the

Funded by the European Union under Grant Agreement No 101096056. Views and opinions expressed are however those of the author(s) only and do not necessarily reflect those of the European Union or CINEA. Neither the European Union nor the granting authority can be held responsible for them.

microclimate systems. Future steps include detailed analysis of the collected data and potential system adjustments to improve performance.

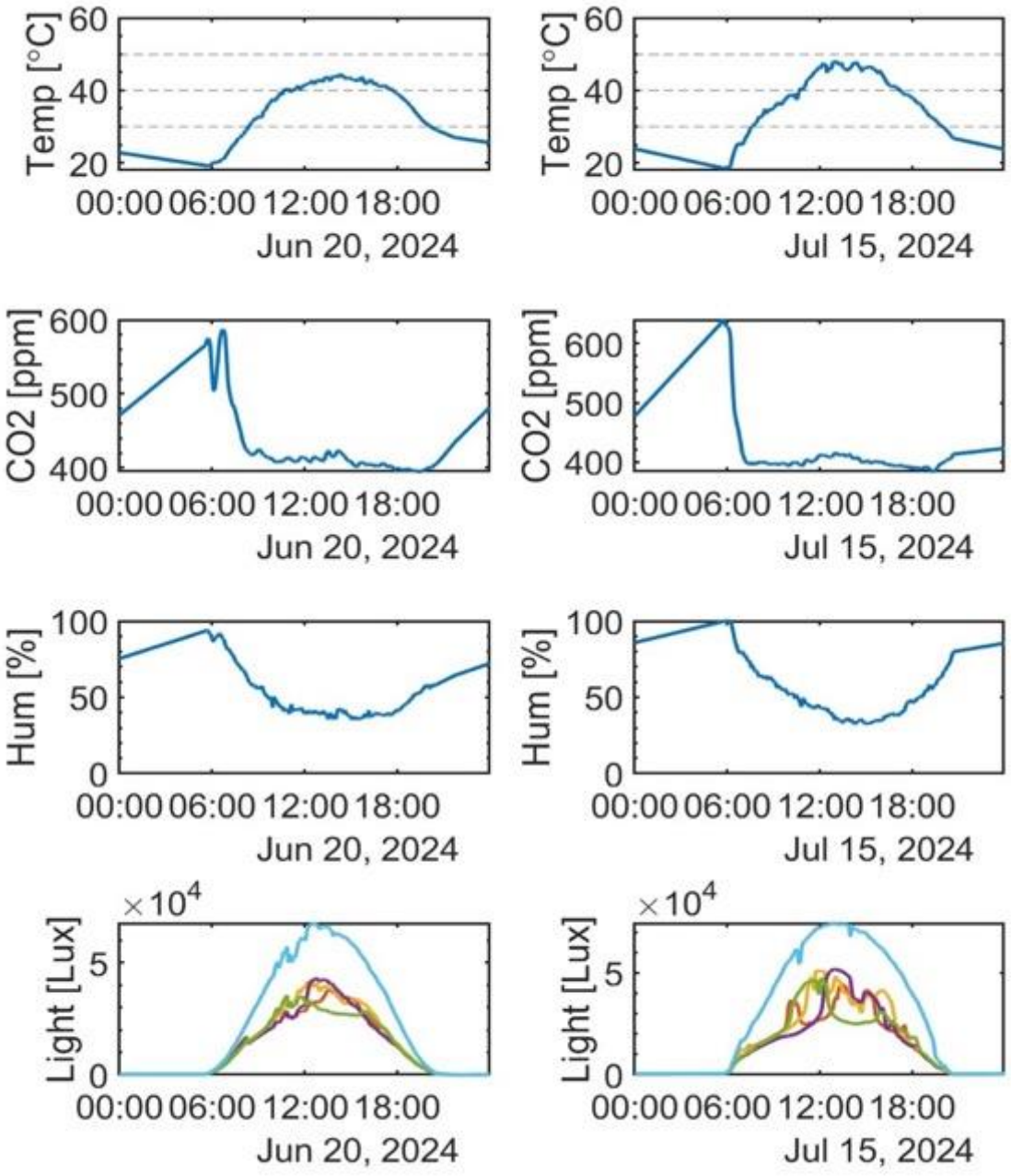

Figure 6. Italy site greenhouse microclimate and electric power production in days from June and July as indicated below.

Watzkendorf -Germany

In Germany, the Watzkendorf site is fully prepared with data acquisition systems functional, pending the completion of the electricity supply, (the system suffers under internet interruption). The setup includes greenhouses with PV tracking systems, microclimate sensors, and crop response monitoring.

Funded by the European Union under Grant Agreement No 101096056. Views and opinions expressed are however those of the author(s) only and do not necessarily reflect those of the European Union or CINEA. Neither the European Union nor the granting authority can be held responsible for them.

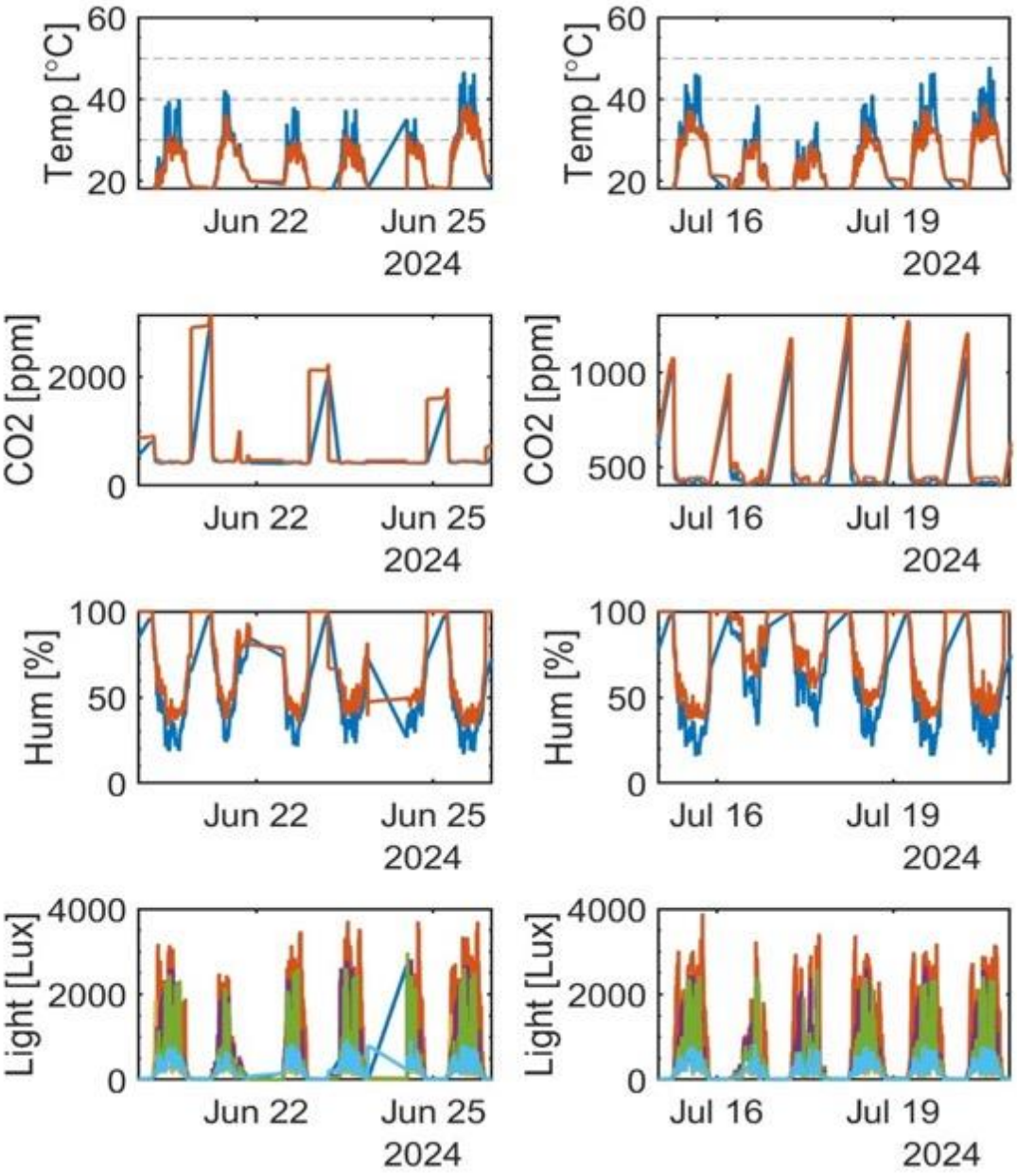

Figure 7. Watzkendorf site microclimate data collection

Humboldt University-Germany

In Berlin, the installation is pending the arrival of an inverter, expected to be operational within the next weeks. Interim data on microclimate and crop responses are being collected, with full data collection to commence once the inverter is installed. This setup will allow for comprehensive monitoring of PV system performance and its impact on greenhouse conditions, ensuring optimal system functionality.

Funded by the European Union under Grant Agreement No 101096056. Views and opinions expressed are however those of the author(s) only and do not necessarily reflect those of the European Union or CINEA. Neither the European Union nor the granting authority can be held responsible for them.

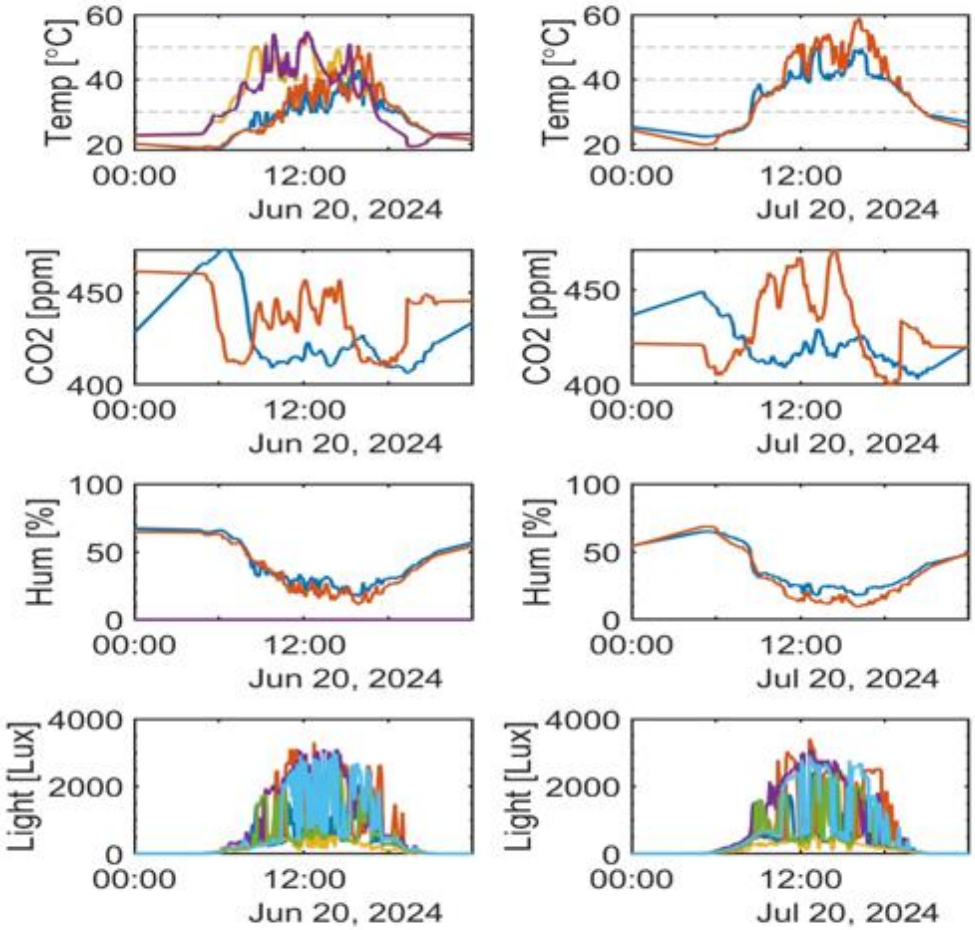

Figure 8. Humbolt site microclimate data collection

BUKO University - Vienna

The Vienna site has completed all installations, with greenhouses equipped with PV tracking systems and microclimate sensors. The focus is on collecting data on the crop effects caused by the tracking systems. Due to restrictions on connecting the system to the grid, alternative methods for power conversion data acquisition are being explored. Current efforts aim to find solutions for this issue, while continuous monitoring of crop responses provides valuable insights into the agronomic impacts of the PV installations. This data is crucial for understanding the effects of PV tracking systems on plant growth and optimizing the greenhouse environment.

Funded by the European Union under Grant Agreement No 101096056. Views and opinions expressed are however those of the author(s) only and do not necessarily reflect those of the European Union or CINEA. Neither the European Union nor the granting authority can be held responsible for them.

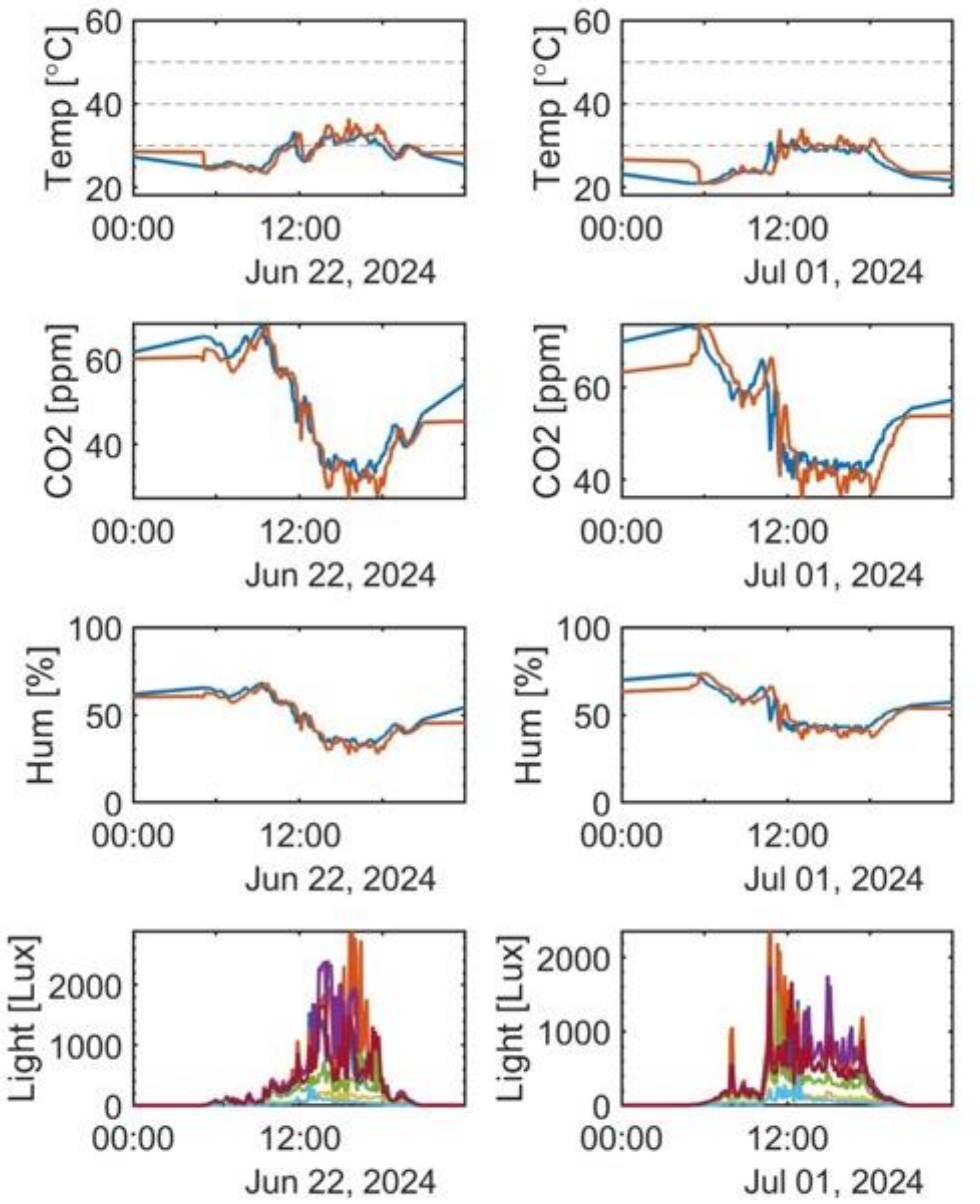

Figure 8. BUKO site microclimate data collection

Thessaly university-Greece

The installation in Greece is currently in the planning stages, with full operational status expected before August. The planned setup includes greenhouses with PV tracking systems, microclimate sensors, and crop response monitoring. All necessary equipment and systems are prepared for installation once agreements are finalized. Data collection methodologies will mirror those at other REGACE sites, focusing on microclimate conditions, crop responses, and PV system performance. Preparations are underway to ensure an efficient and timely setup, which will contribute to the

Funded by the European Union under Grant Agreement No 101096056. Views and opinions expressed are however those of the author(s) only and do not necessarily reflect those of the European Union or CINEA. Neither the European Union nor the granting authority can be held responsible for them.

overall goals of the REGACE project by providing additional data and insights from a new geographic location.

Effects of solar panels on Microclimate

Light Distribution

The integration of PV panels within greenhouses significantly impacts light distribution, which is crucial for optimal plant growth. The sun radiation simulation using COMSOL (Figure 5) demonstrates how light diffuses across the tunnel greenhouse, creating an almost uniform pattern beneath the solar panels. This uniformity is essential for ensuring that the plants receive consistent light for optimal growth. The propagation of radiation over time, shown in subfigures a-0c, indicates how the greenhouse design effectively manages light distribution, minimizing shading effects and ensuring sufficient light penetration for plant growth throughout the day.

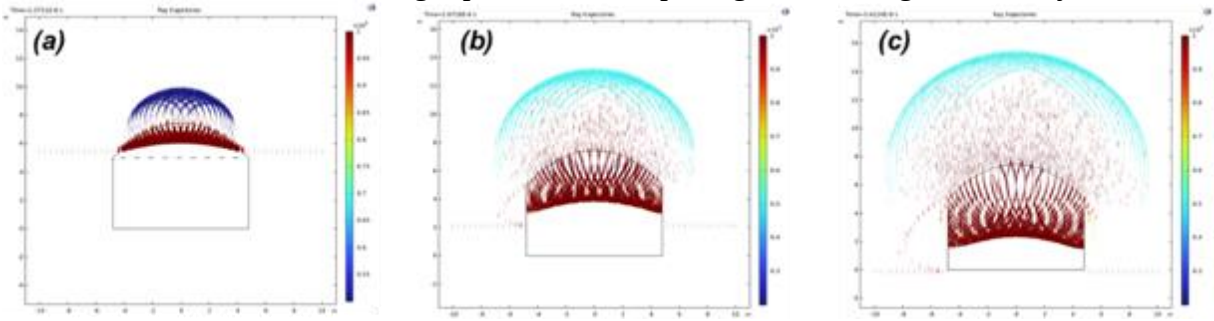

Figure 9. Sun Radiation simulated in COMSOL shows the reflected and transmitted radiation across tunnel greenhouse. (a-0c) propagation through time.

AZ Site

At the AZ site, sensors have been strategically placed within the greenhouses to measure light intensity at various points (Figure 6). The data reveals that light intensity is highest above the panels, decreases between the panels, and is lowest below them. Despite this gradient, the light levels beneath the panels remain adequate for plant growth. The observed oscillations in light intensity are due to the movement of the sun, causing small, consistent shading patterns. This information is crucial for understanding the light dynamics within the greenhouse and their impact on plant growth. The light intensity inside the greenhouse is affected from the type of the greenhouse cover (transparency and defused) also from dust accumulation.

Funded by the European Union under Grant Agreement No 101096056. Views and opinions expressed are however those of the author(s) only and do not necessarily reflect those of the European Union or CINEA. Neither the European Union nor the granting authority can be held responsible for them.

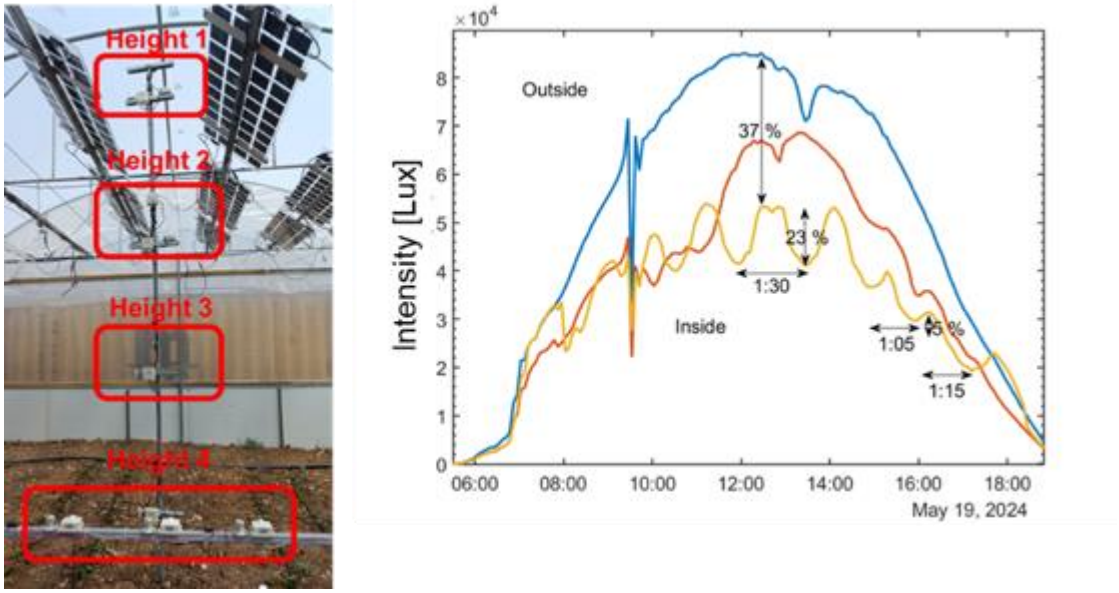

Figure 10. Sensors in green house (Left) Corresponding Radiation Patterns in Lux are outside the greenhouse panels (blue curve) at panels level (Red curve) one meter bellow the panels (yellow curve).

Comparison to Other Sites

Similar light distribution patterns are observed at other REGACE project sites. At the Circeo site, the PV tracking systems are designed to optimize sunlight capture, and the microclimate sensors capture the variations in light intensity throughout the day. The measurements indicate that light intensity levels for one day inside the greenhouses at the Italy site are lower than those at AZ, showing lower light levels for plant growth and lower energy production per panel. This nonuniformity across different sites underscores the effectiveness of the greenhouse designs (structure type and cover properties) and PV systems in maintaining suitable light conditions for plant growth.

Data from other sites, such as the Humboldt site, Watzkendorf site and Buko site, further corroborate these findings. Measurements taken at different points within these greenhouses (Figure 7) show that while there are fluctuations in light levels due to the movement of the sun and the structural elements of the greenhouses, the overall light distribution remains conducive to plant growth. These patterns are crucial for understanding how PV panels impact greenhouse environments and for optimizing the design and placement of sensors to ensure accurate monitoring of light conditions.

Funded by the European Union under Grant Agreement No 101096056. Views and opinions expressed are however those of the author(s) only and do not necessarily reflect those of the European Union or CINEA. Neither the European Union nor the granting authority can be held responsible for them.

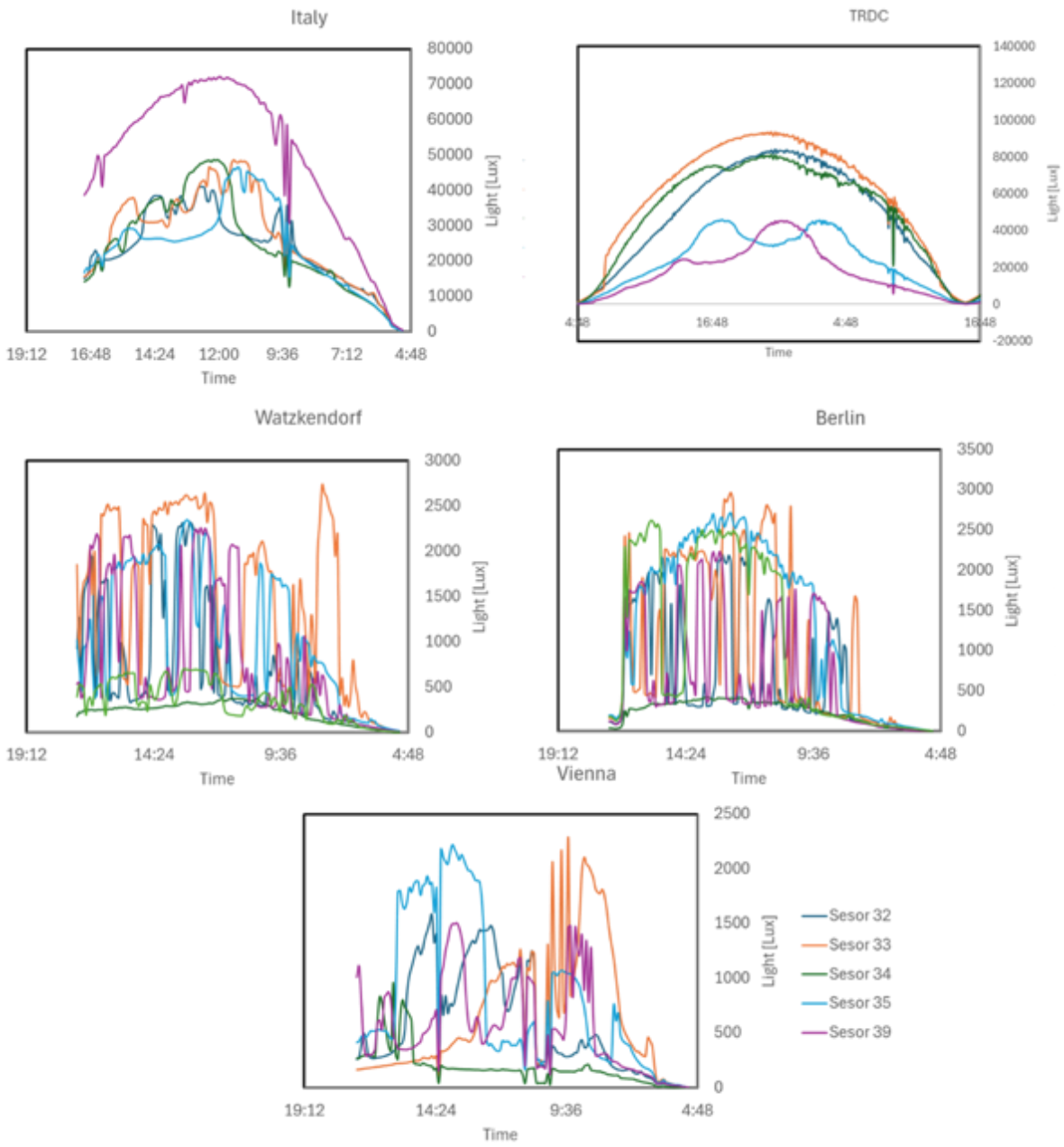

Figure 11. Light Intensity levels for one sunny day measurements inside greenhouse at different sites.

Funded by the European Union under Grant Agreement No 101096056. Views and opinions expressed are however those of the author(s) only and do not necessarily reflect those of the European Union or CINEA. Neither the European Union nor the granting authority can be held responsible for them.

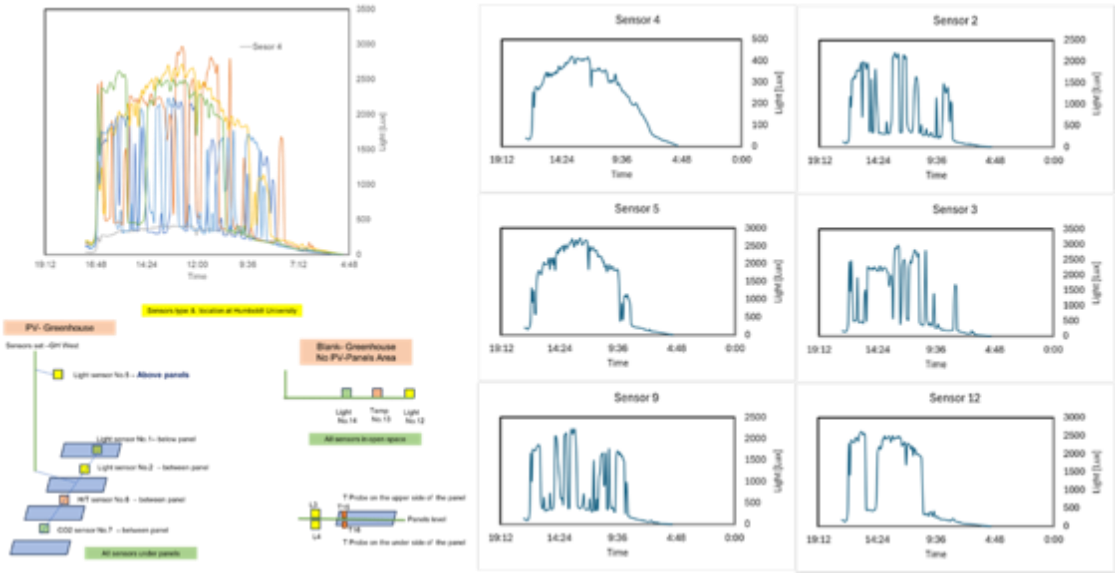

Figure 12. Daily light intensity for differently located sensors in Humboldt university shows architecture interruption on light intensity due to the metallic roof. Sensor number 4 shows the ground reflected light with very low intensity (max 400 Lux) Compared with the blank reaching above 2500 Lux.

Figure 12 illustrates the daily light intensity measurements from various sensors located in the greenhouse at Humboldt University, highlighting the impact of the greenhouse's architectural elements on light distribution. The data shows significant light intensity interruptions caused by the metallic roof, with Sensor 4 detecting ground-reflected light at a maximum of 400 Lux, in stark contrast to other areas that reach above 2500 Lux. This shading effect from the greenhouse construction poses a challenge for distinguishing it from cloud cover. To optimize the performance of responsive PV systems in supporting crop growth, it is crucial to develop methods that can accurately differentiate between shading caused by structural elements and that caused by clouds. This will enable the responsive PV systems to adjust more effectively to real-time light conditions, ensuring that crops receive adequate illumination while maximizing energy production.

General Summary

Overall, the integration of PV panels within greenhouses affects light distribution in ways that can be both beneficial and challenging for plant growth. By diffusing light and creating shaded areas, PV panels create nonuniform light distribution, which should be carefully investigated. However, the structural elements of the greenhouses and the small size of the sensors can cause localized shading that may not fully represent the light conditions experienced by the plants. Continuous monitoring and data analysis from different sites provide valuable insights into optimizing light distribution and improving the overall performance of agrivoltaic systems. The radiation variations observed are within the limits of normal plant growth, ensuring that the plants receive adequate light for their development.

Temperature Distribution

Funded by the European Union under Grant Agreement No 101096056. Views and opinions expressed are however those of the author(s) only and do not necessarily reflect those of the European Union or CINEA. Neither the European Union nor the granting authority can be held responsible for them.

The integration of PV panels within greenhouses has a substantial impact on temperature distribution, which is critical for plant growth and energy efficiency. Temperature variations within the greenhouses are influenced by the presence of PV panels, the greenhouse structure, and external environmental conditions.

AZ Site

Thermal images taken with an infrared camera inside and outside the greenhouses at AZ site (Figure 13) provide insights into the temperature distribution. These images show that the soil and panels are the hottest areas, with tracking panels inside the greenhouse being hotter than non-tracking panels. Panels outside the greenhouse are even hotter, suggesting that the greenhouse structure provides some thermal regulation. This differential heating indicates that the PV panels absorb and retain heat, contributing to higher temperatures in their vicinity.

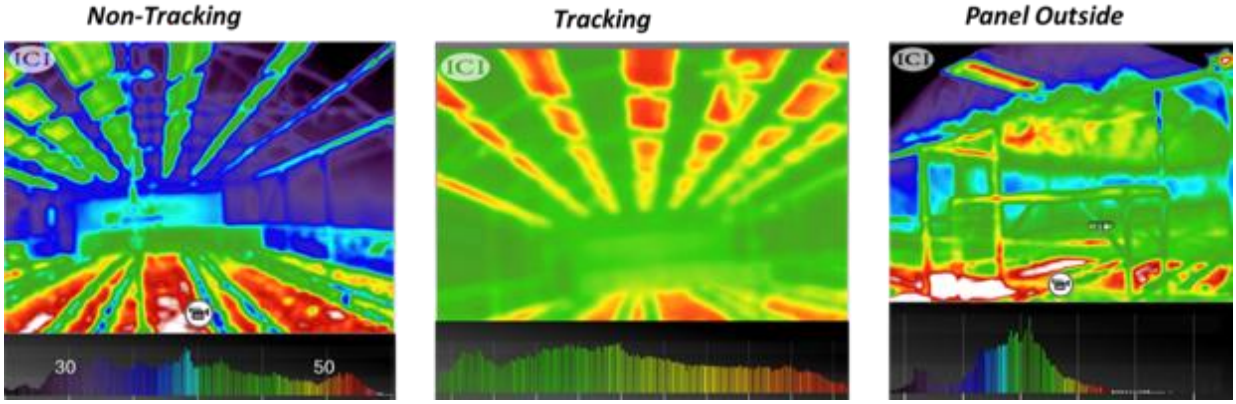

Figure 13. Thermal images taken in IR camera inside and outside the green house with tracking and non-tracking panels.

Further data collected on temperature levels within the AZ greenhouses (Figure 14) shows distinct differences between greenhouses with and without solar tracking panels. In greenhouses equipped with solar tracking panels, temperatures are higher in the upper space and lower near the ground. This gradient indicates that the panels not only absorb sunlight but also contribute to heating the air in the upper regions of the greenhouse. The movement and orientation of the tracking panels likely enhance this effect by maximizing sunlight capture, which increases the temperature in the upper space. In contrast, greenhouses without solar panels exhibit a more uniform temperature distribution, with lower temperatures in the upper space compared to those with PV panels but higher near the ground. This suggests that the absence of PV panels allows for more even sunlight penetration and heat distribution throughout the greenhouse.

Funded by the European Union under Grant Agreement No 101096056. Views and opinions expressed are however those of the author(s) only and do not necessarily reflect those of the European Union or CINEA. Neither the European Union nor the granting authority can be held responsible for them.

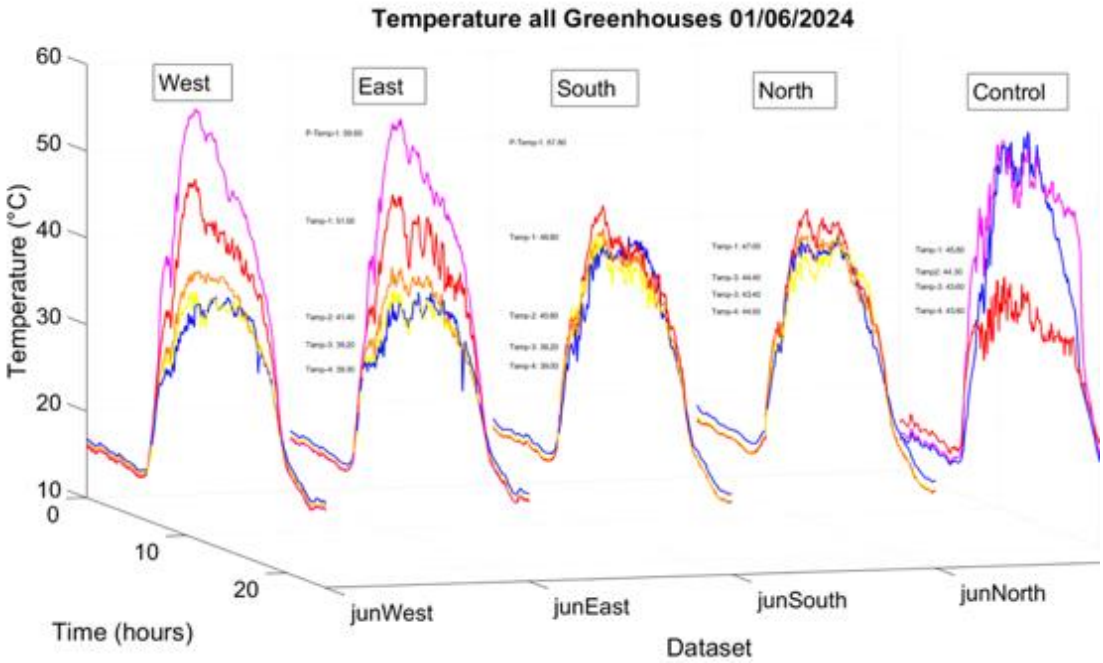

Figure 14.1 Temperature level in four greenhouses located at AZ including control outside the green house. The panels temperature inside the GH shows 5℃ higher than those outside the GH. Main while the air temperature outside 20 ℃ lower from the panel temperature. The temperature on crops level in GH with PV panels lower about 7 ℃ than those without PV Panels. The Controls are the temperature on top and bellow (blue-pink) the panel outside the green house and the temperature outside (red).

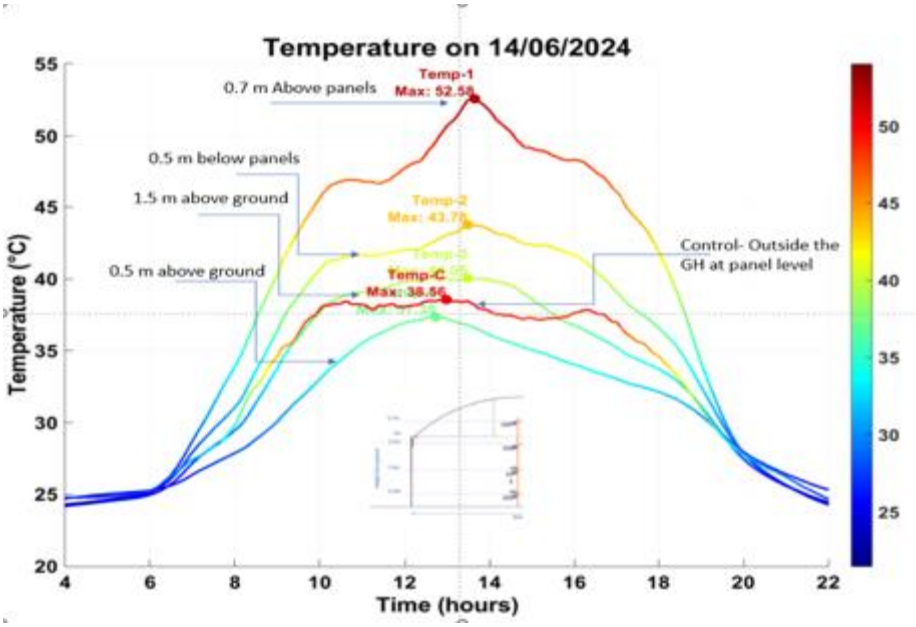

Figure 14.2 Temperature level in PV greenhouse located at AZ including control outside the green house. The temperature inside the GH shows approximately 15℃ differences between sensors at top and bottom. The Control shows the temperature outside the GH at panel level (red).

Funded by the European Union under Grant Agreement No 101096056. Views and opinions expressed are however those of the author(s) only and do not necessarily reflect those of the European Union or CINEA. Neither the European Union nor the granting authority can be held responsible for them.

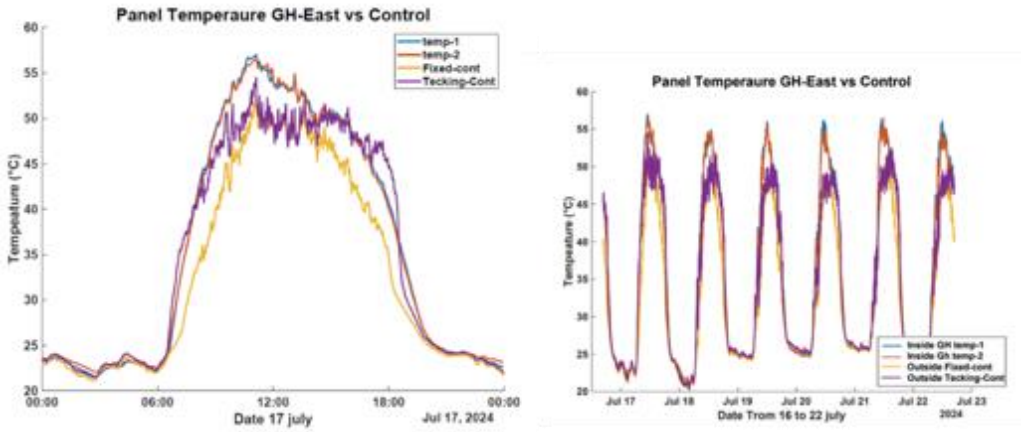

Figure 14.3 Panel Temperature compression inside and outside the GH located at AZ. The panel temperature inside the GH shows approximately 5℃ higher temperature than outside panels.

Funded by the European Union under Grant Agreement No 101096056. Views and opinions expressed are however those of the author(s) only and do not necessarily reflect those of the European Union or CINEA. Neither the European Union nor the granting authority can be held responsible for them.

Comparison to Other Sites

Temperature measurements taken at other REGACE project sites (Figure 10) show similar patterns. In the greenhouses at different sites, temperature variations follow a similar trend where areas under PV panels tend to be hotter. The data collected for one day inside the greenhouses at different sites further confirm that the presence of PV panels influences the internal temperature distribution, contributing to a hotter environment near the panels and a cooler environment near the ground.

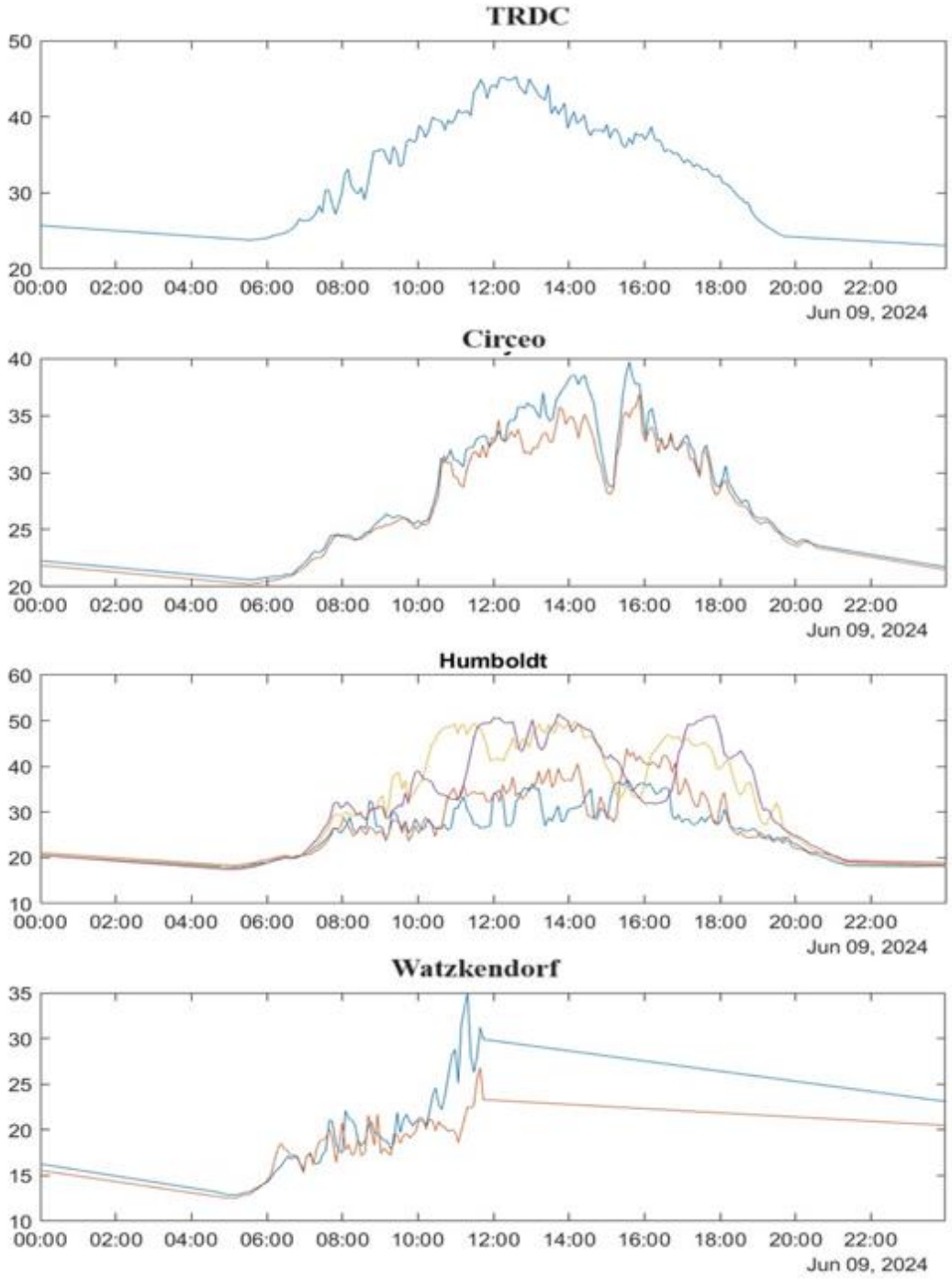

Figure 15. Temperature levels for one day measurements inside the GH at different sites.

General Summary

Funded by the European Union under Grant Agreement No 101096056. Views and opinions expressed are however those of the author(s) only and do not necessarily reflect those of the European Union or CINEA. Neither the European Union nor the granting authority can be held responsible for them.

The integration of PV panels within greenhouses significantly impacts temperature distribution. PV panels absorb and retain heat, leading to higher temperatures in their vicinity, particularly in the upper regions of the greenhouse. This heating effect can create a gradient where the air near the panels is hotter, and the air near the ground is cooler. In greenhouses without PV panels, the temperature distribution is more uniform, suggesting that the absence of panels allows for more even sunlight penetration and heat distribution. Continuous monitoring and data analysis from different sites provide valuable insights into optimizing temperature conditions and improving the overall performance of agrivoltaic systems. Understanding these temperature dynamics is crucial for optimizing greenhouse conditions to ensure that plants receive the optimal temperature range for growth and development.

CO2 Concentration

The presence and operation of PV panels within greenhouses can also affect CO2 levels, which are crucial for plant photosynthesis and growth.

AZ Site

In AZ, the data indicates that increased light intensity leads to higher CO2 levels within the greenhouses. The oscillations in CO2 concentration are more closely correlated with the shading patterns created by the PV panels. These variations are important for understanding how the greenhouse microclimate responds to changes in light distribution caused by the PV panels.

Circeo Site

At Circeo site, the greenhouses are partially open, resulting in more stable CO2 levels with minimal fluctuations. The average CO2 concentration is around 400 ppm, which is the typical ambient level. This stability contrasts with other sites where the CO2 levels can rise up to 450-500 ppm due to the enclosed environment and the influence of PV panels.

Comparison to Other Sites

Figure 11 illustrates the CO2 data collection in ppm across different sites in one day. It shows the variations in CO2 concentrations, highlighting the differences between open and enclosed greenhouse environments and the influence of PV panels on these levels.

Funded by the European Union under Grant Agreement No 101096056. Views and opinions expressed are however those of the author(s) only and do not necessarily reflect those of the European Union or CINEA. Neither the European Union nor the granting authority can be held responsible for them.

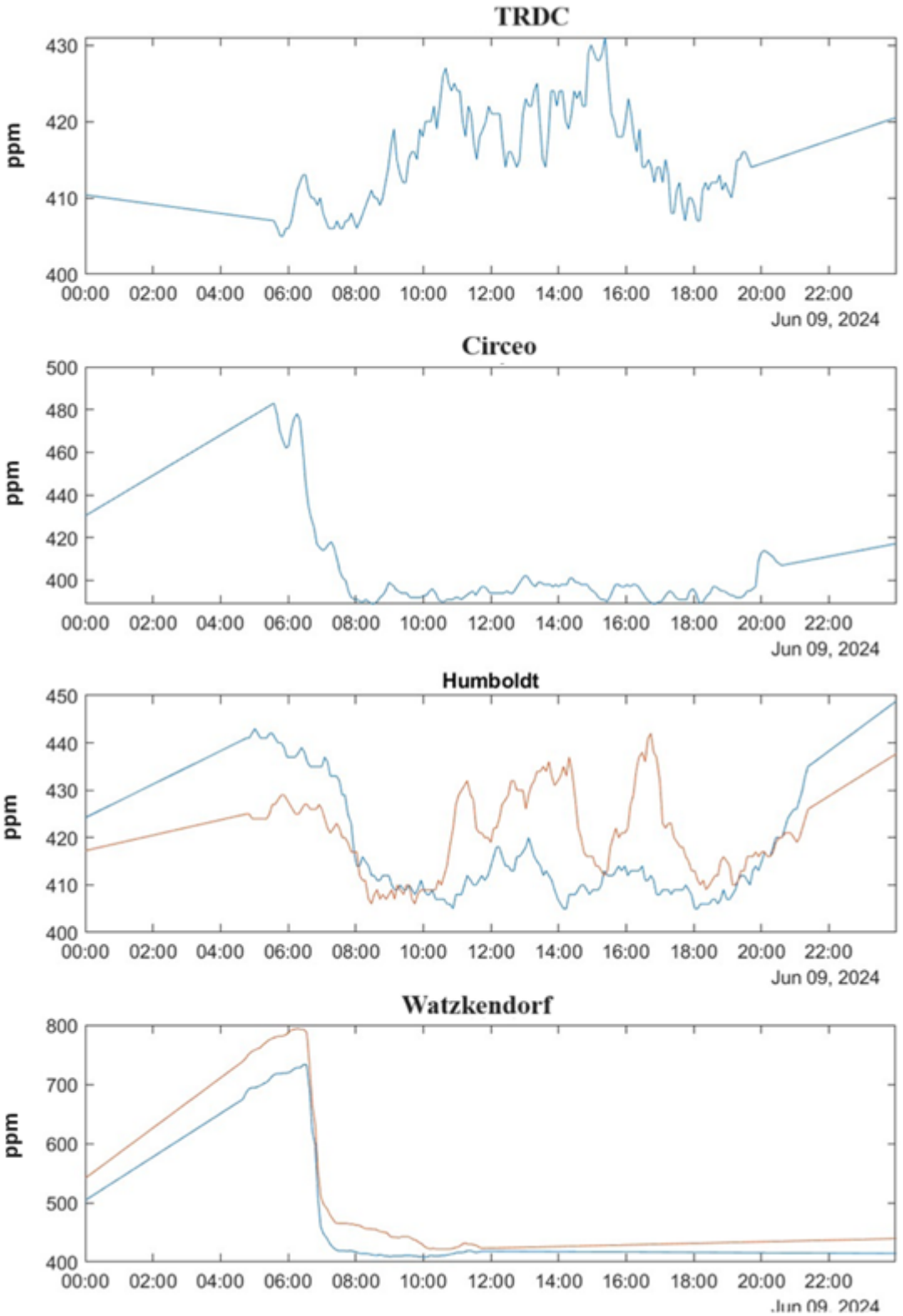

Figure 16.1 CO2 data collection in different sites in one day

Funded by the European Union under Grant Agreement No 101096056. Views and opinions expressed are however those of the author(s) only and do not necessarily reflect those of the European Union or CINEA. Neither the European Union nor the granting authority can be held responsible for them.

Figure 16.2 CO2 data collection over last month in Watzkendorf GH shows abnormal CO2 concentration values (above 3000 ppm) and slowdown to 1300 ppm in the mid of July 24. Our hypothesis is that the farmer introduced new compost, which increased the CO2 concentration.

General Summary

Overall, the data indicates that the presence of PV panels and the resulting light distribution significantly influence CO2 levels within greenhouses. While partially open greenhouses like those in Circeo maintain stable CO2 levels around 400 ppm, enclosed greenhouses with PV panels, such as those in AZ, can see levels rise to 450 ppm. Further detailed and comprehensive analysis will be conducted to examine these effects more thoroughly as outlined in the work packages (WPs) of this project. Understanding these dynamics is crucial for optimizing greenhouse conditions and enhancing plant growth and productivity.

Power Production

Figure 12 shows the daily electricity production at the Circeo site in Italy for February, March and April for the system in sun-tracking mode. As expected, as the season changes from winter to spring, with increasing daylight hours and light intensities, the total electricity yield increased due to these seasonal light variations, from 192kWh in February to 480kWh in April. In should be noted though that the data shown here is for 27 days in February, 31 days in March and 30 days in April.

Funded by the European Union under Grant Agreement No 101096056. Views and opinions expressed are however those of the author(s) only and do not necessarily reflect those of the European Union or CINEA. Neither the European Union nor the granting authority can be held responsible for them.

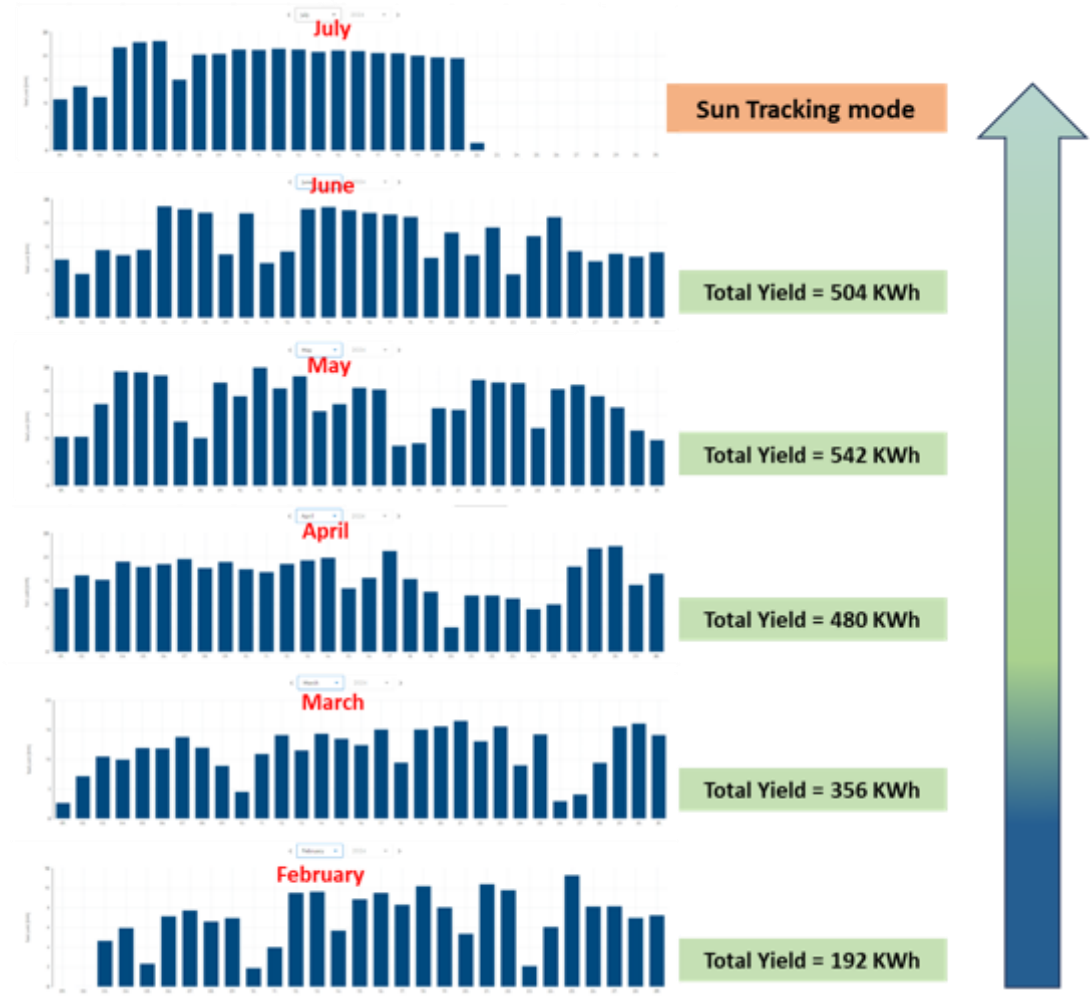

Figure 17. Daily power production in Circeo site in Italy in different months and to the left summarized total energy production.

Comparison Between Circeo and AZ Sites

When comparing the power production between Circeo and AZ sites, several factors come into play. The AZ site generally receives more light due to the type of plastic cover used in the greenhouses (86%), which has a higher light transmission rate compared to the cover used at the Circeo site (73%). Additionally, the AZ site has twice the number of PV panels compared to the Circeo site, resulting in a higher overall light conversion efficiency.

Impact of Tracking Systems

Another significant factor contributing to the difference in energy production is the use of tracking systems. Tracking systems on a single axis allow the PV panels to follow the sun's path throughout the day, maximizing sunlight capture and energy production meanwhile increasing the panel temperature. Data shows that tracking systems can increase energy production by more than 20% compared to fixed panels, especially in greenhouses. This increase in energy production is also influenced by seasonal changes, with higher gains observed during periods of longer daylight hours and higher solar irradiance. The impact of the bifaciality of the panels on the power

Funded by the European Union under Grant Agreement No 101096056. Views and opinions expressed are however those of the author(s) only and do not necessarily reflect those of the European Union or CINEA. Neither the European Union nor the granting authority can be held responsible for them.

yield inside the greenhouse is still being studied. The current collected data does not allow us to deliver clear results at this point in time.

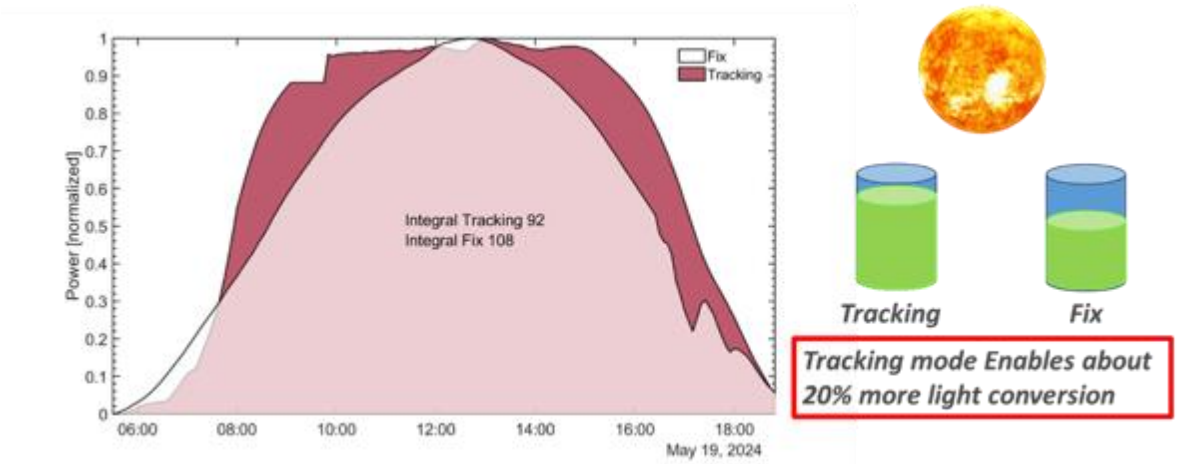

Figure 18. Power conversion in tracking vs no tracking mode in two different days with similar irradiance.

Figure 15 illustrates the comparative view between the agrivoltaic systems at Circeo and AZ sites, including microclimate and energy production. This comparison shows that while AZ site has relative higher energy production due to better plastic cover transparency and the higher global light intensity conditions, the efficiency of light conversion to energy is about 85% of that in Circeo.

Funded by the European Union under Grant Agreement No 101096056. Views and opinions expressed are however those of the author(s) only and do not necessarily reflect those of the European Union or CINEA. Neither the European Union nor the granting authority can be held responsible for them.

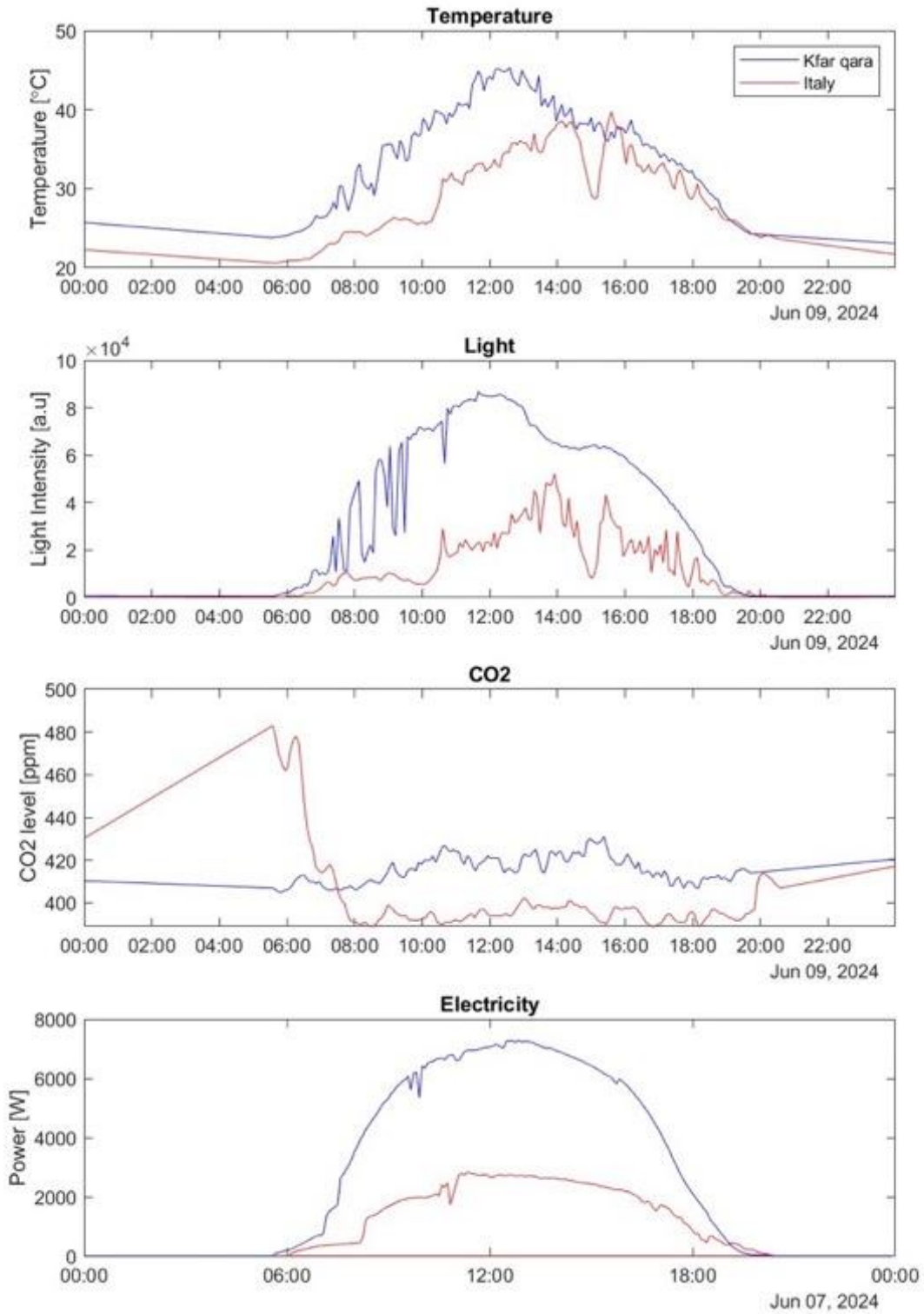

Figure 19. The comparative view between agrivoltaics systems in Circeo and AZ including microclimate and energy production. The Energy production per KWp in AZ vs Circeo is about 72% in favor AZ, due to the intensity of radiation, type of the plastic cover and greenhouse orientation.

Seasonal Dependence

Funded by the European Union under Grant Agreement No 101096056. Views and opinions expressed are however those of the author(s) only and do not necessarily reflect those of the European Union or CINEA. Neither the European Union nor the granting authority can be held responsible for them.

The effectiveness of tracking systems is also season dependent. During the winter months, when the sun's path is lower in the sky, tracking systems are particularly beneficial in maximizing sunlight exposure. Conversely, during the summer months, when there is naturally more sunlight, the relative gain from tracking systems is still significant but slightly reduced due to increasing the panel temperature. This seasonality is crucial for understanding the performance dynamics of PV systems in agrivoltaics applications and for planning energy management strategies.

General Summary

The increasing trend in energy production observed at Circeo site from February to April 2024 highlights the impact of seasonal changes on PV system performance. The comparison with AZ site demonstrates how different environmental and structural factors, such as the type of plastic cover, global light intensity and the orientation of the greenhouse, can influence overall energy production. The inclusion of tracking systems further enhances energy production by over 20%, emphasizing the importance of dynamic systems in maximizing efficiency. Moving forward, detailed analysis of sensor data from all sites will be conducted to assess the performance of the PV systems and their impact on the greenhouse microclimate and crop growth.

This analysis will include comparative analysis of different sites, temporal analysis to understand diurnal and seasonal patterns, and evaluation of the PV systems' impact on the greenhouse environment and crop growth. The goal is to develop strategies to optimize the PV system performance and greenhouse conditions, enhancing energy efficiency and crop productivity. By conducting this comprehensive analysis, we aim to gain a deeper understanding of the interactions between the PV systems, greenhouse environment, and crop growth, refining the design and operation of agrivoltaics systems to achieve optimal performance and sustainability.

Overall Summary

The REGACE project aims to integrate advanced photovoltaic (PV) technologies with greenhouse systems to optimize energy production, crop yield, and environmental control. This report has provided a comprehensive analysis of the microclimate conditions and system performance across various installation sites, including AZ, Circeo, Humboldt, Watzkendorf and Buko.

Key findings include:

1. **Light Distribution**: The sun radiation simulation using COMSOL demonstrated effective light diffusion across the tunnel greenhouse, ensuring consistent light for optimal plant growth. Light distribution patterns observed in Kfar Qare' and Italy, supported by sensor data, indicate adequate light levels for plant growth even under PV panels.
2. **Temperature Distribution**: Thermal images and sensor data revealed significant temperature variations within the greenhouses. PV panels contribute to higher temperatures in their vicinity, particularly in the upper regions of the greenhouse. This heating effect creates a gradient where the air near the panels is hotter, and the air near the ground is cooler. In greenhouses without PV panels, the temperature distribution is more uniform.

Funded by the European Union under Grant Agreement No 101096056. Views and opinions expressed are however those of the author(s) only and do not necessarily reflect those of the European Union or CINEA. Neither the European Union nor the granting authority can be held responsible for them.

3. **CO2 Concentration**: At the Kfar Qare' site, increased light intensity correlates with higher CO2 levels, with oscillations influenced by shading from the PV panels. In contrast, the Italy site maintains stable CO2 levels around 400 ppm due to its open greenhouse structure. Other sites showed CO2 levels rising up to 450 ppm in enclosed environments.
4. **Power Production**: The data from the Italy site showed an increasing trend in energy production due to seasonal changes. Comparing power production between Italy and Kfar Qare', the latter had higher overall energy production due to more panels and better light conditions. Tracking systems, which increase energy production by more than 20%, were also highlighted for their efficiency, especially in different seasons.

Conclusion

This report underscores the importance of understanding the interactions between PV systems, greenhouse environments, and crop growth. The detailed analysis of light distribution, temperature variations, CO2 levels, and power production across multiple sites provides valuable insights into optimizing greenhouse conditions and PV system performance.

Moving forward, the REGACE project will continue to analyze sensor data from all sites to refine strategies for enhancing energy efficiency and crop productivity. This comprehensive analysis will include comparative analysis of different sites, temporal analysis to understand diurnal and seasonal patterns, and evaluation of the PV systems' impact on the greenhouse environment and crop growth. The goal is to develop strategies to optimize the PV system performance and greenhouse conditions, contributing to the development of sustainable and efficient agrivoltaic systems.

By conducting this ongoing research and analysis, the REGACE project aims to advance the integration of renewable energy technologies in agriculture, promoting sustainability and higher yields in agrivoltaic systems.

Funded by the European Union under Grant Agreement No 101096056. Views and opinions expressed are however those of the author(s) only and do not necessarily reflect those of the European Union or CINEA. Neither the European Union nor the granting authority can be held responsible for them.

Task 4.1 Dynamic modelling of the greenhouse microclimate and energy demand

Introduction

This deliverable marks the halfway point of Task 4.1 within Work Package (WP) 4, focusing on the dynamic modeling of greenhouse microclimates and energy demand. The primary objective of this task is to build a dynamic model of greenhouses using advanced software for Dynamic Building Simulation (DBS), considering plant interaction with the environment. DBS is a powerful tool for estimating trends in indoor environmental variables and energy demand as climatic conditions change and as a function of the building envelope characteristics. Although greenhouses can be simulated in dynamic conditions like buildings, their thermal field is influenced by additional physical processes, such as plant growth and water use, which must be accurately represented within the model.

The progress made so far is in line with the project's timeline, with significant advancements in developing and refining the dynamic model. The model has been calibrated and validated using data provided by the monitoring activities of WP 3, enhancing our understanding of the thermo-hygrometric behaviour of the greenhouse system and allowing for precise evaluation of its energy demand. The pilot greenhouse, where the model was applied, belongs to the University of Thessaly (UTH) and is located in Central Greece. It consists of six independent chambers used for various cultivations, each equipped with advanced systems for microclimate control, including continuous roof vents, cooling systems, central heating, and thermal/shading screens. These systems are essential for maintaining optimal growing conditions and ensuring efficient energy use.

A critical aspect of our approach involves improving the IDA Indoor Climate and Energy (IDA ICE) software's capability to simulate the microclimate inside a greenhouse by implementing the evapotranspiration equations directly into the energy balance of the thermal zone of the tool. This new custom zone accounts for the hygrothermal interaction of the plants with the greenhouse's microclimate. The progress made in this area is crucial for developing a reliable Digital Twin (DT) of the greenhouse system, which will be instrumental in better understanding the physics behind greenhouse operations and optimizing their performance.

At this halfway point, the work done so far aligns with the project's planned activities and milestones, setting a strong foundation for the subsequent phases. The integration of the dynamic model with data from WP 3 and the enhancements to the simulation software ensure that we are on track to meet the final objectives of WP 4. Moving forward, the focus will be on further refining the model, integrating additional data, and validating the outputs to ensure the comprehensive and accurate simulation of greenhouse microclimates and energy demand. This progress underscores the critical role of Task 4.1 in achieving the overall goals of Work Package 4 and the broader project.

Funded by the European Union under Grant Agreement No 101096056. Views and opinions expressed are however those of the author(s) only and do not necessarily reflect those of the European Union or CINEA. Neither the European Union nor the granting authority can be held responsible for them.

Simulation of energy properties of the greenhouse

Introduction

In the face of escalating global challenges such as climate change, resource depletion, and increasing population demand, there is an urgent need to develop innovative and sustainable solutions in agriculture. One promising avenue is Agri-Photovoltaics (Agri-PV), which has emerged as a viable approach to optimize land use by combining solar energy harvesting with agricultural activities (Dinesh and Pearce 2016; Schweiger and Pataczek 2023). Greenhouses (GHs) provide a controlled environment for optimizing crop growth, extending growing seasons, and protecting plants from adverse weather conditions. The integration of photovoltaic (PV) technology within greenhouse structures represents a progressive step toward achieving sustainability and energy efficiency in agricultural practices. In this framework, the project REGACE (www.regaceproject.com), funded by Horizon Europe will develop and validate a disruptive innovative technology to generate renewable electricity in greenhouses in all seasons of the year to enable the constant production of food without energy limitations.

In the last 20 years, several studies have been focused on different aspects of energy optimization in greenhouse production (Rodríguez et al. 2015). Either the focus has been on the introduction of new technologies, e.g., infrastructure (glass and screen types), light-emitting diodes, or other types of equipment. Various projects have focused on the development of various IT and decision support systems for improved climate control that balances optimal photosynthesis and plant growth (or transpiration) with energy consumption and cost (Zhang et al. 2020).
However, there is a lack of correlation between morphological plant development, optimization of energy consumption, and production. In greenhouses, energy optimization, product flow, and artificial climate are currently operated as three separate systems. In practice, these systems are undoubtedly interconnected in greenhouse production. The REGACE approach aims to create a DT ecosystem, REGACE DT that integrates crop production, PV production, and microclimate modelling with the final objective of integrating these aspects using Artificial Intelligence techniques.

The main goal of the work here presented is to build a dynamic model of the greenhouse using an advanced software for DBS taking into account the plant interaction with the environment. DBS is a powerful means of estimating trends in indoor environmental variables and energy demand as climatic conditions change and as a function of the building envelope characteristics. The greenhouse, being an enclosed space, can be assimilated to a building and as such can be simulated in dynamic conditions using the tools that are commonly used for building simulation. The thermal field inside the greenhouse, however, is also affected by a number of physical processes such as plant growth and water use that must be properly considered within the dynamic model (Baglivo et al. 2020; Ouazzani Chahidi et al. 2021).

In the current discourse of greenhouse optimization, various researchers have dedicated efforts to study structural configurations, ventilation systems, and the implications of evapotranspiration on environmental parameters such as temperature

Funded by the European Union under Grant Agreement No 101096056. Views and opinions expressed are however those of the author(s) only and do not necessarily reflect those of the European Union or CINEA. Neither the European Union nor the granting authority can be held responsible for them.

and humidity. Stanciu et al. (Stanciu, Stanciu, and Dobrovicescu 2016) provided insight into the thermal dynamics within a polyethylene greenhouse, analysing the effects of different orientations and ventilation regimes in seasonal extremes of Bucharest (Romania), emphasizing the role of evapotranspiration. Similarly, (Abdel-Ghany and Kozai 2006) evaluated a small glass greenhouse in Tokyo, Japan, focusing on temperature and humidity fluctuations during a short summer period, highlighting evapotranspiration's significant impact.

In contrast, (Mobtaker et al. 2019) prioritized the study of thermal transmittance through different glass roof shapes and orientations in Tabriz, Iran, without considering evapotranspiration or ventilation systems. Similarly (Singh, Singh, and Singh 2018) modelled a large greenhouse in Punjab, India, with a double gothic arch structure, integrating natural ventilation and a thorough analysis of evapotranspiration's comprehensive impact using Matlab-Simulink.
(Fitz-Rodríguez et al. 2010) have developed a variable model applicable to various U.S. locations, considering different heights and roof shapes of greenhouses, including the effects of material selection, evapotranspiration, and integrated heating/cooling systems.

Innovation in greenhouse energy sustainability was represented by (Ouazzani Chahidi et al. 2021), who simulated a glass-covered greenhouse integrated with PV panels and a geothermal pump in Albania, focusing on internal temperature regulation, energy efficiency, and solar energy utilization.
(Baglivo et al. 2020) employed TRNSYS software for a detailed simulation of a greenhouse in Crotone, Italy, taking into account plant evapotranspiration, natural ventilation, and temperature control systems, presenting data over varying time scales.

This software's versatility was further echoed in the studies of (Opeyemi Ogunlowo et al. 2023) and (Brækken et al. 2023), who employed TRNSYS and IDA ICE for dynamic greenhouse modelling, examining the influence of structural designs, climatic conditions, and operational systems on yearly temperature, humidity, and energy patterns.

In our approach we aim to improve the capability of the software IDA ICE to simulate the microclimate inside a greenhouse by implementing the evapotranspiration equations directly into the energy balance of the thermal zone of the tool. In this way, we create a new custom zone that could take into account for the hygrothermal interaction of the plants with the greenhouses microclimate. The findings of our work will be used to better understand the physics behind the greenhouse system and together with data gathered in the pilot will contribute to the development of a reliable DT of the system.

Funded by the European Union under Grant Agreement No 101096056. Views and opinions expressed are however those of the author(s) only and do not necessarily reflect those of the European Union or CINEA. Neither the European Union nor the granting authority can be held responsible for them.

Pilot greenhouse description

The pilot greenhouse, where the model of University of Rome Tor Vergata (UR) was applied, belongs to UTH and it is located in Central Greece (on the coastal area of Eastern Thessaly) near to Volos with latitude of 39.22 °N, longitude of 22.44 °E, and altitude of 85 m, as pointed in Figure 1.

Figure 1. Location of UTH pilot greenhouse, Greece

Geometry

The pilot greenhouse consists of six independent chambers with NE-SW orientation, as presented in Figure 2. The greenhouse ground area is 1440 m^2 and the cultivated area is 800 m^2.

Funded by the European Union under Grant Agreement No 101096056. Views and opinions expressed are however those of the author(s) only and do not necessarily reflect those of the European Union or CINEA. Neither the European Union nor the granting authority can be held responsible for them.

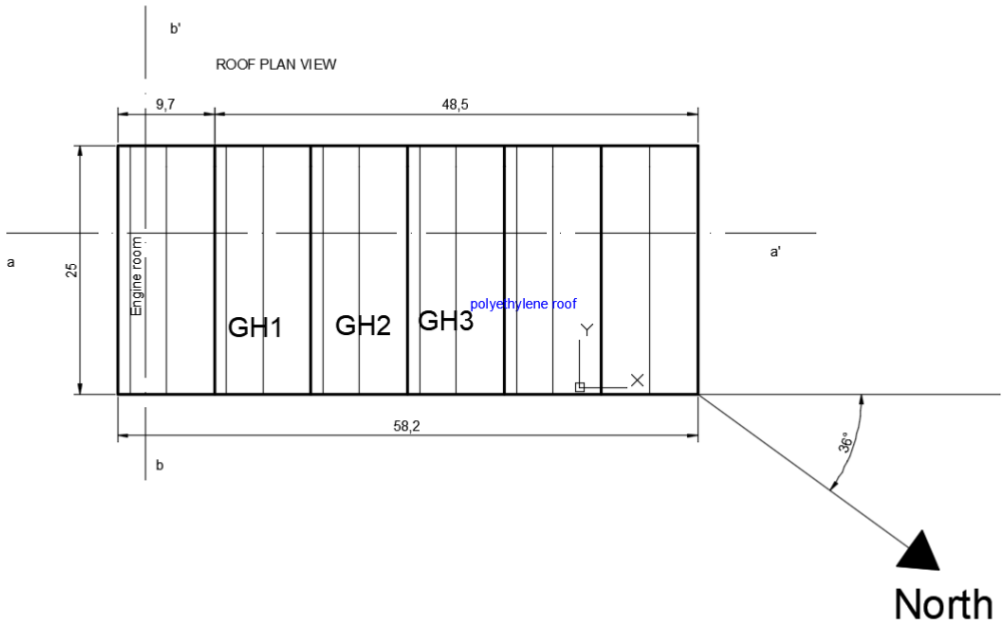

Figure 2. Plan and orientation of pilot greenhouse; all the dimensions are in meters.

The first chamber is the engine room, while the other five chambers are identical and used for various cultivations. The dimensions are introduced in Figure 2, and based on that, each chamber is 9.6 meters wide and 25 meters long. Moreover, the greenhouse has a gothic shape roof with a gutter height of 5.0 m and ridge height of 7.35 m, as presented in Figure 3.

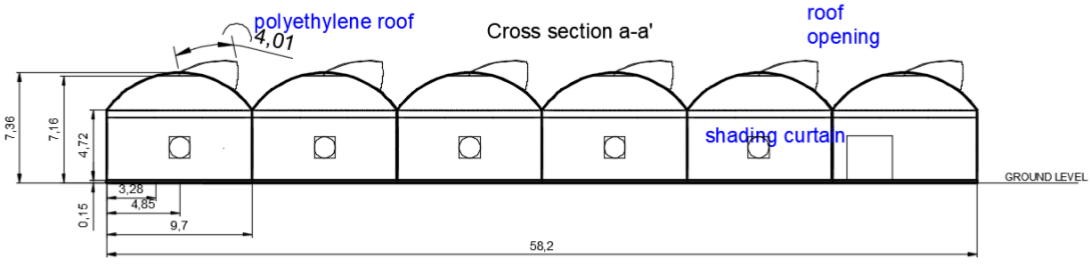

Figure 3. Greenhouse's cross-section a-a' shown in Figure 2

Materials

The side walls of the greenhouse are covered by corrugated polycarbonate sheets (thickness of 0.08 cm) while the roof is covered by polyethylene films (thickness of 180 μm, light transmission of 93%). Polycarbonate sheets are also used to cover the internal side walls between the six spans. Furthermore, the floor is covered partly by concrete and partly by geotextile.

Crops

Funded by the European Union under Grant Agreement No 101096056. Views and opinions expressed are however those of the author(s) only and do not necessarily reflect those of the European Union or CINEA. Neither the European Union nor the granting authority can be held responsible for them.

Each greenhouse compartment is equipped with six hydroponic gutters of 20 m each located 0.5 m above the ground in a distance of 1.6 m between each others, holding 19 perlite slabs of 35 L each (average substrate water content of 25-30%) the substrates used for rooting/cultivation of the crop. A drip irrigation system was also used for the crop fertigation needs with 5 drippers per slab. Additionally, the crops in chambers were:

- The chambers GH1 and GH2 from March to November had tomato crops.
- The chambers GH3 and GH4 from March to November had leafy vegetables.

Electromechanical equipment for microclimate control

Each greenhouse compartment is equipped with:

a) A continuous roof vent
b) A cooling system consisting of a cellulose paper evaporative pad (15 cm thick, 9.6 m width/per chamber and 2.0 m height) and an exhaust fan (diameter 1.4 m, capacity of 35 000 m^3/h, 1.1 kW) for tunnel operation. The evaporative pads are served by a water pump of 2.2 kW and a DC motor of 0.37 kW.
c) A central heating system consisting of: (i) A heat generation system (an oil boiler for all the five chambers) of 291.4 kW with 80% heating efficiency, located in engineering room, (ii) A distribution system consisting of a circular pipe PR-P Φ70, and (iii) A heat emission system by a pipe rail (12 metallic pipes of 5.1 cm diameter in each chamber) with max pipe temperature set at 60 °C (the hot water leaves the boiler at 70 ºC and returns at 50 ºC). The heat distribution system is supported by a circulator of 0.87 kW and the water rate is 18 m^3/h (3.6 m^3/h per chamber).
d) A thermal/shading screen with the light transmission of about 50% and energy saving of 60%.

The crop gutters and the heating, ventilation and cooling systems are indicatively presented in the plan view and the cross-section of chamber GH1 in Figures 4 and 5, respectively. In Figure 6, a picture of the GH1 interior is given with the heat distribution system.

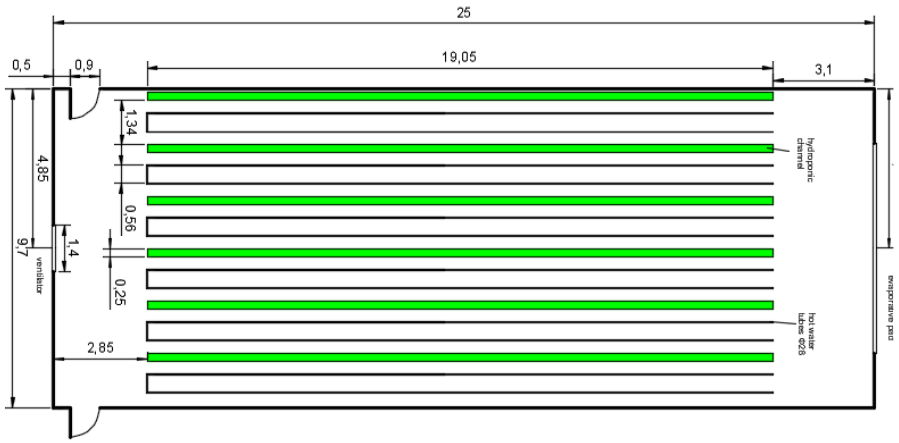

Figure 4. Plan view of GH1; all dimensions are in meters.

Funded by the European Union under Grant Agreement No 101096056. Views and opinions expressed are however those of the author(s) only and do not necessarily reflect those of the European Union or CINEA. Neither the European Union nor the granting authority can be held responsible for them.

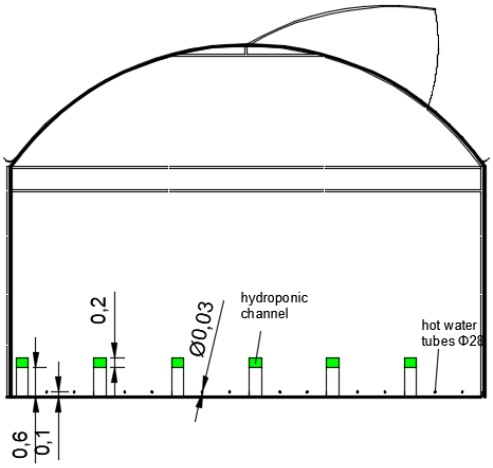

Figure 5. Cross section of GH1

Production electromechanical equipment for microclimate control

Apart from the equipment used for the internal microclimate control, the greenhouse is also served by production equipment, located either inside the chambers, or in the engine room, or outside the greenhouse: a) A drilling pump of 35 kW and 160 m head, b) Two irrigation pumps of 1.91 kW, with 46 m head and 14 m^3/h water flow, and c) Eight fertigation pumps of 0.83 kW, 38 m head and 2.5 m^3/h flow rate.

Available measurements

The available measurements concern the following parameters of external and internal microclimate of GH 1. The measurements cover the all the 2020 year with 15-minute averaged values.

External microclimate

- Outdoor air temperature [^{o}C]
- Outdoor air Relative humidity [%]
- Total radiation [W/m^2]
- Daily total irradiance [J/m^2]
- Precipitation [mm]
- External air wind velocity [m/s]
- External air wind direction [grd]

Internal microclimate

- Air temperature inside GH 1 [^{o}C]
- Relative humidity inside GH 1 [%]
- Column L: Ventilation windows percentage opening [%]

Funded by the European Union under Grant Agreement No 101096056. Views and opinions expressed are however those of the author(s) only and do not necessarily reflect those of the European Union or CINEA. Neither the European Union nor the granting authority can be held responsible for them.

Figure 6. Heat distribution system

Greenhouse operational characteristics (set points)

The design day temperature (the temperature inside the greenhouse be ideally maintained during the day) is 23 ºC and the design night temperature is 17 ºC. The design relative humidity is also 75 – 85%. The operational strategy during the measurement period can be summarized as following:

- The roof vent opens when (there is "or" between conditions):
  - The greenhouse air temperature exceeds 21ºC during the day and 18 ºC during the night
  - The greenhouse air relative humidity exceeds 95% during the day and 87% during the night (The maximum vent opening for dehumidification of 10%).
- The evaporative pad cooling system operates when the air temperature exceeds 25 ºC.
- The heating system operates so to maintain a greenhouse air temperature of 18 ºC during the day and 14 ºC during the night.
- The thermal/shading screen closes whenever (There is "or" between conditions):
  - The outside temperature drops two degrees below the heating set point
  - The outside solar radiation exceeded 750 W/m^2.

Funded by the European Union under Grant Agreement No 101096056. Views and opinions expressed are however those of the author(s) only and do not necessarily reflect those of the European Union or CINEA. Neither the European Union nor the granting authority can be held responsible for them.

Pilot greenhouse description

The approach consists of the construction of a DBS model in the IDA ICE 4.8 (Sahlin et al. 2003) for environment of one of the five pilot greenhouses of the REGACE project. The objective is to reproduce the indoor microclimate also considering the evapotranspiration process due to the presence of crops. Evapotranspiration is a combined mechanism that comprises the loss of water from the soil both by evaporation from the soil surface and by transpiration from the leaves of the plants through their stomas.

In order to take into account for this mechanism in the greenhouse simulation, the regular thermal zone model implemented in the software has been modified integrating the heat and moisture balance equations with the evapotranspiration model of Penman-Monteith (Monteith 1965).

Fig. 1: Aerial and front view of the pilot greenhouses from Google Maps

The simulations were performed for a six-span N-S oriented gothic arch greenhouse, located in UTH near Volos (Latitude of 39.22 °N, Longitude of 22.44 °E, and altitude of 85 m), on the coastal area of Eastern Greece. According to the Köppen-Geiger classification, the prevailing climate in this region is categorized as Csa (Hot-summer Mediterranean climate).

The external environmental data were obtained through on-site measurements (referred to year 2020). These data include parameters such as temperature, humidity, radiation, wind speed and direction, and rainfall. The internal measurements of temperature and humidity within the six zones at ground level were also recorded. Table 1 shows type of main sensors, accuracy and scan rate.

Table 1 – Characteristics of the sensors installed outside and inside the greenhouses in Volos

Variable	Type	Accuracy	Scan rate
Temperature	PT100	0.1 °C	15 min

Funded by the European Union under Grant Agreement No 101096056. Views and opinions expressed are however those of the author(s) only and do not necessarily reflect those of the European Union or CINEA. Neither the European Union nor the granting authority can be held responsible for them.

Relative Humidity	Capacity	±3%	15 min
Solar irradiance	Thermopile	±10 W/m²	15 min

A critical aspect of this study involved decomposing measured global solar irradiance into the direct and diffuse components as requested by the IDA ICE local climate file ingested by the model. We used the decomposition model by Erbs implemented in PVLib (Jensen et al. 2023) collaborative platform for PV simulation to calculate direct normal irradiance (DNI) and diffuse horizontal irradiance (DHI) based on global horizontal irradiance (GHI), zenith angle, and day of the year.

IDA-ICE modelling of the greenhouse

The GH geometry and materials together with the evaporative cooling system have been implemented in IDA ICE 4.8 (Fig. 2) and the regular thermal zone has been replaced with a new custom zone that considers the evapotranspiration mechanism. Table 2 shows the main thermal properties of the GH cover (polycarbonate for the side walls and polyethylene for the roof).
IDA ICE provides direct and indirect evaporative cooling system in its environment. Suitable modifications have been applied to the components to fit the specifications of the real fan-pad (only direct evaporative cooling).

This component was developed to closely mimic the system's functionality. Observations from the simulation revealed that the air exiting the pad was cooler compared to the incoming air, particularly during periods of high summer temperatures.

Table 2 – Thermal properties of the GH envelope

TYPE	g	Tsol	Tvis	Uw (W/m²K)
Polycarbonate Corrugated	0.773	0.631	0.636	2.527
Polyethylene	0.830	0.771	0.884	5.299

Additionally, the trends in absolute humidity showed an increase when there was a divergence in temperatures, indicating the effective operation of the fan and pad setup. Furthermore, in the testing greenhouse, a Natural Ventilation and Temperature Control system was implemented. Natural ventilation was facilitated by opening windows located on the roof of each zone. As a first attempt the temperature setpoint for windows opening has been set at 20°C

In the simulation of shading, an integrated window shading approach was adopted for all the roof windows. The control of the shading curtains was based on the measurements of global radiation components, specifically DNI and DHI.

Funded by the European Union under Grant Agreement No 101096056. Views and opinions expressed are however those of the author(s) only and do not necessarily reflect those of the European Union or CINEA. Neither the European Union nor the granting authority can be held responsible for them.

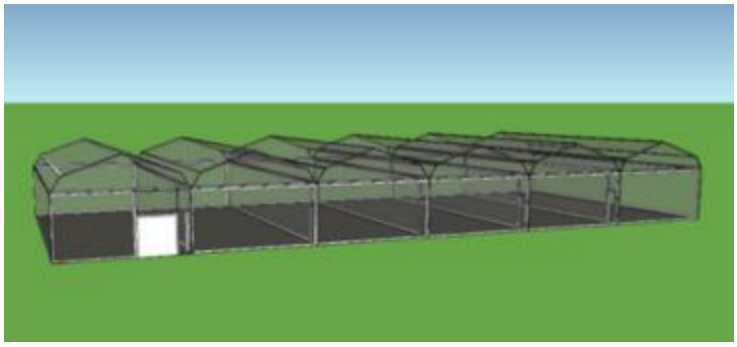

Fig. 2: IDA ICE greenhouse representation

Evapotranspiration due to plants

In order to take into account the plants evapotranspiration in the greenhouses we develop a tool within IDA-ICE 4.8. For doing that, we have designed a custom zone within DBS software that considers the crop evapotranspiration process. This is modelled as proposed in (Katsoulas and Stanghellini 2019). In particular, the Penman-Monteith equation is used to compute the evapotranspiration mass flow, $\dot{m}_{ET_0}$ (in $kg\ s^{-1}$) (Monteith 1965):

$$\dot{m}_{ET_0} = A_c \frac{\Delta R_n + \rho C_p D_i g_a}{\lambda \left[\Delta + \gamma \left(1 + \frac{g_a}{g_c} \right) \right]} \quad (1)$$

where R_n is the net radiation intercepted by the crop (Wm^{-2}), D_i is the vapor deficit of the air (kPa), g_a and g_c are the crop aerodynamic and stomatal conductances (ms^{-1}), Δ is the slope of the saturation vapor pressure-temperature relationship ($kPa\ K^{-1}$), γ is the psychrometric constant ($kPa\ K^{-1}$), A_c is the crop area (m^2), and ρ, C_p, λ are the air density (kgm^{-3}), specific heat capacity ($J\ kg^{-1}K^{-1}$) and latent heat of vaporization ($J\ Kg^{-1}$). In the zonal model, the aerodynamic and stomatal conductances (g_a, g_c) are assumed to be constant and must be provided by the user. On the other hand, Δ is computed as:

$$\Delta = \frac{4098 P_{v,sat}}{(T + 237.3)^2} \quad (2)$$

with T and $P_{v,sat}$ being the air temperature (°C) and the saturation vapor pressure (kPa).

Following (Katsoulas and Stanghellini 2019), the intercepted net radiation is modelled as:

$$R_n = a\left(1 - e^{-k_s LAI}\right) R_s \quad (3)$$

where R_s is the solar radiation per unit area (Wm^{-2}), a is an empirical constant (indicating the fraction of net radiation absorbed by the crops), k_s is the extinction coefficient for shortwave radiation, and LAI is the leaf area index. In the zonal model, the coefficients a and k_s are set to 0.86 and 0.7. In addition, the solar radiation R_s is calculated as the shortwave radiation reaching the floor divided by its area (since the crops are assumed to be at the ground level). Moreover, the leaf area index is multiplied by a "schedule factor" in IDA ICE, since LAI is not constant throughout the year.

Finally, the latent power related to the evapotranspiration mass flow is calculated as in (Baglivo et al. 2020):

$$P_{ET} = \dot{m}_{ET_0} \left(\lambda + C_{p,v} T \right) \quad (4)$$

($C_{p,v}$ is the specific heat capacity of the vapor, $J\ kg^{-1}K^{-1}$).

Funded by the European Union under Grant Agreement No 101096056. Views and opinions expressed are however those of the author(s) only and do not necessarily reflect those of the European Union or CINEA. Neither the European Union nor the granting authority can be held responsible for them.

In the zonal model, the evapotranspiration mass flow is added to the humidity balance equation:

$$\rho V \frac{dW}{dt} = F_{occ} + F_{eqp} + F_{lks} + F_{trm} + F_{lu} + \dot{m}_{ET_0} \qquad (5)$$

where W is the vapor fraction, V is the zone volume, F_{occ} is the vapor flow due to occupants, F_{eqp} and F_{lu} are the vapor flows due to equipment and local units, F_{lks} and F_{trm} are the vapor flows through leaks and air terminals.
On the other hand, the latent evapotranspiration power is included as a sink term in the energy balance equation:

$$\rho V \left(C_p + W C_{p,v}\right) \frac{dT}{dt} + \rho V \lambda \frac{dW}{dt} = \dot{Q}_{occ} + \\ + \dot{Q}_{eqp} + \dot{Q}_{lu} + \dot{Q}_{cv,srf} + \dot{Q}_{cv,lt} + \dot{Q}_{dv} + \dot{Q}_{lks} + \\ + \dot{Q}_{trm} + \dot{Q}_{Loss} - P_{ET} \qquad (6)$$

where $\dot{Q}_{occ}$, $\dot{Q}_{eqp}$ and $\dot{Q}_{lu}$ are the heat flows from occupants, equipment, and local units (both convective and latent contributions), $\dot{Q}_{cv,lt}$ and $\dot{Q}_{dv}$ are the convective heat flows due to lights and convective devices, $\dot{Q}_{lks}$ and $\dot{Q}_{trm}$ are the heat flows due to leaks and terminals, $\dot{Q}_{cv,srf}$ are the convective heat flows at the surfaces, and $\dot{Q}_{Loss}$ are the heat losses to the zone. In this study the simulation was carried out for the most critical summer season with a variable simulation time step with maximal time step of 1.5 hours and an output time step of 1 hour.

Results

The GH model has been built and then, the initial tests on the model functionality have been carried out. A first preliminary validation with the available microclimate data is presented in this report. We focused on the first greenhouse (GH1) cultivated with tomatoes.

Annual Trends of Temperature and Relative Humidity as Affected by Different Cooling Systems

This section presents the outcomes of year-long simulations conducted on the greenhouse model, focusing on GH1 zone while exploring different cooling system configurations. By sequentially implementing various cooling systems, the aim is to illustrate how temperature and relative humidity align with the measured values as the complexity of the cooling systems increases.

The simulation sequences are as follows:

- Initial simulation without any cooling system.
- Simulation with ventilation and window opening control set at 20°C.
- Simulation adding shading to the ventilation setup.
- Simulation incorporating evaporative cooling alongside ventilation and shading.
- Simulation involving ventilation, shading, evaporative cooling, and integrating evapotranspiration theory with minimal crop size.
- Further simulation with ventilation, shading, evaporative cooling, and evapotranspiration theory applied with maximal crop size.

Funded by the European Union under Grant Agreement No 101096056. Views and opinions expressed are however those of the author(s) only and do not necessarily reflect those of the European Union or CINEA. Neither the European Union nor the granting authority can be held responsible for them.

This systematic approach in introducing cooling systems in the simulations provides a deep insight into the impact of each addition on the internal greenhouse climate. Starting from a scenario where neither active nor passive cooling was utilized, the initial simulations were based on the climatic data from the Volos climate file and the greenhouse's geometric model. The temperatures remained below 40°C during the coldest months, but a notable increase was observed from late March to early October, attributed to the substantial incident radiation on the greenhouse covering, leading to an intensified greenhouse effect. Notably, temperatures exceeding 60°C were frequent during the summer months, which severely impacts crop viability.

Although the introduction of a controlled shading system, which affects both direct and diffused radiation, results in a reduction in temperature, this change is not immediately evident from the temporal temperature trend. Furthermore, with the addition of evaporative cooling, an additional 2-5°C reduction in temperature is achieved.

The evaporative cooling system operates continuously throughout the day. The relatively minor variations in temperature and relative humidity can be attributed to changes within the evaporative cooling system. These observations confirm the operation of the evaporative cooling system, although it should be noted that the use of default values and the incremental approach detailed in this study may limit the results to some extent.

Additionally, the subsequent implementation of evapotranspiration into the model introduces the physical presence of crops within the greenhouse system, thereby fundamentally altering the interactions among various internal thermal flows. In the absence of crops, the thermal power reaching the ground is partly exchanged through conduction to deeper layers and partly transmitted through convection towards the internal air and radiation, resulting in increased sensible heat and subsequent temperature rise. However, with the presence of crops, a portion of the available sensible heat is utilized as latent heat for water vapor formation, released into the internal air from the plants and soil. Consequently, the internal air temperature is expected to decrease while humidity rises, with variations largely dependent on the size of the plants. Initially, a model representing the plants during their early growth stage, where their impact on internal temperature and relative humidity variation is minimal, was implemented (LAI = 1).

As final step we added the evapotranspiration model into the simulation dynamics, focusing on how this influences internal air conditions such as temperature and relative humidity. Analysis of the internal temperature trends during hot summer months (Fig. 3) revealed a decrease in temperature up to 20-35°C accompanied by increasing humidity levels (exceeding 50%) as plants grow (LAI = 4).

These fluctuations align with the maximum and minimum evapotranspiration rates. Monthly average analyses revealed temperature decreases from non-cooled to the maximum evapotranspiration cases in warmer months, while relative humidity showed an opposite trend, increasing with cooling system complexity during hot periods.

Funded by the European Union under Grant Agreement No 101096056. Views and opinions expressed are however those of the author(s) only and do not necessarily reflect those of the European Union or CINEA. Neither the European Union nor the granting authority can be held responsible for them.

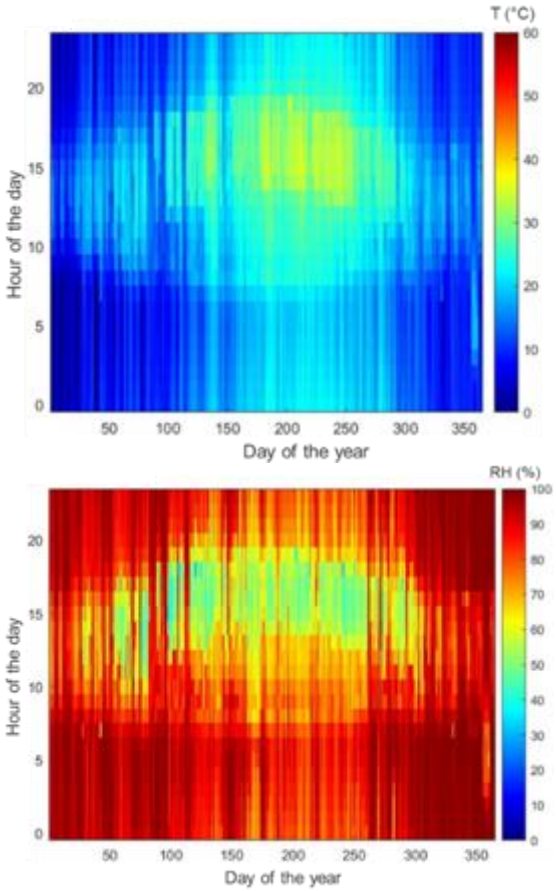

Fig. 3: Carpet plot for yearly values of greenhouse internal temperature and relative humidity with ventilation, shading, evaporative cooling and maximum evapotranspiration (LAI = 4).

Daily Trends of Temperature and Relative Humidity Inside the Greenhouse

Results from the daily variability shows that the most substantial deviations in measured values typically occurred during the months of July and August, between 3:00 PM and 7:00 PM or 8:00 PM on the same day, with deviations averaging up to 6°C for temperature and 20% for relative humidity. Fig. 4 shows the first ten days of June, where, on the contrary, the agreement with the measured values is fairly good.

In this case, the maximum evapotranspiration (LAI = 4) was considered. Despite the abovementioned variations, the introduction of cooling systems brought about significant daily enhancements in both thermal conditions and humidity levels compared to scenarios with no cooling in place. Among the systems analysed, natural ventilation, shading, and the natural variability in crop size through evapotranspiration emerged as key contributors to the improvement of the internal greenhouse climate.

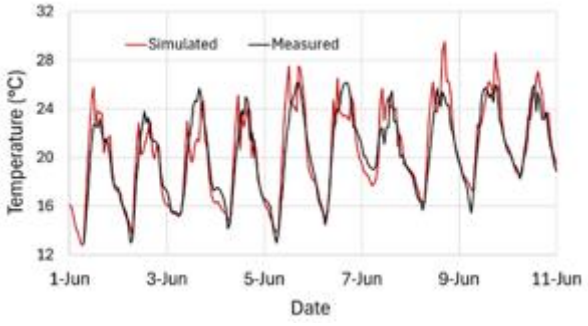

Funded by the European Union under Grant Agreement No 101096056. Views and opinions expressed are however those of the author(s) only and do not necessarily reflect those of the European Union or CINEA. Neither the European Union nor the granting authority can be held responsible for them.

Fig. 4: The first 10 days of comparison in June between simulated internal temperature of the greenhouse with ventilation, shading, evaporative cooling and maximum evapotranspiration (LAI = 4) and the measured temperature

While natural ventilation exhibited high efficiency, it showed limitations in maintaining optimal relative humidity levels between 11:00 AM and 3:00 PM, prompting evaporative cooling and other complementary systems to become notably effective during this period, establishing an optimal synergy among multiple subsystems.

Comparison between GH1 and the Area without Crops

In the study, comparisons were made among greenhouse conditions featuring different cooling systems in the presence of crops (GH1) and an area without plants (Zone 1). The analysis aimed to emphasize the role of evapotranspiration in greenhouses and its impact on overall cooling effectiveness. Initially, a scenario was considered where all cooling systems were active but with minimal evapotranspiration (LAI = 1). It was observed that in winter, the temperature deviation between Zone 1 and GH1 was minor, but this difference became more pronounced in the warmer months due to the increased radiation and enhanced evapotranspiration effects. Subsequent simulations with the maximum evapotranspiration (LAI = 4) revealed significant deviations in temperatures during the summer, with GH1 showing up to a 10°C advantage due to the cooling effect of evapotranspiration.
Further comparisons of measured and simulated temperature and humidity trends for all greenhouse zones, particularly in July, highlighted the influence of shading effects on different zones relative to the sun's position.

Conclusion

In this study, we developed a dynamic greenhouse simulation model using the IDA ICE software, to simulate a greenhouse located near Volos, Greece.
The findings from our simulations revealed differences between the model-predicted internal temperatures and humidity levels and those recorded in the greenhouse in the real case. These discrepancies became more pronounced as the external temperatures increased. Despite these discrepancies, the installed cooling systems were effective in significantly mitigating these differences. For instance, in the absence of cooling measures, the internal temperatures could reach up to 70°C, which were reduced to approximately 30-35°C with cooling interventions. Similarly, the minimum relative humidity levels were observed to increase from 10% to a range of 50-60% due to the cooling systems.

A notable challenge encountered in the model pertained to accurately simulating conditions between 3:00 and 7-8:00 pm during summer days. This issue was primarily attributed to the assumptions made regarding the physical properties and placement of shading curtains. These curtains are strategically placed between the greenhouse's upper and lower sections to optimize shading. However, for simplicity and due to the constraints of the simulation software, the model treated these shading elements as if they were fully integrated within the structure. Additionally, the lack of precise data on evaporative cooling led to the reliance on default software values, further contributing to the discrepancies observed. This study underscores the importance of

Funded by the European Union under Grant Agreement No 101096056. Views and opinions expressed are however those of the author(s) only and do not necessarily reflect those of the European Union or CINEA. Neither the European Union nor the granting authority can be held responsible for them.

accurate data and the need for refinement in simulation models to closely mimic real-world conditions.

References

Abdel-Ghany, Ahmed M., and Toyoki Kozai. 2006. "Dynamic Modeling of the Environment in a Naturally Ventilated, Fog-Cooled Greenhouse." Renewable Energy 31 (10): 1521–39. https://doi.org/10.1016/j.renene.2005.07.013.

Baglivo, Cristina, Domenico Mazzeo, Simone Panico, Sara Bonuso, Nicoletta Matera, Paolo Maria Congedo, and Giuseppe Oliveti. 2020. "Complete Greenhouse Dynamic Simulation Tool to Assess the Crop Thermal Well-Being and Energy Needs." Applied Thermal Engineering 179 (October):115698. https://doi.org/10.1016/j.applthermaleng.2020.115698.

Brækken, August, Sigurd Sannan, Ionut Ovidiu Jerca, and Liliana Aurelia Bădulescu. 2023. "Assessment of Heating and Cooling Demands of a Glass Greenhouse in Bucharest, Romania." Thermal Science and Engineering Progress 41 (June):101830. https://doi.org/10.1016/j.tsep.2023.101830.

Dinesh, Harshavardhan, and Joshua M. Pearce. 2016. "The Potential of Agrivoltaic Systems." Renewable and Sustainable Energy Reviews 54 (February):299–308. https://doi.org/10.1016/j.rser.2015.10.024.

Fitz-Rodríguez, Efrén, Chieri Kubota, Gene A. Giacomelli, Milton E. Tignor, Sandra B. Wilson, and Margaret McMahon. 2010. "Dynamic Modeling and Simulation of Greenhouse Environments under Several Scenarios: A Web-Based Application." Computers and Electronics in Agriculture 70 (1): 105–16. https://doi.org/10.1016/j.compag.2009.09.010.

Jensen, Adam R., Kevin S. Anderson, William F. Holmgren, Mark A. Mikofski, Clifford W. Hansen, Leland J. Boeman, and Roel Loonen. 2023. "Pvlib Iotools—Open-Source Python Functions for Seamless Access to Solar Irradiance Data." Solar Energy 266 (December):112092. https://doi.org/10.1016/j.solener.2023.112092.

Katsoulas, Nikolaos, and Cecilia Stanghellini. 2019. "Modelling Crop Transpiration in Greenhouses: Different Models for Different Applications." Agronomy 9 (7): 392. https://doi.org/10.3390/agronomy9070392.

Mobtaker, Hassan Ghasemi, Yahya Ajabshirchi, Seyed Faramarz Ranjbar, and Mansour Matloobi. 2019. "Simulation of Thermal Performance of Solar Greenhouse in North-West of Iran: An Experimental Validation." Renewable Energy 135 (May):88–97. https://doi.org/10.1016/j.renene.2018.10.003.

Monteith, JL. 1965. "Evaporation and Environment. 19th Symposia of the Society for Experimental Biology. University Press, Cambridge, 205-234." Symp Soc Exp Biol.

Opeyemi Ogunlowo, Qazeem, Timothy Denen Akpenpuun, Wook Ho Na, Misbaudeen Aderemi Adesanya, Anis Rabiu, Prabhat Dutta, Hyeon-Tae Kim, and Hyun-Woo Lee. 2023. "Simulation of Greenhouse Energy and Strawberry (Seolhyang Sp.) Yield Using TRNSYS DVBES: A Base Case." Solar Energy 266 (December):112196. https://doi.org/10.1016/j.solener.2023.112196.

Ouazzani Chahidi, Laila, Marco Fossa, Antonella Priarone, and Abdellah Mechaqrane. 2021. "Energy Saving Strategies in Sustainable Greenhouse Cultivation in the Mediterranean Climate – A Case Study." Applied Energy 282 (January):116156. https://doi.org/10.1016/j.apenergy.2020.116156.

Rodríguez, Francisco, Manuel Berenguel, José Luis Guzmán, and Armando Ramírez-Arias. 2015. Modeling and Control of Greenhouse Crop Growth. Cham: Springer International Publishing. https://doi.org/10.1007/978-3-319-11134-6.

Funded by the European Union under Grant Agreement No 101096056. Views and opinions expressed are however those of the author(s) only and do not necessarily reflect those of the European Union or CINEA. Neither the European Union nor the granting authority can be held responsible for them.

Sahlin, Per, Lars Eriksson, Pavel Grozman, Hans Johnsson, Alexander Shapovalov, and Mika Vuolle. 2003. “Will Equation-Based Building Simulation Make It? - Experiences from the Introduction of IDA Indoor Climate and Energy.” In Eighth International IBPSA Conference Eindhoven, Netherlands August 11-14, 2003.
Schweiger, Andreas H., and Lisa Pataczek. 2023. “How to Reconcile Renewable Energy and Agricultural Production in a Drying World.” PLANTS, PEOPLE, PLANET 5 (5): 650–61. https://doi.org/10.1002/ppp3.10371.
Singh, Mahesh Chand, J.P. Singh, and K.G. Singh. 2018. “Development of a Microclimate Model for Prediction of Temperatures inside a Naturally Ventilated Greenhouse under Cucumber Crop in Soilless Media.” Computers and Electronics in Agriculture 154 (November):227–38. https://doi.org/10.1016/j.compag.2018.08.044.
Stanciu, Camelia, Dorin Stanciu, and Alexandru Dobrovicescu. 2016. “Effect of Greenhouse Orientation with Respect to E-W Axis on Its Required Heating and Cooling Loads.” Energy Procedia 85 (January):498–504. https://doi.org/10.1016/j.egypro.2015.12.234.
Zhang, Shanhong, Yu Guo, Huajian Zhao, Yang Wang, David Chow, and Yuan Fang. 2020. “Methodologies of Control Strategies for Improving Energy Efficiency in Agricultural Greenhouses.” Journal of Cleaner Production 274 (November):122695. https://doi.org/10.1016/j.jclepro.2020.122695.

Funded by the European Union under Grant Agreement No 101096056. Views and opinions expressed are however those of the author(s) only and do not necessarily reflect those of the European Union or CINEA. Neither the European Union nor the granting authority can be held responsible for them.

Task 4.2 CFD modelling of the greenhouse microclimate

Introduction

This deliverable represents the midpoint of Task 4.2 within Work Package 4, focusing on Computational Fluid Dynamics (CFD) modeling of the greenhouse microclimate. Task 4.2 is led by the University of Thessaly (UTH) with the collaboration of Tor Vergata University of Rome (UR). The primary aim of this task is to simulate the transfer phenomena within greenhouses equipped with photovoltaic (PV) systems, particularly examining the impact of PV panels on the available photosynthetically active radiation (PAR) and other environmental parameters critical for crop growth and energy efficiency.

The progress made thus far aligns well with the project timeline and milestones, reflecting significant advancements in developing and validating the CFD models.

The CFD modeling is structured at two levels:
Radiation Modelling: This involves simulating the radiation transport inside the greenhouse through its cover. This 2D CFD model provides crucial information about available radiation, particularly for greenhouses with arched or gothic geometries. The results from this modeling feed into the energy modeling (Task 4.1) and PV modeling (Task 4.3), forming an integral part of the Digital Twin model.

Internal Microclimate Modelling: This involves simulating the microclimate within the greenhouse, focusing on heat exchange among the incident radiation, heat storage, and heat transport by plants, the structure, and the ground. This includes both 2D and 3D geometries to provide detailed insights into the greenhouse's internal environment. The work done so far includes the development of various submodels and user-defined functions (UDFs) necessary for accurate CFD simulations. These models account for critical factors such as evapotranspiration, CO2 distribution, and the impact of evaporative cooling systems. The validation of these models against real-world data from pilot greenhouses ensures their reliability and accuracy.At the halfway point, the progress includes:

- Completion of state-of-the-art literature research on greenhouse simulation.
- Development and testing of submodels and UDFs.
- Definition of necessary environmental and building variables.
- Acquisition and mapping of real greenhouse designs and data.
- Initial validation of radiation models without the presence of PV, focusing on various greenhouse geometries.

The remaining phases will focus on the continuous improvement and validation of these models, conducting parametric studies to evaluate different geometries, climatic conditions, and cultivation methods. The ultimate goal is to integrate these models into a comprehensive Digital Twin, providing a powerful tool for optimizing greenhouse design, crop production management, energy saving, and microclimate control.

1. **General information for subtask 4.2**

Funded by the European Union under Grant Agreement No 101096056. Views and opinions expressed are however those of the author(s) only and do not necessarily reflect those of the European Union or CINEA. Neither the European Union nor the granting authority can be held responsible for them.

The subject of the subtask is to simulate the transfer phenomena inside greenhouses equipped with photovoltaics (with the photovoltaics located inside the greenhouse under the cover). These simulations will allow to

- Study the effect of photovoltaic presence on the available photosynthetically active radiation (PAR) at the plants level. The development of analytical models for the calculation of radiation propagation through a simple geometry cover may be feasible. But when it comes to arched or gothic roofs the problem becomes more complicated. Furthermore, when photovoltaics is added and reflection and emission of side walls, ground, plants and photovoltaics are accounted for, CFD seems to be the only reliable calculation tool for a detailed study or for feeding information to simpler models.
- Study the effect of photovoltaics on all the parameters that define the microclimate inside the greenhouse. The photovoltaics presence not only prevents some of the PAR to reach the plants but also affects the other light wavelength bands which alter the flow and temperature fields inside the greenhouses.
- Study the effect of photovoltaics on the crop growth.
- Study the effect of the greenhouse microclimate on the PV's operating environment. Temperature negatively affects the performance of the PV, while the increased humidity (due to plants evapotranspiration) modifies the optical properties of the air inside the greenhouse reducing the available radiation for electricity production by the PV.
- Finally, the developed CO2 fields can be studied with CFD simulations, since in REGACE the CO2 will be examined as 'substitute' of reduced PAR for the crop growth.

The developed CFD models will be used for execution of sets of parametric studies that will feed data to the developed digital twin model. In Figure 1 the subtask 4.2 position in the REGACE project is depicted describing the information exchange paths. According to this flow chart info will be fed into T.4.2 from: a) WP1 which will provide info about the greenhouses structure, the used materials and the crops types, b) WP2 which will provide info about the PV structure and operating conditions, and c) WP3 which will provide measurements of environmental parameters which will be used for validation of the developed models. For the development of the CFD model, information will be interchanged with the other subtasks of the WP4 (T.4.1 – dynamic modeling, T.4.3 PV modeling and T.4.5 – digital twin development). ,Finally, data will be fed directly to WP5 for project validation and indirectly to WP6 for sustainability assessment of the developed solutions.

Funded by the European Union under Grant Agreement No 101096056. Views and opinions expressed are however those of the author(s) only and do not necessarily reflect those of the European Union or CINEA. Neither the European Union nor the granting authority can be held responsible for them.

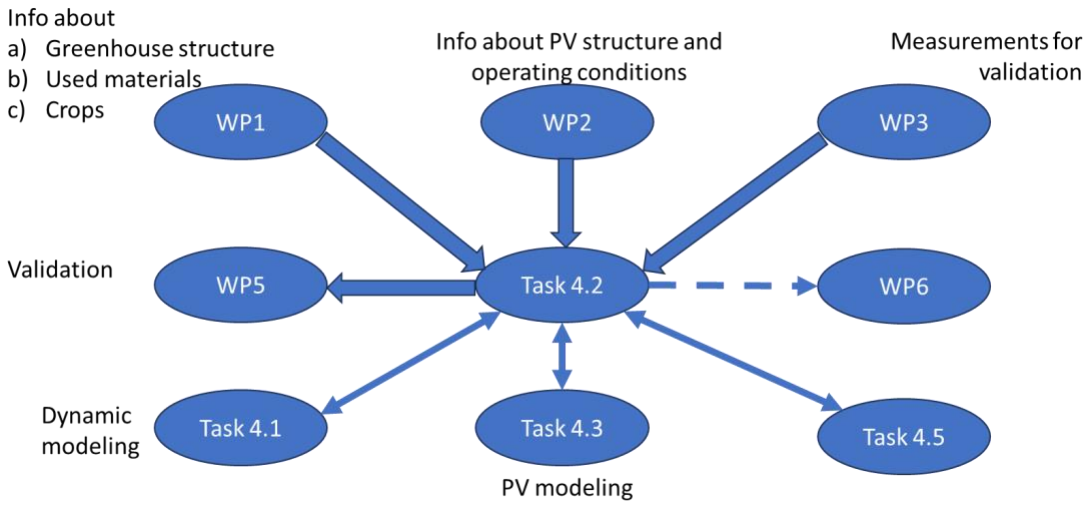

Figure 1. T4.2 position in REGACE project

T.4.2 will be structured in two levels. The first level concerns 2D simulations of greenhouses cross-sections and the second level is about 3D simulations of the whole greenhouse interior.

2D simulation will be used for the assessment of roof and PV effect on the radiation inside the greenhouse. So, they will be applied in all the pilot greenhouses in order to examine at least three types of roof geometry (pitched roof, venlo and gothic roofs).

In particular, it will focus on:

- Detailed simulation of radiation propagation inside the greenhouse (in all pilot greenhouses).
- Validation of radiation modeling.
- Examination of roof shape effect on available radiation.
- Test and validation of submodels related to radiation propagation.
- Interaction with dynamic and PV modeling.

With the radiation model validated and the differentiation due to various roof types estimated, the whole interior of a greenhouse will be studied at the second level with 3D simulation for the geometry of one chamber of the UTH greenhouse (which is the referred greenhouse in the whole WP4. In the 3D models, new models will be developed and added concerning: a) ground interaction, b) evapotranspiration and humidity, c) evaporative pads and d) CO_2 distribution. Thus, detailed simulation of all the transport phenomena developed inside the greenhouse will be achieved. Once the model is validated, it will be used for a set of parametric studies for feeding data to digital twin model.

Given that T.4.2 covers all the project period, it was divided to 14 distinct stages, so to be able to assess its progress. In the following Figure 2 this discretization is presented in a predicted timetable. Then the progress of T.4.2 will be presented according to this schedule.

Funded by the European Union under Grant Agreement No 101096056. Views and opinions expressed are however those of the author(s) only and do not necessarily reflect those of the European Union or CINEA. Neither the European Union nor the granting authority can be held responsible for them.

		Feb 2023	Mar 2023	Apr 2023	May 2023	June 2023	July 2023	Aug 2023	Sep 2023	Oct 2023	Nov 2023	Dec 2023	Jan 2024	Feb 2024	Mar 2024	Apr 2024	May 2024	June 2024	July 2024	Aug 2024	Sep 2024	Oct 2024	Nov 2024	Dec 2024	Jan 2025	Feb 2025	Mar 2025	Apr 2025	May 2025	June 2025	July 2025	Aug 2025	Sep 2025	Oct 2025	Nov 2025	Dec 2025	Jan 2026
WP	Description	1	2	3	4	5	6	7	8	9	10	11	12	13	14	15	16	17	18	19	20	21	22	23	24	25	26	27	28	29	30	31	32	33	34	35	36
4	**Modelling & Digital Twins**																																				
4.2	***CFD modelling of the greenhouse microclimate***																																				
4.2.1	*State of the art of greenhouse simulation: literature research*					x																														
4.2.2	Identification and testing of the sumodels and software (UDFs - FLUENT - OpenFoam)																																				
4.2.3	Definition of the environmental and building variables needed										x																										
4.2.4	Acquisition of the real greenhouses design and identification of the suitable greenhouses																																				
4.2.5	Mapping of available data in terms of measured variables and time intervals																																				
4.2.6	Definition of studied geometries and cases - development of grids																																				
4.2.7	Definition of data format for exchange																																				
4.2.8	Start of data acquisition from the greenhouses																																				
4.2.9	Validation of models and submodels and calibration of models																																				
4.2.10	Initial simulation with synthetic datasets																																				
4.2.11	Parametric studies for various geometries																																				
4.2.12	Parametric studies for various climatic conditions																																				
4.2.13	Parametric studies for various cultivation and PV electricity generation modes																																				
4.2.14	Final results and definition of optimal model setup																																				

Figure 2. T.4.2 stages time table

With crosses (x) are indicated completed stages of the T.4.2 which resulted in internal reports

- 4.2.1 State of the art of greenhouse simulation: literature research
- 4.2.3 Definition of environmental and building variables needed

Funded by the European Union under Grant Agreement No 101096056. Views and opinions expressed are however those of the author(s) only and do not necessarily reflect those of the European Union or CINEA. Neither the European Union nor the granting authority can be held responsible for them.

Subtask 4.2.1 – literature review

In a short historical review, the use of CFD for describing the transport phenomena inside a greenhouse with Computational Fluid Dynamics (CFD) techniques began at the late 1990' (Kacira et al. 1998) and early 2000 (Bartzanas and Kittas, 2001) where CFD was used for the simulation of transport phenomena inside greenhouse and the determination of the developed microclimate (distribution of temperature, humidity, air speed, etc.) mainly using the finite volume method. Initially, these kinds of studies were focused on the ventilation systems' efficiency as it was marked out in a relevant literature review (Bournet and Boulard, 2010). Later, many submodels were developed for the study of various transport phenomena inside greenhouses (Kacira et al. 2008, Bartzanas et al. 2013) like evapotranspiration (Kichah et al. 2012), heating and cooling (Couto et al. 2012) of greenhouses, energy balance of individual elements (Nebbali et al. 2012), condensation (Piscia et al. 2012), humidity (Kim et al. 2008) etc. The issue of radiation was initially approached indirectly. One approach is to use analytical models in order to calculate the surface temperatures developed due to radiation (short and long wave) (Molina-Aiz et al. 2004). The next step was to model the effect of radiation as heat source terms in the energy equation attributed to short wave solar radiation and to long wave thermal radiation emitted by the greenhouses' heated surfaces (Campen and Bot, 2003), but without solving a radiation transport equation (RTE). Later radiation models were used to solve the RTE. The most popular is the Discrete Ordinate (DO) model. In some cases, solar radiation is calculated indirectly: the DO model is used for the calculation of thermal radiation in one wave band (Wang et al. 2013, Chen et al. 2015). In a further step, solar radiation too is solved inside the greenhouse, but using the solar radiation inside the greenhouse (calculated analytically according to the cover materials properties) as a boundary condition (Nebbali et al. 2012). Kuroyanagi 2017 investigated air leakage and wind pressure coefficients of single-span plastic greenhouses. Sciuto et al. 2018 simulated a typical bioclimate greenhouse in winter on cloudy days. Jiao et al. 2020 examine the growth of a celery plant inside a double-film greenhouses in terms of developed temperature and humidity fields.

The concurrent use of CFD and Computational Heat Transfer (CHT) method for the handling of NS equations (pressure, momentum and turbulence) and the holistic energy equation treatment (energy transport and radiation transmittance) inside the greenhouse was initiated by (Baxevanou et al. 2008). In this view, for the first time the optical properties of plants and cover materials were considered and the effect of cover materials on the PAR levels inside the canopies of greenhouse at certain hours of a summer day was examined (Baxevanou et al. 2010). Under the same perspective and mathematical background, the transport phenomena were observed for an entire solar day in an arched greenhouse examining specific cover material (Fidaros et al. 2010).

According to the Choab et al. 2019 review, the interactive components that are accounted for in CFD simulation of greenhouse operations are: (i) the cover, (ii) the crop, (iii) floor as surface or as a material with depth in one or more layers, (iv) the plant surface, (v) the inside air in one or more vertical or horizontal zones, (vi) the growing media, (vii) the air inside the crop, and (viii) greenhouse walls.

This project has received funding from the European Commission's Horizon Europe programme under grant agreement number 101096056.

Since the transport phenomena related to the greenhouse operation and the modelling of interaction with crop growth are numerous and complicated, most of the researchers adopt some assumptions in order to simplify them. According to the Choab et al. 2019 review, the most commonly adopted assumptions are: (i) Cover thermal properties constant in time, (ii) Negligible absorption of solar radiation by the cover, (iii) Negligible absorption and heat capacity of the air inside the greenhouse, (iv) No radiative exchange between greenhouse constructions, (v) Not accounting for temperature stratification, (vi) Plants thermal properties the same as water, (vii) Not accounting for humidity stratification, (viii) Ground conduction in steady state condition, (ix) Negligible heat capacity of cover, (x) No condensation on the plants, (xi) Greenhouse cover transparent to long wave radiation, (xii) Negligible heat storage capacity of greenhouse thermal mass, (xiii) Negligible soil evaporation and transpiration, (xiv) Inside air homogenous, (xv) Crop canopy as a big leaf, (xvi) Inside air does not participate in radiation, (xvii) greenhouse construction elements are considered as lumped systems, (xviii) negligible condensation inside the greenhouse, and (xix) no ventilation. However, as the models evolve, usually the different groups of researchers start developing a model which they then evolve further, many of these assumptions are removed and more detailed and accurate modeling is adopted.

According to recent review works (Rezvani et al. 2021, Choab et al. 2019 and Bournet and Rojano 2022) the existing works considering the simulated transport phenomena are categorized as following.

New challenges

Much more accurate simulation of mechanical ventilation would be the inclusion of fans in the computational domain and the approach of them as pressure jump that would determine the exit velocity according to the pressure drop inside the greenhouse and the available inlet area.

Simulation of evaporative pad as porous material and as heat sink, humidity source and pressure drop including the evaporative pads in the computational domain through UDFs accounting for the air velocity, as formed by the tunnel operation and the external air temperature and humidity.

Full simulation of plant function which will include, in addition to known evapotranspiration models, the plants' interaction with radiation (there exist already some approaches) in various wavelength bands accounting for beam and diffusive parts of solar radiation and the heat storage in plants, as well as the interaction with CO2 and the heat storage in crop mass.

As far the ground modeling is concerned, two main approaches emerge: a) modeling as isothermal surface calculating the temperature through an energy balance model that will be integrated in the simulation procedure as UDFs accounting for the incident radiation (per wave length), the internal air temperature and humidity, the optical and thermophysical properties of ground and the ground temperature at a depth where it could be estimated through analytical models from available climatic conditions, b) including a layer of the ground at the appropriate depth in the computational domain where the isothermal temperature could be calculated according to climatic conditions through UDFs.

This project has received funding from the European Commission's Horizon Europe programme under grant agreement number 101096056.

Challenges addressed during the project

In the present project two approaches will be adopted. The first is related to the propagation of solar radiation inside the greenhouse at the presence of photovoltaic panels with variable orientation/inclination (depends on the greenhouse orientation). The second is the prediction of the internal microclimate (including the CO2 distribution) in mechanically ventilated greenhouses with various heating/cooling/ventilation systems.

In the first part, 2D cross sections of various greenhouse geometries will be studied in unsteady-state simulations for representative solar days, trying two approaches: a) constant orientation (or inclination) angle (depending on the greenhouse orientation, during the solar day, b) continually change of orientation (or inclination) angle of the photovoltaics either with different grids or with moving grid. The purpose will be the estimation of available radiation on the photovoltaics surface as well as for the crop in terms of wavelength bands, on radiation type (beam or diffusive) as instantaneous and average daily values.

The 2nd approach is the simulation of one 3D geometry with photovoltaics where steady-state and unsteady calculations will be performed for the study of the developed flow, temperature, humidity, radiation (in four wavelength bands) and CO2 concentration fields accounting for: a) including the evaporative pads in the computational domain, b) including the exhaust fans in the computational domain, c) modeling the ground adequately, d) incorporating the evapotranspiration model as well as the operation of plants as porous materials, heat storage, mass and radiation exchange, e) incorporating CO2 sources.

Subtask 4.2.2 – Models development

Stage 4.2.2 concerns the development of the above described submodels, along with the UDFs that will be used in the CFD modeling and it is ongoing. Until now, there have been developed the 7 out of 8 submodels of which the relevant UDFs have been developed for the 3. One more model with its UDFs and 3 more UDFs remain to be prepared.

Finished submodels and UDFs

- All incident radiation submodels and UDFs
  Three approaches of incident solar radiation have been prepared
    - Calculating the vertical component of solar radiation to each segment of cover (according to each segment inclination angle) each moment. This is the approach used until now in relative works (Baxevanou et al. 2008, 2010, 2018 and 2020, Fidaros et al 2010) which produced quite good results when the PV were not inside the greenhouse
    - Calculating the magnitude of solar radiation and the incidence angle on each segment of cover (according to each segment inclination angle) each moment. this will allow to account for the direction of the beam part of solar radiation inside the greenhouse
    - Considering a computational domain which will extend far enough from the greenhouse to allow only the radiation measure and the angle of incidence on the

This project has received funding from the European Commission's Horizon Europe programme under grant agreement number 101096056.

horizontal plane to be determined. This makes the calculations and the required UDFs easier but restricts the accuracy inside the greenhouse. However, the pixelization of DO model will define the accuracy of calculations

- Shading submodels and UDFs
  In multispan greenhouses the cover of each chamber is partially shaded by its neighbor chamber. Thus, a model was developed. For each segment of the cover (each moment) the following elements are evaluated: a) the ellipse resulting from the intersection of a cylinder and a plane vertical to horizon including the solar position, b) the line on the vertical plan which begins from the center of the cover segment and it is tangential to the ellipse and c) the line that begins from the segment center to the solar position. Then the incidence angle of the two lines is compared and it is identified whether the specific segment at the specific moment is shaded or not. If it is shaded, only the diffuse and reflected components of solar radiation are compared
- Plants model as heat storage and thermal radiation sources and UDFs
  Plants can store heat according to their specific heat capacity and their mass and emit thermal radiation according to their temperature and their emission coefficient

Finished submodels

- Energy balance model for ground
  The participation of ground in the transport phenomena in most cases is addressed either as isothermal wall or as constant heat flux wall. However, both approaches are very crude and reduce the accuracy of calculations (especially when the greenhouse temperature is one of the most important factors that will dictate the PV inclination angle). Thus, two approaches have been prepared and will be assessed.
  - Creating an energy balance model that calculates ground temperature according to greenhouse temperature, incident radiation, shading, ground thermal and optical properties and soil temperature at a depth of 3 meters depending on the day of the year and the external climatic conditions. This information is evaluated for each moment, at each ground computational boundary cell
  - Considering a computational domain extended for 3 meters in depth, where the soil temperature will be defined by the day of the year and the external climatic conditions
- Evapotranspiration model
  The plants are considered as sources of humidity and sinks of heat. The rates of humidity production and cooling depend on the plants type, age, geometry, foliage characteristics and moisture content
- Evaporative pads models
  The evaporative pads usually are not included in the computational domain and they are addressed as surfaces with knownvalues of air velocity, temperature and humidity. A model was prepared for the inclusion of evaporative pads in the computational domain where the final velocity will be calculated according to the exhaust fans operation and the evaporative pad characteristics, and the temperature and humidity content according to the external air conditions and the evaporative pads operational characteristics
- Model for humidity effect on air optical properties

This project has received funding from the European Commission's Horizon Europe programme under grant agreement number 101096056.

Usually, air is considered as a medium with unity refraction index and zero extinction coefficient. The truth is that the presence of vapors in the air alterates its optical properties and this is calculated in each computational cell according to the humidity concentration and the solved wavelength band.

UDFs under development

- UDFs for energy balance model for the ground
- UDFs for evapotranspiration
- UDF for humidity effect on air optical properties

Submodels and UDFs under development

- CO_2 submodels and UDFs

  The plants are CO_2 sinks during the day and CO_2 sources during the night. The rates of production and consumption depend on plants characteristics (type, size, density etc.) and on the available solar radiation. The relative model and UDFs will be developed in the second part of the project.

Subtask 4.2.3 – Definition of needed variables

For the preparation of simulations, the following information should be collected

- Identification of simulated greenhouse and crops characteristics.
- Identification of involved materials.
- Identification of needed thermophysical properties.
- Identification of needed optical properties.
- Identification of needed crop properties.
- Identification of required information of internal climate control technologies.
- Identification of crops required environmental conditions.
- Identification of required information about external climatic conditions.

As far the required thermophysical properties are concerned, the following information should be gathered for each involved material

- Number of layers
- Material of each layer
- Thickness of each layer
- Solid
  - Density, ρ [kg/m3]
  - Thermal conductivity, k [W/mK]
  - Specific heat capacity [J/kgK]
- Fluid
  - Density, ρ [kg/m3]
  - Thermal conductivity, k [W/mK]
  - Specific heat capacity [J/kgK]

This project has received funding from the European Commission's Horizon Europe programme under grant agreement number 101096056.

- Viscosity, μ [Pa.sec]
- Thermal expansion coefficient [1/K]

Concerning the optical properties Table 1 should be filled for each involved material
Table 1 Materials required optical properties

Property	UV (0.1-0.4 μm)	PAR (0.4-0.76 μm)	NIR (0.76 – 1.4 μm)	IR >1.4 μm
Refraction index				
Extinction coefficient				
Emission coefficient				
Albedo*				

- Albedo: is the fraction of sunlight that is diffusely reflected by a body

For the plants the following information should be gathered additionally:

a. Pressure drop across the crops

- Porosity (percentage of solid and percentage of fluid)
- Viscus resistance, $(1/\alpha)$, $[1/m^2]$ per direction
- Inertial resistance, C_2, 1/m

b. Latent heat released by crops

- Evapotranspiration rate
- LAI

c. Geometrical properties of crops

- Dimensions
- Position of crop inside the greenhouse (imprint on a plane)

d. Growth material

- Geometry
- Position of growth inside the greenhouse (imprint on a plane)
- Material
  - Thermophysical properties of material
  - Optical properties of material per wavelength band.

Status of subtasks 4.2.4 – 4.2.8

T. 4.2.4 Acquisition of the real greenhouses design and identification of the suitable greenhouses

- Status: on going
- Finished
  - All the data has been acquired for UTH greenhouse
  - Almost all the data has been acquired for AZS greenhouse
  - For the greenhouses of BOKU and HU information given to UR for their modelling is available

This project has received funding from the European Commission's Horizon Europe programme under grant agreement number 101096056.

- Pends
    - AZS greenhouse required data about the openings of the greenhouse (position, dimensions and operation modus)
    - For the greenhouses of BOKU and HU additional information will be asked in the frame of bilateral meeting scheduled in the near future

T. 4.2.5 Mapping of available data in terms of measured variables and time intervals

- Status: on going
- Finished
    - Mapping of available data for measurements for UTH greenhouse and for AZS greenhouse
    - Mapping of available data for measurements for BOkU and HU according to the information gathered by UR
- Pends
    - Additional information about data for measurements for BOkU and HU greenhouses will be gathered in the near future
    - No available information for FSC greenhouse

T. 4.2.6 Definition of studied geometries and cases - development of grids

- Status – on going
- Finished
    - Almost all the studied geometries have been identified
    - Studied cases for UTH greenhouse have been defined
- Pends
    - Development of grids for UTH greenhouse is ongoing
    - Studied cases for the rest pilot greenhouse subject remains to be defined (may now)
    - The development of grids for the other pilot greenhouses has not been started yet

T. 4.2.7 Definition of data format for exchange

- Status – on going
- Finished
    - The data format for exchange is completed only for the UTH greenhouse
- Pends
    - The data format for exchange in all the other pilot greenhouses is subject to discussion with all the partners running pilot greenhouses

T. 4.2.8 Start of data acquisition from the greenhouses

- Status – on going
- The data acquisition has started
    - in UTH greenhouses for chambers without PV from beginning of March
        - Total radiation in 6 positions
        - Diffuse radiation in 1 position
        - Temperature and humidity
        - External climatic conditions
    - In AZS greenhouses – available positions of instrumentations not yet set of measurements

This project has received funding from the European Commission's Horizon Europe programme under grant agreement number 101096056.

Current planning of 2D simulations

As a first step, 2D simulations will be implemented in the geometry of UTH greenhouse (gothic roof multi span) and then 2D simulation will continue with the AZS greenhouse (arch roof single span), Berlin greenhouse (venlo multispan). Later, the necessity to simulate the facilities of Vienna (small venlo) and Mecklenburg (pitched roof single span) in 2D will be considered.

What we wish to achieve with 2D simulations in UTH greenhouse is the following

- Choose the appropriate radiation modeling approach (normal at the cover, magnitude and incidence angle at the cover, magnitude and incident away from the greenhouse)
- Validate the radiation propagation model
    - In all the wavelength bands
    - Optical properties
    - Handling of different boundary conditions
    - PV effects
- 'Transfer' of boundary conditions to the side walls of the internal chambers
- Parametric studies for the production of information about
    - Available PAR at plants level
    - Available PAR and NIR at the PV surfaces (front and back)

In the case of a multispan greenhouse, when one wants to study a single chamber, one faces the problem of defining the boundary conditions on the intermediate side walls (mainly temperature and radiation). With parametric studies and regression analysis we will estimate the incident radiation on the intermediate walls according to the external climatic conditions. This way we will 'transfer' the external boundary conditions to the side walls of the chambers where PV will be installed. And this will be used in both 2D detailed simulation of the chambers equipped with PV, in different positions, with steady state and unsteady conditions as well as in the 3D simulation of one single chamber with the complete model (including all the submodels developed in T.4.2.2. The organization of 2D simulations in the UTH greenhouse is presented below.

In the first step the whole greenhouse cross section is accounted for under different conditions. In Figure 3 the first examined geometry is presented with no plants, no curtains and no PV. In Figure 4 the geometry with no plants and PV but with curtain is presented. In Figure 5 the third geometry is presented with young plants, no curtain and no PV. In Figure 6 the fourth geometry is presented with mature plants, no curtain and no PV. In Figure 7 the fifth geometry is presented with young plants and curtain but not PV. And finally, in Figure 8 the sixth whole cross section geometry is presented with mature plants, curtain but no PV.

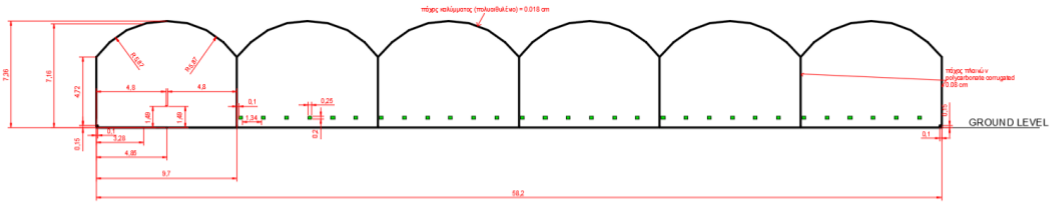

This project has received funding from the European Commission's Horizon Europe programme under grant agreement number 101096056.

Figure 3. Whole cross section, no plants, no curtain, no PV

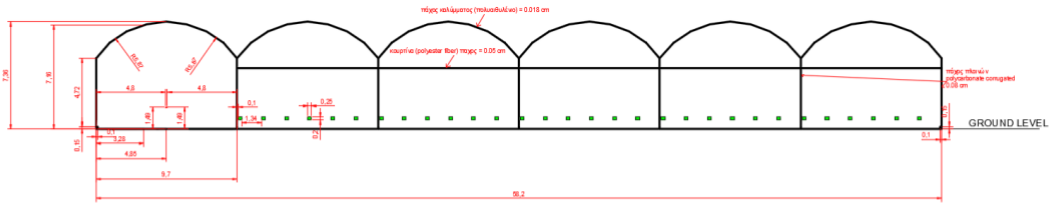

Figure 4. Whole cross section, no plants, with curtain, no PV

TOTAL CROSS SECTION 3 (no curtain + young plants)

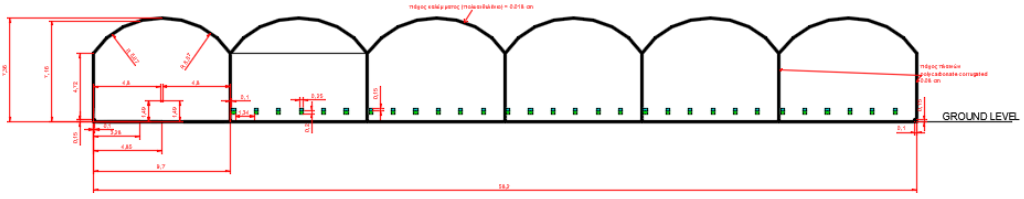

Figure 5. Whole cross section, young plants, no curtain, no PV

TOTAL CROSS SECTION 5 (no curtains + old plants)

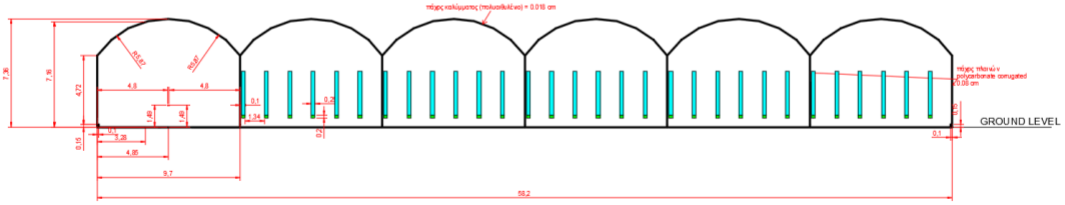

Figure 6. Whole cross section, mature plants, no curtain, no PV

TOTAL CROSS SECTION 4 (with curtains + young plants)

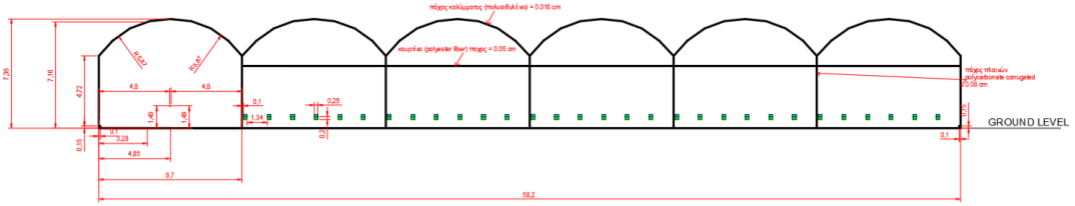

Figure 7. Whole cross section, young plants, with curtain, no PV

This project has received funding from the European Commission's Horizon Europe programme under grant agreement number 101096056.

TOTAL CROSS SECTION 6 (with curtains + old plants)

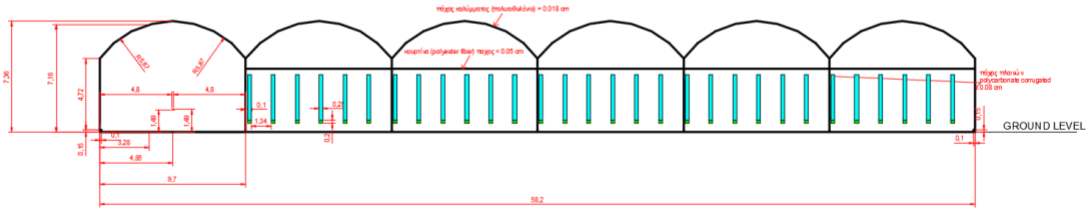

Figure 8. Whole cross section, mature plants, with curtain, no PV

The above geometries will be used for the validation of radiation models without the presence of PV and in order to choose the most appropriate of the 3 radiation models developed in T.4.2.2. The simulations will be validated against measurements of internal microclimate in chambers 3 and 4 (where the PV will be installed later). According to the nomenclature adopted in WP4, these chambers are named GH1 and GH2, since chamber1 hosts the control room. The measurements were carried out from the beginning of March to the middle of June and concern cucumber cultivation. In Figure 9 and 10 the position of the measurement devices is presented.

PLAN VIEW

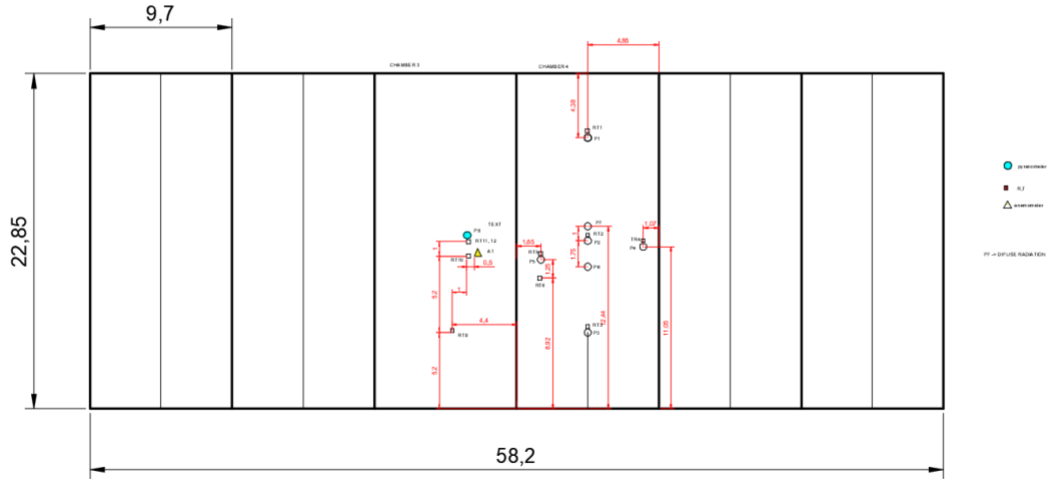

Figure 9. Plan view measurement devices

This project has received funding from the European Commission's Horizon Europe programme under grant agreement number 101096056.

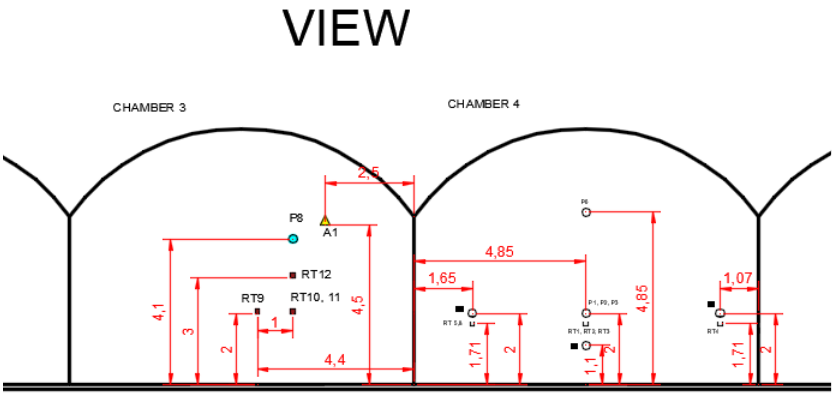

Figure 10. Cross section measurement devices

Using the results of the above-described simulation and elaborating the data with regression analysis, using as independent parameters: a) the external radiation, b) the position of curtain, c) the age of the plants, d) external temperature and e) the internal air humidity, a rule will be created for the calculation of radiation in the side intermediate walls of chambers 3 and 4. This will allow the 'transfer' of external boundary conditions, concerning mainly radiation and secondary temperature to the internal side walls.

Then the second phase of 2D simulations will begin, focusing on the chambers where the PV will be installed. Three basic geometries will be considered as presented inFigure 11, cross-sections with PV, without plants, with young and with mature plants.

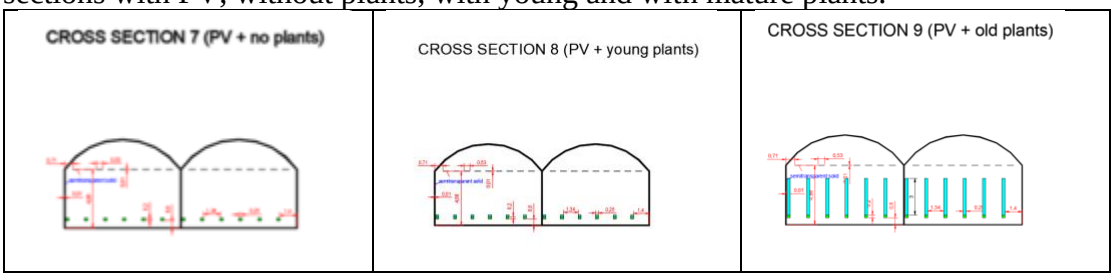

Figure 11. Basic 2D geometries with PV

Then, and in collaboration with the other partners, the necessity to investigate the behavior with open roof openings as shown in Figure 12 will be considered.

This project has received funding from the European Commission's Horizon Europe programme under grant agreement number 101096056.

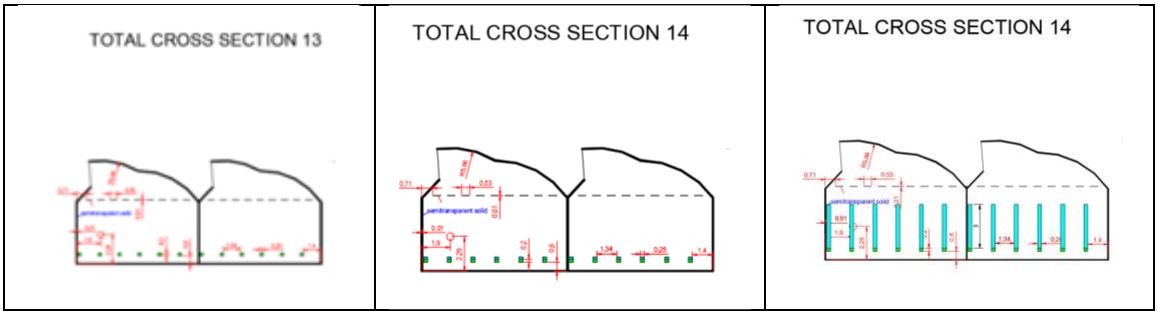

Figure 12. Basic 2D geometry with PV and open the roof openings

Finally, the final stage of 2D simulations in the UTH greenhouses will be scheduled with steady-state simulations with PV twisted in extreme and intermediate positions and with unsteady simulation with moving grids considering the continuous rotation of the PV modules.

References

Bartzanas, T., Kittas, C., 2001. Optimisation of greenhouses ventilation performance with computational fluid dynamics. In 2nd Southeastern Europe Fluent Users Group Meeting, Bucharest Romania, CD-ROM, Simtec Eds., Thessaloniki, Greece.

Bartzanas, T., Kacira, M., Zhu, H., Karmakar, S., Tamimi, E., Katsoulas, N., Lee, I.-B., Kittas, C., 2013. Computational fluid dynamics applications to improve crop production systems. Computers and Electronics in Agriculture 93 151–167

Baxevanou , C., Bartzanas, Th., Fidaros, D., Kittas, C., 2008. Solar radiation distribution in a tunnel greenhouse. Acta Horticulturare. 801, 855-862.

Baxevanou C, Fidaros D., Bartzanas Th. And C.Kittas, 'Numerical simulation of solar radiation, air flow and temperature distribution in a naturally ventilated tunnel greenhouse', CIGR Journal, Volume 12, No 3, Pages 48-67, 2010

Baxevanou C, Fidaros D, Bartzanas Th, Kittas C, 'Yearly numerical evaluation of greenhouse cover materials', Computers and Electronics in Agricultrure, Vol. 149, pp.54-70, 2018

Baxevanou C, Fidaros D, Katsoulas N, Mekeridis E, Varlamis Chr, Zachariadis A and St. Logothetidis, Simulation of Radiation and Crop Activity in a Greenhouse Covered with Semitransparent Organic Photovoltaics, Appl. Sci. 2020, 10, 2550

Bournet P.E., Boulard, T., 2010. Effect of ventilation configuration on the distributed climate of greenhouses: A review of experimental and CFD studies. Computers and Electronics in Agriculture, 74, 195 – 217

Campen, J.B, Bot, G.P.A., 2003. Determination of Greenhouse-specific Aspects of Ventilation using Three-dimensional Computational Fluid Dynamics', Biosystems Engineering 84 (1), 69–77.

Chen, J., Xu, F., Tan, D., Shen, Z., Zhang, L., Ai, Q., 2015. A control method for agricultural greenhouses heating based on computational fluid dynamics and energy prediction model. Applied Energy 141, 106–118.

Choab N., Allouhi A., El Maakoul A., Kousksou T., Saadeddine S., Jamil A., Review on greenhouse microclimate and application: Design parameters, thermal modeling and simulation, climate controlling technologies (2018), Solar Energy 191 (2019) 109–137

This project has received funding from the European Commission's Horizon Europe programme under grant agreement number 101096056.

Couto, N., Rouboa, A., Monteiro, E., Viera, J. 2012. Computational Fluid Dynamics Analysis of Greenhouses with Artificial Heat Tube., World Journal of Mechanics 2, 181-187.

Fidaros, D.K., Baxevanou, C.A., Bartzanas Th., Kittas, C., 2010. Numerical simulation of thermal behavior of a ventilated arc greenhouse during a solar day. Renewable Energy. 35 (7), 1380 – 1386.

Jiao, W., Liu, Q., Lijun, G., Liu, K., Shi, R., & Ta, N. (2020). Computational fluid dynamics-based simulation of crop canopy temperature and humidity in double-film solar greenhouse. Hindawi Journal of Sensors, 15. https://doi.org/10.1155/2020/8874468. Article ID 8874468

Kacira, M., Short, T.H., Stowell, R.R., 1998. A CFD evaluation of naturally ventilated, multi-span, sawtooth greenhouses. Trans. Am. Soc. Agric. Eng. 41 (3), 833–836

Kacira, M., Sase, S., Ikeguchi, A., Ishii, M., Giacomelli, G., Sabeh, N., 2008. Effect of vent configuration and wind speed on three-dimensional temperature distributions in a naturally ventilated multi-span greenhouse by wind tunnel experiments. Acta Horticulturae 801(1) 393-400

Kichah, A., Bournet, P.-E., Migeon, C., Boulard, T., 2012. Measurement and CFD simulation of microclimate characteristics and transpiration of an Impatiens pot plant crop in a greenhouse. Biosystems Engineering 112(1) 22–34.

Kim, K., Yoon, J.-Y., Kwon, H.-J., Han, J.-H., Son, J.E., Nam, S.-W., Giacomelli, G.A., Lee, I.-B., 2008. 3-D CFD analysis of relative humidity distribution in greenhouse with a fog cooling system and refrigerative dehumidifiers. Biosystems Engineering 100, 245 – 255.

Kuroyanagi, T., 2017. Investigating air leakage and wind pressure coefficients of singlespan plastic greenhouses using computational fluid dynamics. Biosyst. Eng. 163, 15–27.

Molina-Aiz, F.D., Valera D.L., Álvarez, A.J., 2004. Measurement and simulation of climate inside Almerıa-type greenhouses using computational fluid dynamics. Agricultural and Forest Meteorology 125, 33–51.

Nebbali, R., Roy, J.C., Boulard, T. 2012. Dynamic simulation of the distributed radiative and convective climate within a cropped greenhouse, Renewable Energy 43, 111-129.

Piscia, D., Montero, J.I., Baeza, E., Bailey, B.J. 2012. A CFD greenhouse night-time condensation model', Biosystems Engineering 111, 1410154.

Sciuto, G.L., Cammarata, G., Capizzi, G., Coco, S., 2018. June). Numerical simulation of a typical bioclimate greenhouse in winter on cloudy days. In: 2018 International Symposium on Power Electronics, Electrical Drives, Automation and Motion (SPEEDAM). IEEE, pp. 779–785

Wang, X.-W., Luo, J.-Y., Li, X.-P. 2013. CFD Based Study of Heterogeneous Microclimate in a Typical Chinese Greenhouse in Central China', Journal of Integrative Agriculture 12(5), 914-923.

This project has received funding from the European Commission's Horizon Europe programme under grant agreement number 101096056.

Task 4.3: Modelling of the PV modules performance

Introduction

This deliverable marks the halfway point of Task 4.3 within Work Package 4, focusing on the modeling of photovoltaic (PV) modules performance. Task 4.3 is led by Università Degli Studi di Roma Tor Vergata (UR) with the participation of the University of Thessaly (UTH) and AZ. The primary objective of this task is to develop a comprehensive performance model for bifacial PV modules, which are integral to the project due to their ability to capture irradiance on both the front and rear sides, enhancing overall energy production.

Here the performance of PV modules in real operating conditions is effectively represented by the Performance Ratio (PR) parameter. PR measures the ratio between the outdoor efficiency and the nameplate efficiency measured at Standard Test Conditions (STC). For crystalline modules, PR is influenced by temperature, irradiance, spectral effects, and reflection effects, which account for changes in module efficiency under varying conditions different from the STC. Given the specific bifacial technology employed in this project, it is crucial to consider the contribution from the rear side of the module. Task 4.3 involves a detailed review of available PV performance models for bifacial technologies. Based on this review, a semi-empirical performance model has been customized for the specific module architecture used in the project, utilizing parameters measured in WP3 (Characterization of PV modules in outdoor conditions).

The model will be calibrated and tested using experimental data collected by WP3.
The progress made so far is in line with the project timeline and includes significant advancements in developing and refining the semi-empirical performance model. Key accomplishments include:

- Conducting a comprehensive review of existing PV performance models for bifacial technologies.
- Developing a semi-empirical model tailored to the project's specific PV module architecture.
- Calibrating the model using data from WP3.
- Validating the model against real-world data to ensure its accuracy and reliability.

The work carried out so far has created a solid foundation for the subsequent phases of Task 4.3. Model development and calibration is critical to accurately predicting the performance of bifacial PV modules under different operating conditions.

As we move forward, the focus will be on further refining the model, conducting additional validation with expanded datasets, and integrating the results into the overall project framework. The completion of these steps will ensure that the performance modeling of PV modules is robust and reliable, providing essential insights for optimizing the design and operation of PV systems within greenhouses.

Bifacial modelling

This project has received funding from the European Commission's Horizon Europe programme under grant agreement number 101096056.

There is an increasing tendency towards application of bifacial photovoltaic (BFPV) technologies to overcome the current energy crises all around the world [1, 2]. The 14th International Technology Roadmap for Photovoltaic (ITRPV) [3] has estimated that the current shares of monofacial photovoltaic (MFPV) and BFPV in the world market are ~65% and ~35%, respectively. In 2027, BFPV is forecasted to take the lead with the contribution of ~55%. Three years later, i.e., in 2030, BFPV share will be ~60%. The change in the market shares is accompanied by the increase in the installed capacity, as well. The new installations are planned to be installed in different forms, such as power plants, building integrated technologies, vehicle integration, and so on. Application in the agriculture to use land more efficiently, which is known as Agri PV, is another sector. Agri PV is planned to occupy a huge share of the installed capacity during the upcoming years and it is forecasted Agri PV will reach $9.3 billion global market by 2031 [4]. Due to ability to received irradiance from the both sides, BFPV systems are very popular to be used in Agri PV.

For a BFPV system either in working or in design stage, power estimation is of great importance [5]. Power could be estimated using some packages. One package that has been commonly used is PVlib [6]. Application of PVlib for BFPV has been reported in several works, including Refs. [7, 8] (Power production assessment), Refs. [9, 10] (Techno-economic evaluation), Refs. [11, 12] (Performance optimization), and so on. In PVlib, monofacial PV (MFPV) estimation model is used for BFPV power, which receives an effective irradiance (G_E) as the input.

In addition to the developed packages, BFPV power estimation could be done by means of the approaches presented by researchers in the literature. In some of the research works, the proposed approach has been able to estimate current and voltage separately, while the power could be determined as multiplication of them. Semi-empirical equations to estimate current and voltage of a BFPV have been provided by Bouchakour et al. [13, 14]. There were two coefficients for each of the current and voltage equation. In addition to the module specifications, temperature and G_E were the input variables of the current equation. They were also the input variables of the voltage equation, to which thermal voltage and number of cells in series had been also added. The accuracy of the semi-empirical model was evaluated compared to values estimated by analytical approach of Ortiz Rivera et al. [15]. The results showed that the accuracy of both analytical and semi-empirical models declined when irradiance decreased. Moreover, analytical model was found more accurate than the semi-empirical one for the investigated case-study, which was a fixed-tilted (FT) system in Terrassa, Spain.

In addition, a digital twin was proposed by Yuan et al. [16] to determine current and voltage of a BFPV system. The digital twin worked based on two-diode equivalent circuit with a boosted parameter estimation using four-state Jaya evolutionary algorithm. The input flow to the digital twin included a number of variables, including GE, temperature, and module characteristics.

Accuracy assessment using the recorded data for a stand-alone module with FT configuration indicated a good agreement between simulation and experiment. Furthermore, a comparative study by Mannino et al. [17] was done to compare some semi-empirical equations for current and voltage estimation of a BFPV plant. Their comparison covered Sandia Array Performance Model (SAPM) [18], as well as the approaches provided by Cristaldi et al. [19] and Faifer et al. [20]. Parameters of models were extracted for a FT BFPV system in Catania, Italy, in which a number

This project has received funding from the European Commission's Horizon Europe programme under grant agreement number 101096056.

of variables including GE was required. The results were found to be highly dependent on the fitting method.

Instead of separate estimation of current and voltage, in another group of the studies, the developed approach obtained the power directly. An ANN was provided by Ghenai et al. [21] which could estimate power of a FT BFPV on a rooftop of a building in Sharjah, the UAE, as a function of many parameters, such as front and back irradiance values. The input data was supplied from PVSyst simulation. High correlation coefficient had been observed. Additionally, the in study of Yunqiao and Yan [22], BFPV power modeling was done using bidirectional gated recurrent unit network considering a FT system in Jiuquan, China, where a more accurate GE was given as the input variable by correction based on the criteria such as clearness of module.

While good accuracy had been seen, quantifying the reflection and module clearness were detected as two serious challenges. May et al. [23] also compared the ability of two machine learning methods, namely random forest and AdaBoost to estimate power output of different photovoltaic (PV) technologies mounted on a FT track in Pretoria, South Africa. The system contained BFPV. Module specifications, in addition to the wind speed, module and ambient temperature values, and plane of array irradiance were the input variables of models. High accuracy of AdaBoost for all the technologies had been observed based on the conducted analysis.

As the summation of power in a specific period of time, some investigations introduced ways to estimate the yield directly. An equation, which was a linear function of height, albedo, and tilt angle, had been given by Castillo-Aguilella and Hauser [24] to find bifacial energy energy gain. Accuracy evaluation was carried out for a number of FT BFPV systems with different tilt angles, located in New York and Arizona, USA, where a satisfactory level of error-related criteria had been reported. Furthermore, Ghenai et al. [25] simulated the performance of a BFPV unit by PVsyst. First, a parametric study was carried out to analyze the impact height, albedo, and tilt angle on annual energy production and bifacial energy gain. Then, response surface methodology (RSM) was utilized and quadratic polynomials were found for the annual energy production and bifacial energy gain, which were the function of the three investigated variables in the parametric study. A similar study was also done by Radwan et al. [26] for a BFPV system in Sharjah, UAE, where in addition to the height, albedo, and tilt angle, module spacing had been added to the considered variables. The module height had been indicated as the variable with the lowest impact on both annual energy and bifacial energy gain among the four.

In another work, Rodriguez-Pastor et al. [27] simulated the performance of a BFPV in agriculture application (AgriPV) using combination of the electrical modeling, heat transfer calculations, and view factors. Having developed and validated their model, some plots were drawn to see correlation between predicted values. The plots included the predicted energy vs. predicted front and rear irradiance. Correlation was also employed to find empirical models in the investigations of Alam et al. [28, 29]. Three correlations were taken into account for a FT BFPV system in Heriot-Watt University, Edinburgh, the UK, namely, RTI and bifacial energy gain, GE and power output, and total clearness index and RTI.

This project has received funding from the European Commission's Horizon Europe programme under grant agreement number 101096056.

The given GE for modeling could be an assumed value. It could also come from the recorded experimental data, or it could be obtained by some models to determine irradiance on the front and back of the module. Separate from all the studies reviewed so far, a part of literature with the subject of "BFPV modeling" has covered the investigations with the topic of finding the simulation ways to overcome the challenge of estimation of GTI and RTI, and consequently, GE accurately. A simple model to find RTI for a BFPV was proposed by Sahu et al. [30], which utilized solar geometry approach. The model was validated by comparing with PVSyst simulation and after validation, employed to calculate the energy annual energy yield for FT configuration in 4 places of India. The research had been followed by the investigation of Ref. [31]. In [31], RTI and after that the energy yield during a year were estimated using the same method (geometry approach). The model was approved using the experimental data and then, used to introduce the optimal tilt, spacing, and orientation for a FT BFPV in Kharagpur, India. Ernst et al. [32] utilized Monte Carlo ray tracing technique to estimate the amount of received irradiance on a FT BFPV system mounted on the rooftop of a building. They coupled the ray tracing method with electrical modeling to evaluate the system in terms of gain in the energy yield for Australia. A comparative study was also carried out by Longares et al. [33] between numerical irradiance models of PVsyst and Multiphysics based finite element method of COMSOL. The difference had been found considerable when sun is perpendicular to the ground and overcast conditions. Another comparative study between irradiance simulation ways had been conducted by Grommes et al. [34]. In that study, raytracing and view factor methodologies were combined. the obtained results were compared with only raytracing for both FT and SAT configuration in Germany and the USA, where the superiority of their proposed approach had been observed. Raytracing was found to have continues positive deviation. In addition, Sun et al. [35] presented an improved view-factor based methodology to calculate amount of the received irradiance for a BFPV system, which met the anisotropic irradiance assumption for the vertical, horizontal, and tilted mounting. Model validation was done using the data gathered from experiments, where lower accuracy was observed for higher albedo condition.

Reviewing the literature has shown that despite the valuable performed studies, there is still the gap of not availability of physical data-driven models for power estimation of a BFPV by which the contribution of the rear side to the power production could be determined separately. In addition, for the developed models in the previous works, RTI or albedo has been an input parameter but for many cases they are not available. Moreover, using simulation ways to determine RTI or albedo often imposes high computational cost, time, and difficulty, while their accuracy drops by increasing albedo. Taking these points into consideration, this work package aims at providing novel data-driven models to estimate BFPV power. One of the proposed models works with RTI as the input. However, as mentioned, RTI is not available for some cases, and therefore, another model is also presented which does not need RTI or albedo, and the input parameters consist of only the angle of incidence, sun elevation and azimuth angles, and clearness index.

The model development and input parameters selection are done in a way that it reflects a meaningful description of the process, which means it is also a physical model. Different tracking strategies and albedo conditions are investigated. Since the data has not been available for the greenhouse, the investigation considers other case studies. One of the case-studies is a FT plant in DTU, Roskilde, Denmark (indicated by DTU) [36, 37], these data are open access.

This project has received funding from the European Commission's Horizon Europe programme under grant agreement number 101096056.

Another, which is in Bolzano, Italy (indicated by BZ), is a SAT one, with both black and white color ground. The modeling results are compared with PVlib simulation, as the common way for this purpose.Tthe data used for SAT case are kindly provided by Eurac within the framework of the Horizon project, Trust-PV [38].

Methodology and data used

The methodology applied in this work has been discussed here. First, in the next section the developed approach is explained. After that, the employed way for data filtering is discussed. Finally, the considered case studies are introduced.

Developed approach

In the developed approach of this study, BFPV power (P^{BF}) is considered in the form of:

$$P^{BF} = P^{MF} + P_n^{BF,front} \times DBPG \quad (1)$$

Eq. (1) is schematically shown in Figure 1, as well.

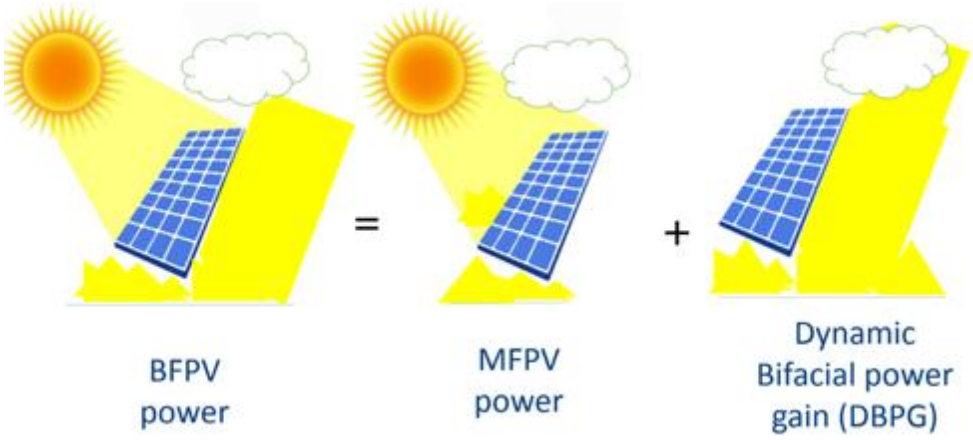

Figure 1. The graphical representation of the proposed approach.

In Eq. (1), $P_n^{BF,front}$ indicates the nominal power of the front side of BFPV, and P^{MF} denotes power of MFPV at the same global tilt irradiance (GTI) and ambient temperature (T_{amb}) as BFPV. Dynamic Bifacial Power Gain ($DBPG$), is also defined as ($DBPG$ should not be confused with the bifaciality coefficient):

$$DBPG = \frac{P^{BF} - P^{MF}}{P_n^{BF,front}} \quad (2)$$

Our Data Driven Model (DDM) estimates $DBPG$ with a polynomial function. If RTI is available, for both FT and SAT configurations, $DBPG$ is calculated from Eq. (3):

This project has received funding from the European Commission's Horizon Europe programme under grant agreement number 101096056.

$$DBPG^{(est\ model)_{DDM}} = PR_{rear} \times \left(\frac{RTI}{1000}\right) \quad (3)$$

On the other hand, if RTI is not available, the polynomial is a function of clearness index (K_{CS}), as a representative of solar radiation, and cosine of angle of incidence ($\cos(AOI)$) as a factor reflecting the relative position of BFPV compared to the sun for FT. For SAT, azimuth and elevation angles (AZ and EL) should be also added to the effective parameters. It means:

$$DBPG^{(est\ model)_{DDM}} = \begin{cases} g_{FT}(cos(AOI), K_{CS}) & Fixed-tilt\ (FT) \\ g_{SAT}(cos(AOI), K_{CS}, AZ, EL) & Single-axis\ tracking\ (SAT) \end{cases} \quad (4)$$

In which the superscript 'est' represents estimation. An installed BFPV plant usually consists of only bifacial modules and there is no MFPV with the same front side specifications there (like the investigated case-studies). Consequently, simulation is utilized to obtain MFPV power, and using the proposed model, BFPV power is estimated by Eq. (4):

$$P^{BF(est\ model)_{DDM}} = P^{MF(est\ model)_{PVlib}}(GTI, T_{amb}) + P_n^{BF,front} \times DBPG^{(est\ model)_{DDM}} \quad (5)$$

$P^{MF(est\ model)_{PVlib}}(GTI, T_{amb})$ is the simulated power of MFPV, which is a function of GTI and T_{amb}.

In contrast, PVlib approach is to use the monofacial estimation model but inputting the effective irradiance G_E [6]:

$$P^{BF(est\ model)_{PVlib}} = P^{MF(est\ model)_{PVlib}}(G_E, T_{amb}) \quad (6)$$

Where:

$$G_E = GTI + \varphi\ RTI \quad (7)$$

In which, φ is the bifaciality coefficient.

It is worth noting that $P^{MF(est\ model)_{PVlib}}$ in all the equations is MFPV power obtained by PVlib.

Data filtering

Developing DDM is done using the data refined by removing nights and after that, passing a statistical filter. The criterion for statistical filter is the performance ratio which is corrected by considering the temperature effect ($PR^*_{Temp\_corr}$):

$$PR^*_{Temp\_corr} = \frac{\frac{P^{BF}}{P_n^{BF,front}}}{(1+\gamma(T_{PV}-25))(\frac{GTI}{1000}+\varphi\frac{RTI}{1000})} \quad (8)$$

In which T_{PV} is temperature of PV. Additionally, γ denotes temperature coefficient of the maximum power. $P_n^{BF,front}$ also indicates the nominal power of front side of BFPV. In Eq. (8), $P_n^{BF,front}$ has been utilized to make BFPV power dimensionless and the superscript '*' is applied for PR to emphasize on that.

Case-studies

This project has received funding from the European Commission's Horizon Europe programme under grant agreement number 101096056.

As indicated before, the data for greenhouse has not been available yet, and therefore, DDM is developed for BFPV systems in two other locations. One is a FT plant in DTU, Roskilde, Denmark, while another is a SAT BFPV system. They are introduced in this part.

DTU: Fixed-Tilted configuration

The considered BFPV system consists of 4 rows. There are 22 modules per each row, resulting in 88 in total. The tilt angle is 25° for all of them. The data had been recorded for 11 months, from April 2019 to March 2020. Resolution of the recorded data is 1 hour. The important information of the utilized PV modules has been given in Table 1, while references [36, 37] are given for further details.

Table 1. The information of the modules for investigated case-studies

Parameter	Value/Condition	
	DTU	**BZ**
Number of PV (rows×PV per row)	4×22	2×12
BFPV technology	Passivated emitter and rear contact (PERC)	Heterojunction technology (HJT)
Nominal front capacity of the used modules ($P_n^{BF,\ Front}$)	295 W	375 W
Average bifaciality, lab measured (φ)	0.67	0.903
The temperature coefficient of maximum power (γ)	-0.39 %/°C	-0.250 %/°C

Single-axis tracking

The investigated case includes 24 modules, mounted on two strings. The share of each string is equal, which means 12 modules for each of them. For this case, the ground was black from July to October of 2022. Then, the ground color had been changed to white by applying the paint. For the white ground, the data measured between October 2022 and February 2024 was used as the input for modeling development. Here, data is available for each 15 minute. The key specifications of the used PV modules for this case are also listed in Table 1.

Results

The historical experimental data, which covers almost one year for DTU case and almost one year and a half for EURAC plant, is used to find the polynomial coefficients to determine $DBPG$ from the two proposed methods (Eq. (3) and Eq. (4)), and BFPV power from Eq. (5) afterwards. Then, the accuracy evaluation has been carried out by comparing with the real data. Comparison is also done with PVlib for BZ case. However, for DTU, PVlib could not be utilized using the real historical data. The reason is in DTU case, there is no historical RTI data.
As indicated, the data first has been filtered using a statistical filter (Eq. (8)) to remove outlier (due to the near shadowing), and then, 70% of the filtered data has been employed for training, while 30% is kept for test. The results are separated for models with and without needs for RTI.
Model with RTI

This project has received funding from the European Commission's Horizon Europe programme under grant agreement number 101096056.

This section starts with finding PR_{rear} values, and continues by comparing estimation of our proposed model with PVlib.

Finding PR_{rear}

70% of the filtered data is utilized for training and using them, PR_{rear} has been obtained. For this purpose, DBPG data against $\frac{RTI}{1000}$ is plotted and the slope of the fitted line is introduced as PR_{rear} (Figure 2a for black ground and Figure 2b for white ground). Figure 2 has indicated that changing ground color from the black to the white leads to bigger *RTI* values, as the range of $\frac{RTI}{1000}$ for white surface is much greater than the black one. The highest value for $\frac{RTI}{1000}$ when ground is black is ~0.12. For white ground it is approximately 3 times more (~0.35). The higher $\frac{RTI}{1000}$ range is accompanied by more DBPG for the white ground color. The maximum of DBPG for black and white ground conditions are ~0.05 and ~0.18, respectively.

The amount of RTI is different for different modules in a BFPV system with a number of modules putting together in strings and rows (Like our case-study). The modules closer to the edge receive greater RTI since around them there is more unshaded ground. The phenomenon is known as the "edge effect". [1] The RTI used to draw Figure 2a and Figure 2b is measured for a place near the center of strings. Since edge effect is more intense for higher albedo conditions [1], at a constant value for measured RTI close to the center, the total received RTI for the whole string is more for the white ground than black ground. Therefore, more energy is available to be converted to the electricity by rear side, and for that reason, the defined PR_{rear} is higher for bigger albedo case, i.e., white ground. Running BFPV on black ground leads to PR_{rear} of 0.2544. Painting the ground to white make it 82.5% more, where it reaches 0.4642. It indicates that application of BFPV in the higher albedo condition provides much greater DBPG, and consequently, total power output.

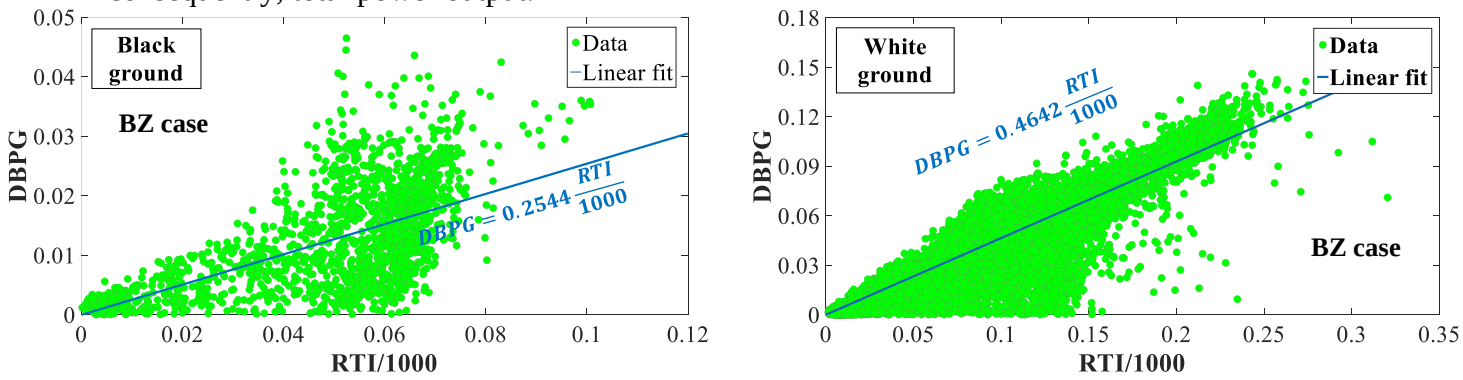

(a) **(b)**

Figure 2. Finding the values of PR_{rear}; (a) Black ground; (b) White ground.

Accuracy evaluation compared to PVlib

The accuracy evaluation of the proposed model is carried out in two ways:

Comparing the error related criteria for the test data, as seen in

Figure 3 (30% of the filtered data is kept for test).

Comparing the estimation for a sample clear-sky day and a sample overcast day (Figure 4).

There has not been any data from the sample days in the training set.

This project has received funding from the European Commission's Horizon Europe programme under grant agreement number 101096056.

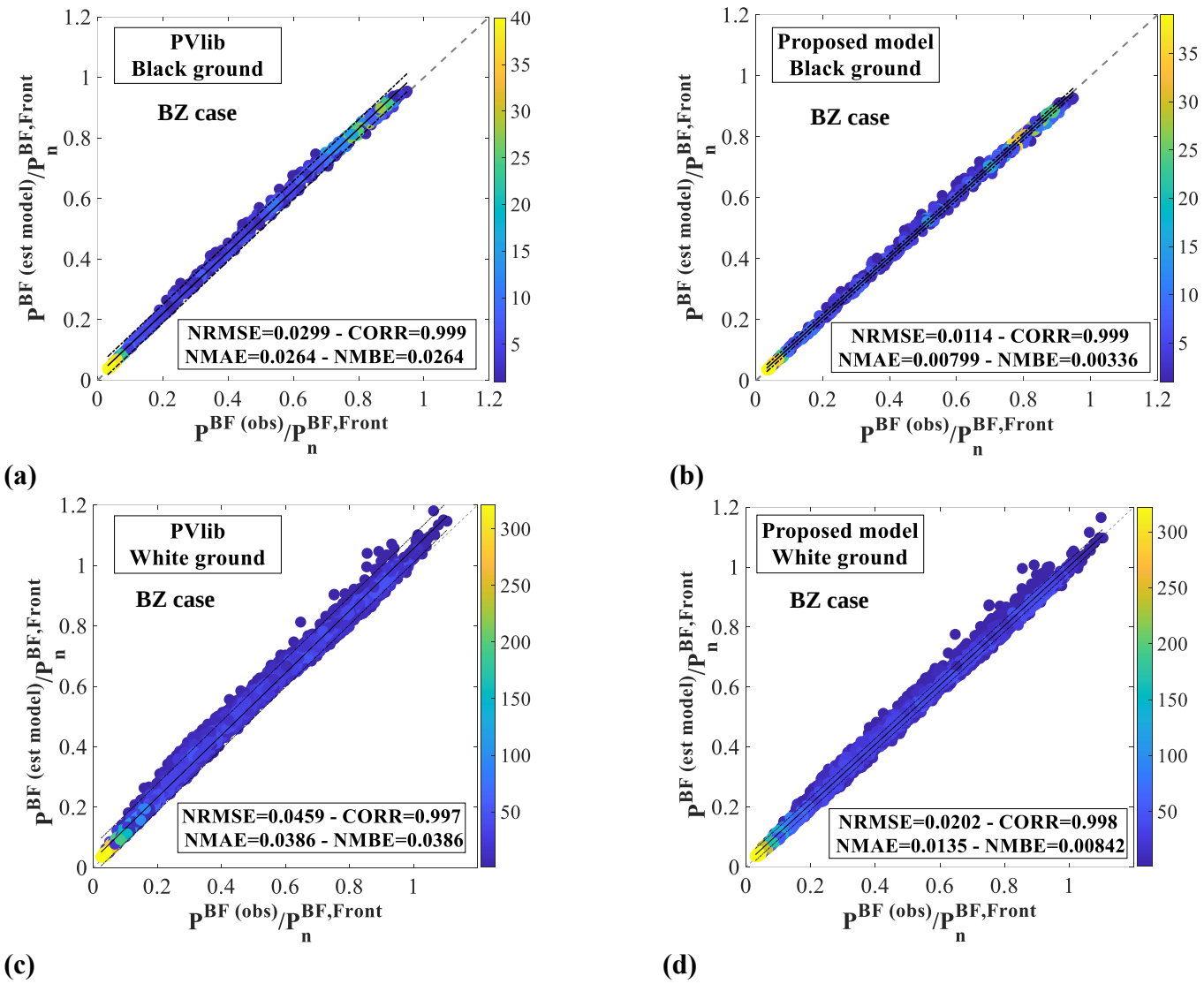

Figure 3. Checking the accuracy using the test data for power estimation by the proposed model with RTI for BZ case (a) PVlib, black ground; (b) Proposed model, black ground; (c) PVlib, white ground; (d) Proposed model, white ground.

Figure 3a and
Figure 3c have shown that for both black and white ground conditions PVlib has overestimation. It could be also seen in the daily profiles of Figure 4a to Figure 4d. One probable reason is a bigger declared bifaciality by manufacturer than the actual one. In addition, degradation has not been considered in the modeling, which is another cause. Another issue is assuming a constant RTI (A value for a place close to center) for the whole string in modeling by PVlib, whereas in reality it is not (Due to phenomena like edge effect). The impact is more when RTI is higher, which results in higher error for white surface.
Overestimation of PVlib decreases when our model has been employed. According to

This project has received funding from the European Commission's Horizon Europe programme under grant agreement number 101096056.

Figure 3, application of the proposed model leads to a significant decrease in normalized mean bias error (NMBE), from 2.64 to 0.34% for the black ground, and from 3.86 to 0.84% for the white ground. Moreover, NRMSE has been improved considerably. It reaches from 2.99% to 1.14% when ground is black. The enhancement is greater for the white surface, where PVlib and our model offer the values of 4.59% and 2.02% respectively. Better operation of the proposed model could be confirmed by checking the daily profiles for the sample clear-sky and overcast days (Figure 4). For both sample days and two ground conditions, the proposed model is able to achieve much closer estimation than PVlib. Even in the times with the near shadow, whose data have not been utilized as the input of modeling, the proposed approach works slightly better.

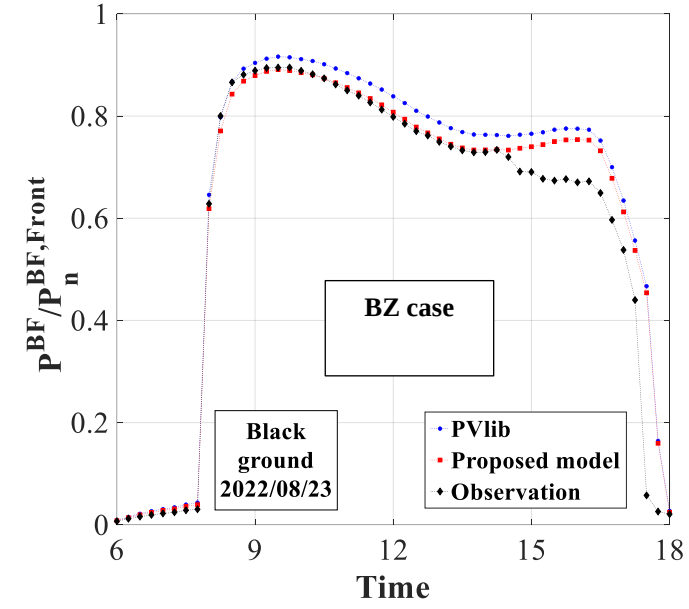

(a)

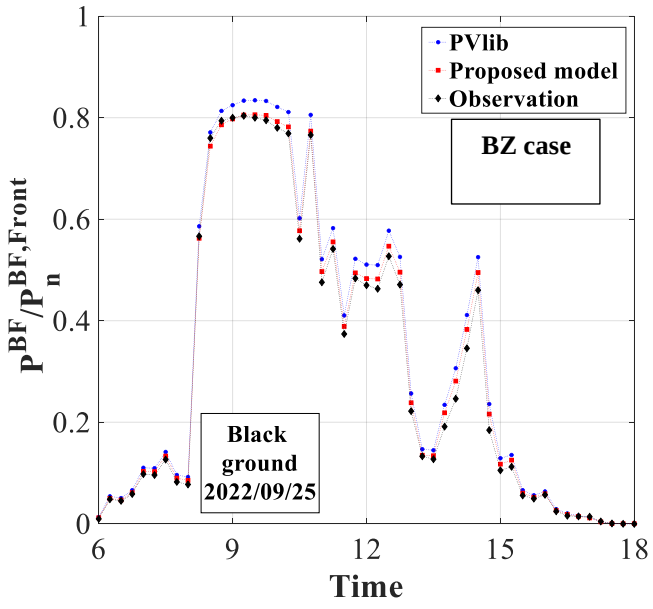

(b)

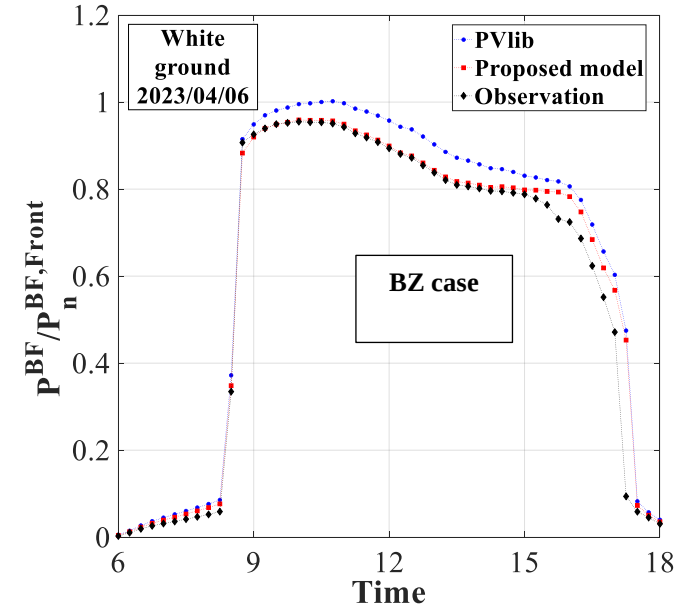

(c)

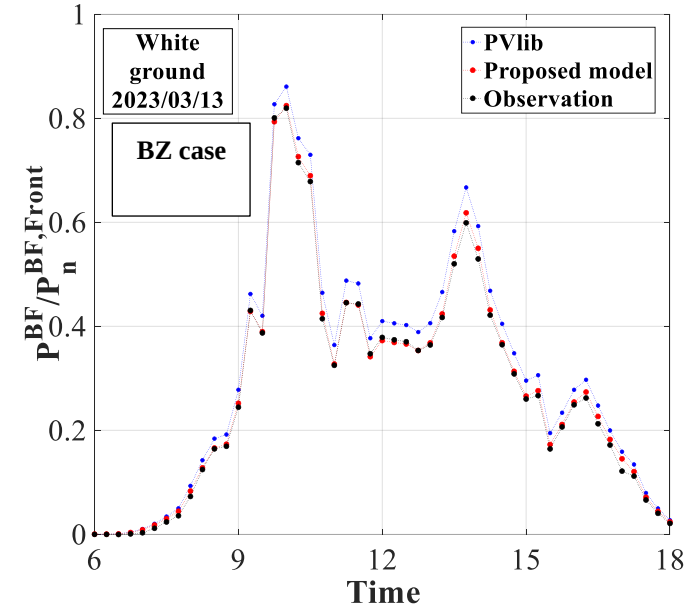

(d)

This project has received funding from the European Commission's Horizon Europe programme under grant agreement number 101096056.

Figure 4. Comparing hourly profiles of power estimated by PVlib and our model (RTI needed) with the observed data for sample days in BZ case (a) PVlib, black ground; (b) Proposed model, black ground; (c) PVlib, white ground; (d) Proposed model, white ground.

Model without RTI

Based on Figure 5b, the developed model reaches NRMSE of 0.98% for BZ plant with black ground, while PVlib estimation obtains just 2.99% (Figure 5a). Here, as per Figure 6a and Figure 7a, PVlib has overestimation, which has been considerably decreased using the data-driven model for the whole days, either the day is clear-sky or overcast. The main reason is that a uniform RTI distribution all-over the strings is assumed (equal to the measured value), while in reality, there is not. Another reason might be smaller bifaciality coefficient than the manufacturer declaration for some modules in the strings.

Power estimation by the proposed model is accompanying by even much better accuracy than PVlib for BZ plant with white ground (Figure 5c and Figure 5d). Our data-driven model improves estimation accuracy by 3.04% with a NRMSE of 1.55% compared to 4.59% of PVlib. The reason for increasing PVlib NRMSE in SAT compared to FT, and white ground in comparison to black ground is that the RTI spatial distribution has got a higher impact on the performance. The PVlib model is unable to consider this, while our model can. Moreover, Figure 6b and Figure 7b indicate the same fashion as black ground for white ground condition. It means much closer estimation by the provided model compared to PVlib remarkable overestimation.

In addition, For DTU plant, with FT configuration, NRMSE is 1.38% (Figure 5e) for our model, while PVlib could not be utilized due to lack of RTI data. Like SAT, for this case, good agreement between the estimation by model and observation has been seen for both clear-sky and overcast days, as per Figure 6c and Figure 7c.

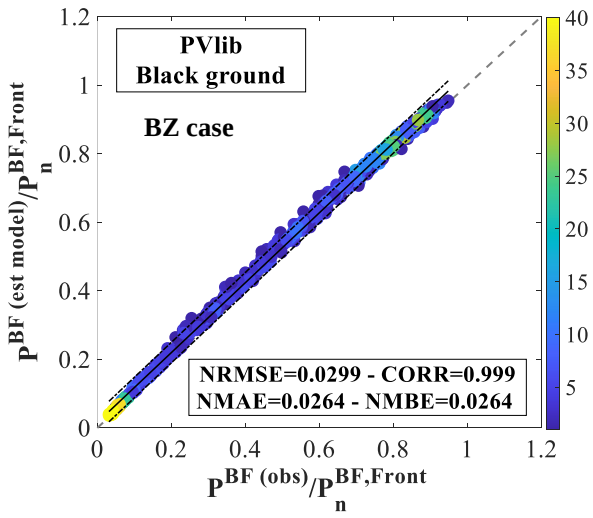

(a)

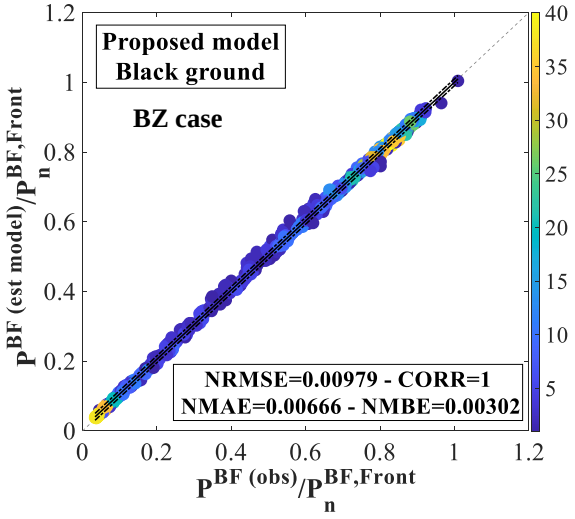

(b)

This project has received funding from the European Commission's Horizon Europe programme under grant agreement number 101096056.

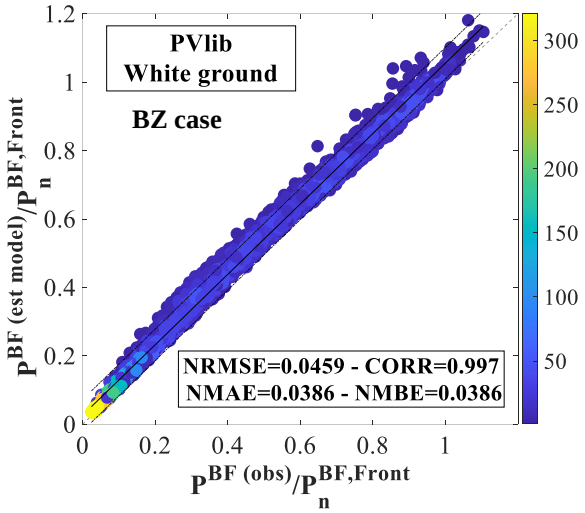

(c)

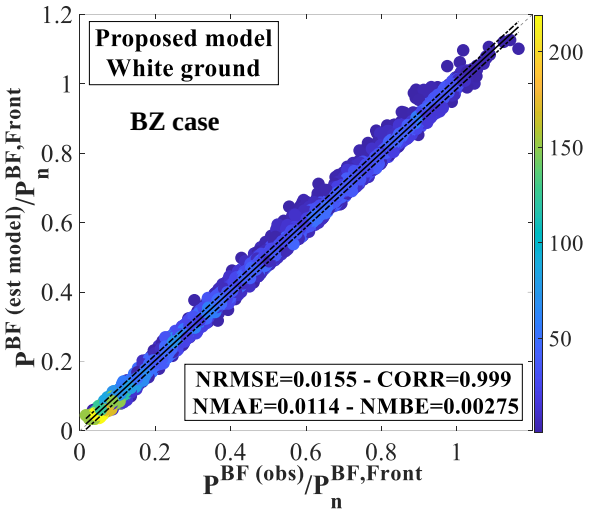

(d)

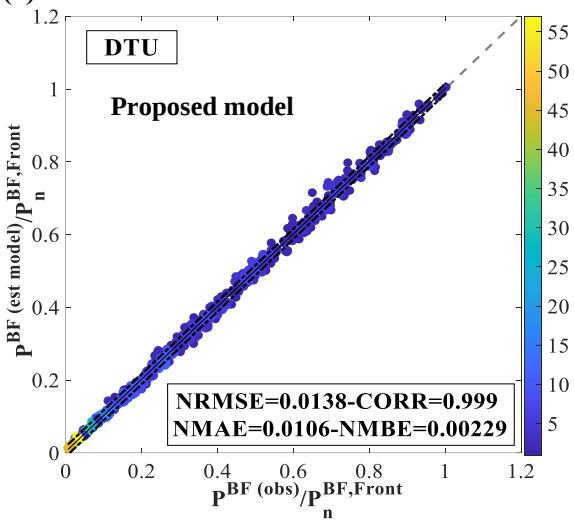

(e)

Figure 5. Checking the accuracy using the test data for power estimation using the proposed model without RIT (a) PVlib, black ground; (b) Proposed model, black ground; (c) PVlib, white ground; (d) Proposed model, white ground.

This project has received funding from the European Commission's Horizon Europe programme under grant agreement number 101096056.

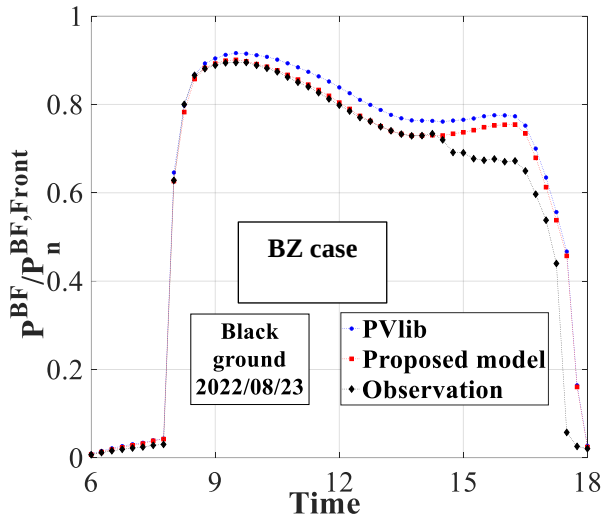

(a)

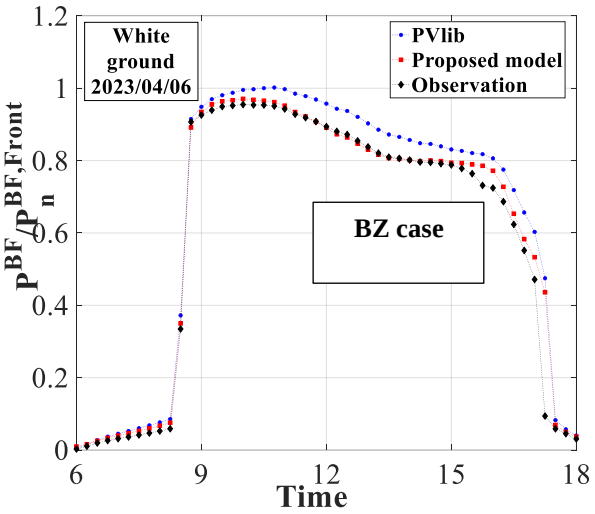

(b)

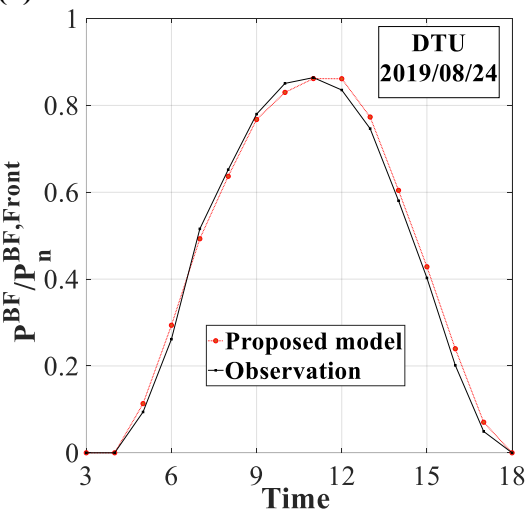

(c)

Figure 6. Comparing the prediction ability of the models with observation for a sample clear-sky day (a) BZ case, black ground; (b) BZ case, white ground; (c) DTU case.

This project has received funding from the European Commission's Horizon Europe programme under grant agreement number 101096056.

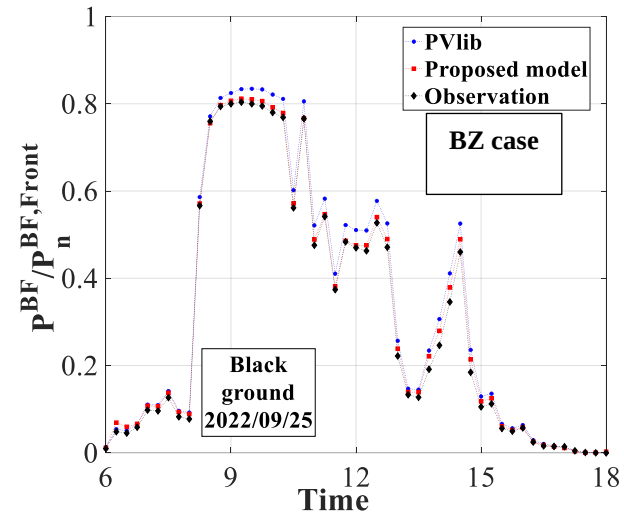

(a)

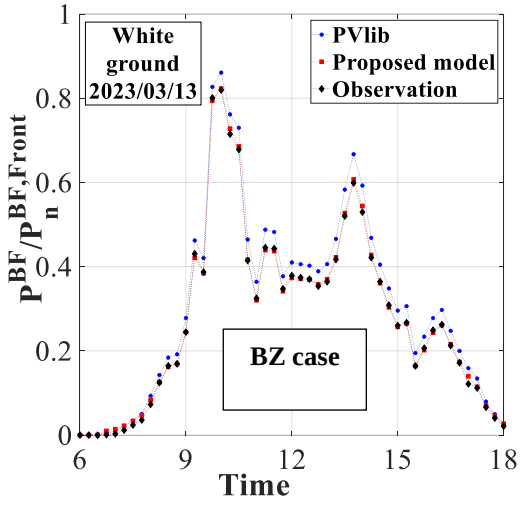

(b)

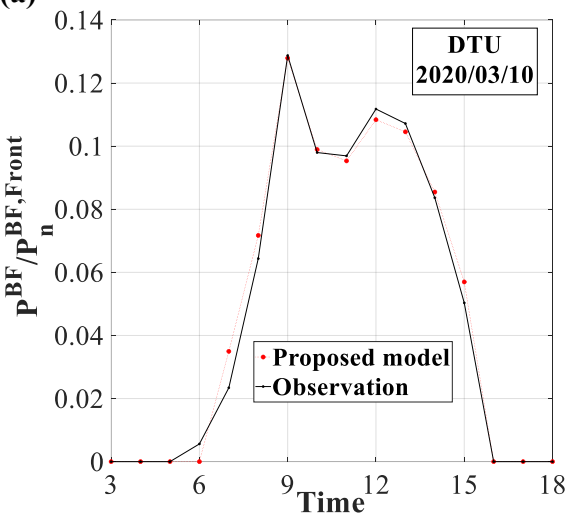

(c)

Figure 7. Comparing the prediction ability of the models with observation for a sample overcase day (a) BZ case, black ground; (b) BZ case, white ground; (c) DTU case.

Conclusion

Data-driven physical models have been proposed here to estimate DBPG, and consequently, the output power of a BFPV. Model development has been carried out for two conditions, namely, with and without RTI. The proposed models have been developed for a FT BFPV system in DTU, Denmark, and a SAT BFPV system, located in Bolzano, Italy, for black and white ground conditions. The accuracy of the proposed models was then compared with PVlib, as the common approach for this purpose. The comparison was done in terms of different error-related criteria, including NRMSE and NMBE. Table 2 summarizes the obtained results.

Table 2. Summary of the results

Parameter	NRMSE			Albedo data	Historical data
	SAT	SAT	FT		

This project has received funding from the European Commission's Horizon Europe programme under grant agreement number 101096056.

	(Black ground)	(White ground)			
PVLib	2.99	4.59	N.A.	✓	X
Data-driven model (RTI available)	1.14	2.02	N.A.	✓	✓
Data driven model (RTI not available)	0.98	1.55	1.38	X	✓

The results have shown the superiority of the both proposed models over PVlib for all the investigated conditions. When RTI data is not available, like DTU case, PVlib could not run since it needs that as input variable. For this case, NRMSE has the low value of 1.38% for our model. In case ground was black and white, PVlib has NRMSE of 2.99 and 4.59%. The corresponding values for the proposed model with RTI were 1.14 and 2.02%, and 0.98 and 1.55% for the presented model without RTI. The improvement compared to PVlib was found greater for the white ground (high albedo) than black ground (low albedo). BFPV systems in most of the applications, including Agri PV, is working in the higher albedo conditions.

Outlook

Within the framework of the work package, as the achievement, accurate models to obtain the power output of BFPV system have been developed and validated for a variety of mounting strategies and albedo condition. In order to go forward, there are a number of problems which should be solved. The most important ones are:

- RTI should be measured at several points (Including edges)
- Finding the impacts of effects on BFPV performance
- Requiring the historical performance data for model development of greenhouse
- Dynamic albedo should be considered
- The next steps also includes:
- BFPV performance characterization to find impact of different effects
- Recording the data for modeling from Greenhouses
- Test the model on data from other Agri-PV systems
- Study interaction of crops and panels (radiation to the crops and dynamic albedo)
- Considering reduction of radiation due to covering in greenhouse

Acknowledgement

Data for FT case comes from DTU open access data [36, 37], which authors acknowledge. Moreover, the research leading to the results for SAT case has received funding from the Horizon 2020 research and innovation programme, under Grant Agreement No. 952957, Trust-PV project. Moreover, Ali Sohani thanks fellowship funding from MUR (Ministero dell'Università e della Ricerca) under PON/DM/1061.

References

[1] Stein J, Reise C, Castro JB, Friesen G, Maugeri G, Urrejola E, et al. Bifacial photovoltaic modules and systems: Experience and results from international research and pilot applications. Sandia National Lab.(SNL-NM), Albuquerque, NM (United States); Fraunhofer …; 2021.
[2] Farghali M, Osman AI, Mohamed IMA, Chen Z, Chen L, Ihara I, et al. Strategies to save energy in the context of the energy crisis: a review. Environmental Chemistry Letters. 2023:1-37.
[3] The 14th International Technology Roadmap for Photovoltaic (ITRPV) < https://www.vdma.org/international-technology-roadmap-photovoltaic>; Accessed on January 31, 2024. . 2023.
[4] Alectris. Agrivoltaics Growth: A $9.3 Billion Market by 2031 <https://alectris.com/2023/11/10/the-growing-landscape-of-agrivoltaics-a-9-3-billion-market-by-2031/>; Accessed on June 15, 2024. 2023.
[5] Ganesan K, Winston DP, Sugumar S, Prasath TH. Performance investigation of n-type PERT bifacial solar photovoltaic module installed at different elevations. Renewable Energy. 2024;227:120526.
[6] Holmgren WF, Hansen CW, Mikofski MA. pvlib python: A python package for modeling solar energy systems. Journal of Open Source Software. 2018;3(29):884.
[7] Sánchez H, Negroni JJ, Meza C, Dittmann S, Gottschalg R. Potential of Vertical Bifacial PV in Chile. Conference Potential of Vertical Bifacial PV in Chile. IEEE, p. 1-5.
[8] Bruhwyler R, Sánchez H, Meza C, Lebeau F, Brunet P, Dabadie G, et al. Vertical agrivoltaics and its potential for electricity production and agricultural water demand: A case study in the area of Chanco, Chile. Sustainable Energy Technologies and Assessments. 2023;60:103425.
[9] Babinec S, Baring-Gould I, Bender AN, Blair N, Li X, Muehleisen RT, et al. Techno-economic analysis of renewable energy generation at the South Pole. Renewable and Sustainable Energy Reviews. 2024;193:114274.
[10] Willockx B, Lavaert C, Cappelle J. Geospatial assessment of elevated agrivoltaics on arable land in Europe to highlight the implications on design, land use and economic level. Energy Reports. 2022;8:8736-51.
[11] Isaza A, Kay M, Evans JP, Prasad A, Bremner S. Maximizing photovoltaic potential and minimizing costs in a future warmer climate: The role of atmospheric aerosols and greenhouse gas emissions. Renewable Energy. 2023;219:119561.
[12] Micheli L, Fernández EF, Aguilera JT, Almonacid F. Economics of seasonal photovoltaic soiling and cleaning optimization scenarios. Energy. 2021;215:119018.
[13] Bouchakour S, Valencia-Caballero D, Luna A, Roman E, Boudjelthia EAK, Rodríguez P. Modelling and simulation of bifacial pv production using monofacial electrical models. Energies. 2021;14(14):4224.
[14] Bouchakour S, Caballero DV, Luna A, Medina ER, El Amin KB, Cortés PR. Monitoring, modelling and simulation of bifacial PV modules over normal and high albedos. Conference Monitoring, modelling and simulation of bifacial PV modules over normal and high albedos. IEEE, p. 252-6.
[15] Ortiz Rivera EI. Modeling and analysis of solar distributed generation. Ph D Thesis. 2006.
[16] Yuan J, Tian Z, Ma J, Man KL, Li B. A Digital Twin Approach for Modeling Electrical Characteristics of Bifacial Solar Panels. Conference A Digital Twin Approach for Modeling Electrical Characteristics of Bifacial Solar Panels. IEEE, p. 317-21.
[17] Mannino G, Tina GM, Jiménez-Castillo G, Cacciato M, Bizzarri F, Canino A. Nonlinear and multivariate regression models of current and voltage at maximum power point of bifacial photovoltaic strings. Solar Energy. 2024;269:112357.

This project has received funding from the European Commission's Horizon Europe programme under grant agreement number 101096056.

[18] King DL, Kratochvil JA, Boyson WE. Photovoltaic array performance model: Citeseer, 2004.
[19] Cristaldi L, Faifer M, Laurano C, Petkovski E, Toscani S, Ottoboni R. An innovative model-based algorithm for power control strategy of photovoltaic panels. Conference An innovative model-based algorithm for power control strategy of photovoltaic panels. IEEE, p. 1-6.
[20] Faifer M, Cristaldi L, Toscani S, Soulantiantork P, Rossi M. Iterative model-based Maximum Power Point Tracker for photovoltaic panels. Conference Iterative model-based Maximum Power Point Tracker for photovoltaic panels. IEEE, p. 1273-8.
[21] Ghenai C, Ahmad FF, Rejeb O, Bettayeb M. Artificial neural networks for power output forecasting from bifacial solar PV system with enhanced building roof surface Albedo. Journal of Building Engineering. 2022;56:104799.
[22] Yunqiao L, Yan F. An innovative power prediction method for bifacial PV modules. Electrical Engineering. 2023;105(4):2151-9.
[23] May SI, Pratt LE, Roro KT, Bokoro P. Power output predictions of photovoltaic system using machine learning. Conference Power output predictions of photovoltaic system using machine learning.
[24] Castillo-Aguilella JE, Hauser PS. Multi-variable bifacial photovoltaic module test results and best-fit annual bifacial energy yield model. Ieee Access. 2016;4:498-506.
[25] Ghenai C, Ahmad FF, Rejeb O, Hamid AK. Sensitivity analysis of design parameters and power gain correlations of bi-facial solar PV system using response surface methodology. Solar Energy. 2021;223:44-53.
[26] Radwan A, Mdallal A, Haridy S, Abdelkareem MA, Alami AH, Olabi AG. Optimizing the annual energy yield of a residential bifacial photovoltaic system using response surface methodology. Renewable Energy. 2024;222:119914.
[27] Rodriguez-Pastor DA, Ildefonso-Sanchez AF, Soltero VM, Peralta ME, Chacartegui R. A new predictive model for the design and evaluation of bifacial photovoltaic plants under the influence of vegetation soils. Journal of Cleaner Production. 2023;385:135701.
[28] Alam M, Gul MS, Muneer T. Performance analysis and comparison between bifacial and monofacial solar photovoltaic at various ground albedo conditions. Renewable Energy Focus. 2023;44:295-316.
[29] Alam M. Energy yield enhancement of bifacial photovoltaic modules. 2023.
[30] Sahu PK, Roy JN, Chakraborty C, Sundaram S. A new model for estimation of energy extraction from bifacial photovoltaic modules. Energies. 2021;14(16):5089.
[31] Sahu PK, Roy JN, Chakraborty C. Performance assessment of a bifacial PV system using a new energy estimation model. Solar Energy. 2023;262:111818.
[32] Ernst M, Liu X, Asselineau CA, Chen D, Huang C, Lennon A. Accurate modelling of the bifacial gain potential of rooftop solar photovoltaic systems. Energy Conversion and Management. 2024;300:117947.
[33] Longares JM, García-Jiménez A, García-Polanco N. Multiphysics simulation of bifacial photovoltaic modules and software comparison. Solar Energy. 2023;257:155-63.
[34] Grommes E-M, Schemann F, Klag F, Nows S, Blieske U. Simulation of the irradiance and yield calculation of bifacial PV systems in the USA and Germany by combining ray tracing and view factor model. EPJ Photovoltaics. 2023;14:11.
[35] Sun B, Lu L, Yuan Y, Ocłoń P. Development and validation of a concise and anisotropic irradiance model for bifacial photovoltaic modules. Renewable Energy. 2023;209:442-52.

This project has received funding from the European Commission's Horizon Europe programme under grant agreement number 101096056.

[36] Riedel N, Berrian D, Alvarez Mira D, Protti AA, Poulsen PB, Libal J, et al. Data used in "Validation of Bifacial Photovoltaic Simulation Software against Monitoring Data from Large-Scale Single-Axis Trackers and Fixed Tilt Systems in Denmark". Technical University of Denmark. Dataset. https://doi.org/10.11583/DTU.13580759.v3. 2021.
[37] Riedel-Lyngskær N, Berrian D, Alvarez Mira D, Aguilar Protti A, Poulsen PB, Libal J, et al. Validation of bifacial photovoltaic simulation software against monitoring data from large-scale single-axis trackers and fixed tilt systems in Denmark. Applied Sciences. 2020;10(23):8487.
[38] TRUSTPV: Solar PV, Performance & Reliability <https://trust-pv.eu/>; Accessed on July 17, 2024.

This project has received funding from the European Commission's Horizon Europe programme under grant agreement number 101096056.

Task 4.4 Water efficiency modelling

Introduction

Task 4.4, focusing on water efficiency modeling, represents a critical component of Work Package 4 (WP4) within the REGACE project. The objective of this task is to optimize water use in PV greenhouses, ensuring that the integration of advanced photovoltaic technologies does not compromise, but rather enhances, the sustainability of agricultural practices. Led by Humboldt University (HU), this task leverages state-of-the-art irrigation systems and detailed water balance analyses to understand and improve water use efficiency in PV greenhouses under varying conditions.

At the Berlin-Dahlem site, a completely closed recirculating irrigation system has been implemented in the greenhouse where the REGACE PV system is installed. This system allows for precise measurement of water inflow and outflow, thereby facilitating the calculation of water balances over an entire growing season. The setup includes water meters for monitoring water input and tipping bucket meters for measuring drainage. This detailed monitoring is essential for comparing water use efficiency under different experimental conditions.
The greenhouse with the PV system, referred to as the collector greenhouse, operates in a closed mode. This mode is enhanced by cooling finned pipes installed under the roof, which not only cool and dehumidify the air but also contribute to cooling the PV panels, potentially increasing their energy yield. Adjacent to the collector greenhouse is an identical reference greenhouse that operates without cooling and PV modules. The comparison between these two setups provides valuable insights into the effects of the PV system on water use efficiency.
Preliminary results have shown significant differences in water consumption between the collector and reference greenhouses. The closed greenhouse maintains a higher relative humidity, resulting in lower plant transpiration rates compared to the collector greenhouse. Moreover, the condensation of water vapor in the closed greenhouse reduces overall water consumption, as the condensed water is returned to the irrigation system. This efficient water recycling mechanism highlights the potential benefits of integrating PV systems with advanced irrigation technologies.

In addition to the Berlin site, water use efficiency is being investigated at other experimental locations. At these sites, irrigation areas under PV modules are equipped with separate water meters, allowing for detailed comparisons with reference areas without PV coverage. This setup enables the assessment of water use efficiency across different greenhouse designs and geographic locations, contributing to a comprehensive understanding of the impacts of PV systems on water consumption.

To further enhance water use efficiency modeling, HU has developed the BERMONIS-plant monitoring system, which includes leaf transpiration sensors and soil moisture sensors. This system has been installed at the Watzkendorf site, enabling precise control of irrigation based on real-time plant and soil data. The BERMONIS system facilitates high-precision irrigation control, ensuring optimal water use while maintaining desired soil moisture levels. This approach not only conserves water but also supports healthy plant growth, maximizing yield.

This project has received funding from the European Commission's Horizon Europe programme under grant agreement number 101096056.

A relevant aspect of this task involves examining the influence of CO2 concentration on water use efficiency. Experiments conducted in a climate chamber have demonstrated that increased CO2 levels can reduce plant transpiration rates and improve water use efficiency. These findings are crucial for developing strategies to enhance the performance of PV greenhouses, especially under conditions of reduced light availability.

In the climate chamber experiments, tomatoes were grown in a hydroponic system under controlled light and CO2 conditions. The results indicated that higher CO2 levels could compensate for reduced light, significantly improving water use efficiency. This research underscores the potential of optimizing CO2 levels to balance water use and enhance crop productivity in PV greenhouses.

The insights gained from Task 4.4 are instrumental in achieving the overall objectives of WP4. By integrating advanced irrigation technologies and detailed water balance analyses with the broader PV greenhouse system models, this task supports the development of sustainable and efficient agrivoltaic systems. The progress made so far aligns with the project's timeline and sets the stage for continued refinement and validation of water use efficiency models.

Activities

In the greenhouse in Berlin-Dahlem where the Regace PV system was installed (collector greenhouse), a water balance was carried out over an entire growing season. The balance was calculated by measuring the water inflow using water meters and the drainage using tipping bucket meters.

The collector greenhouse is operated in closed mode. Cooling finned pipes are installed under the roof. These cool and dehumidify the greenhouse air and cool the PV panels as well, which is expected to result in a higher energy yield. Next to the collector greenhouse is an identical greenhouse (reference greenhouse) without cooling and PV modules with conventional equipment.

There are several reasons for the large differences in water consumption. The relative humidity in the closed greenhouse is much higher than in the collector greenhouse. This results in a lower transpiration performance of the plants (difference between reference and collector without water recirculation in Fig. 1).

This project has received funding from the European Commission's Horizon Europe programme under grant agreement number 101096056.

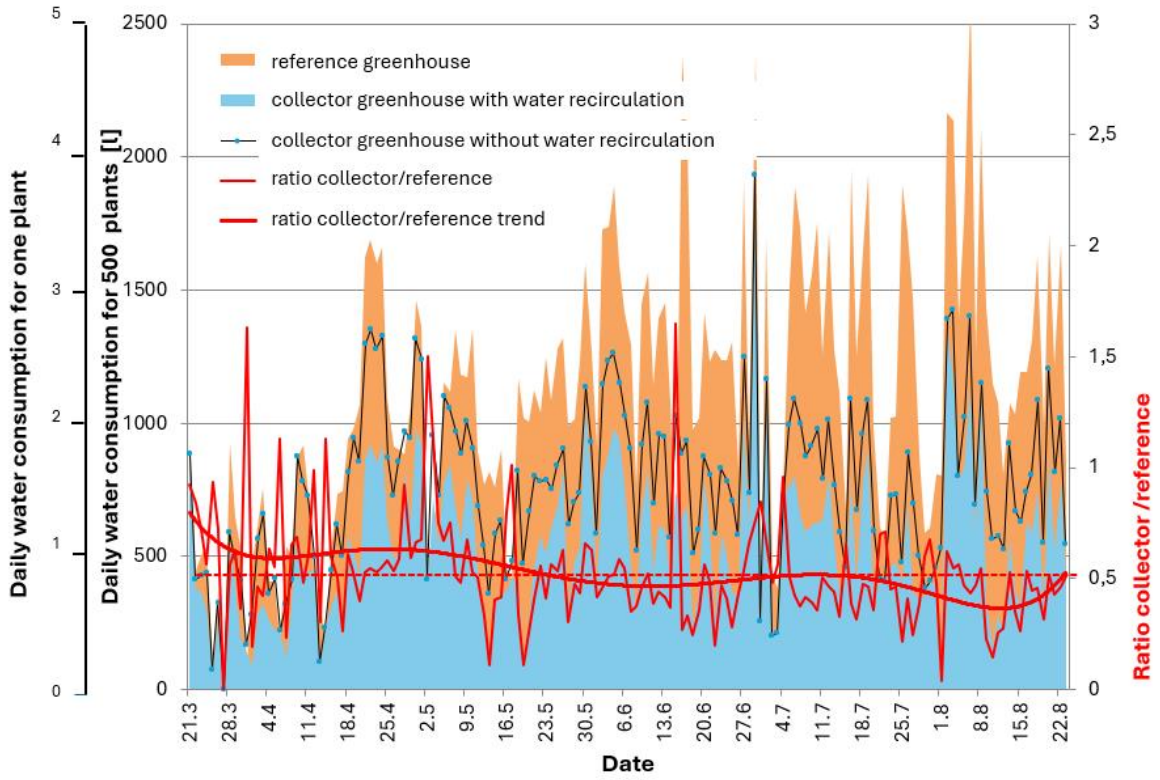

Fig. 1 Water balances of the collector and reference greenhouse

The condensed water from the collector greenhouse is returned to the irrigation system, resulting in a lower water consumption (difference between reference and collector with recirculation).

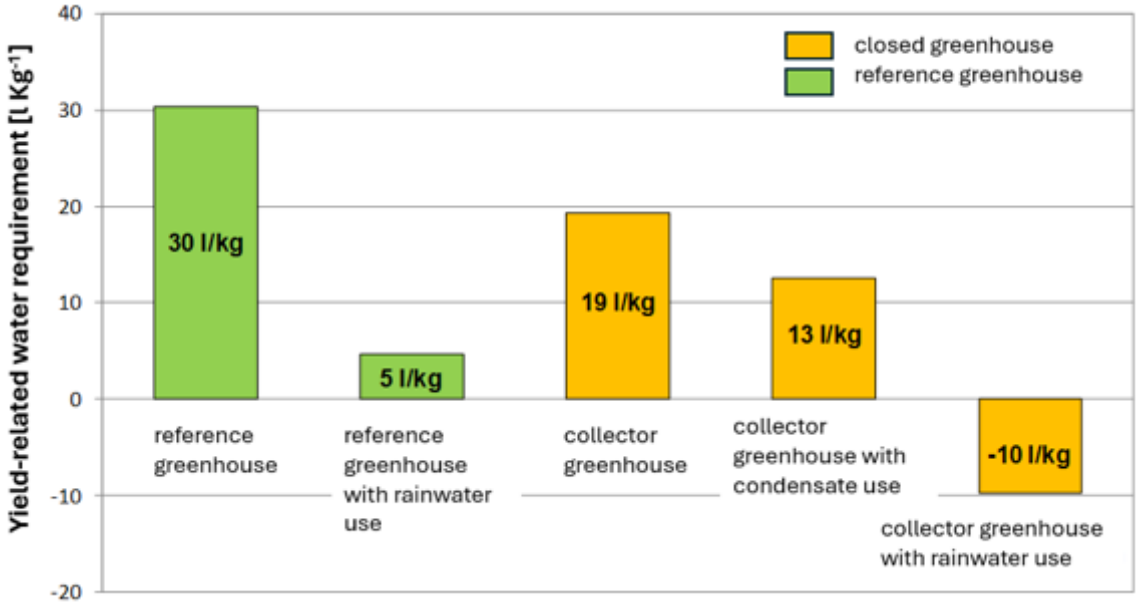

Fig. 2 Scenarios of water demand in tomato cultivation in hydroponic systems and closed greenhouse operation

This project has received funding from the European Commission's Horizon Europe programme under grant agreement number 101096056.

In terms of balancing water requirements, the closed collector greenhouse has the advantage that the recondensation of transpiration water vapor leads to an additional reduction in water turnover. In this case, even with a rainfall of 550 mm at the site, there can be a water surplus of 10 liters per kilogram of crop harvested.

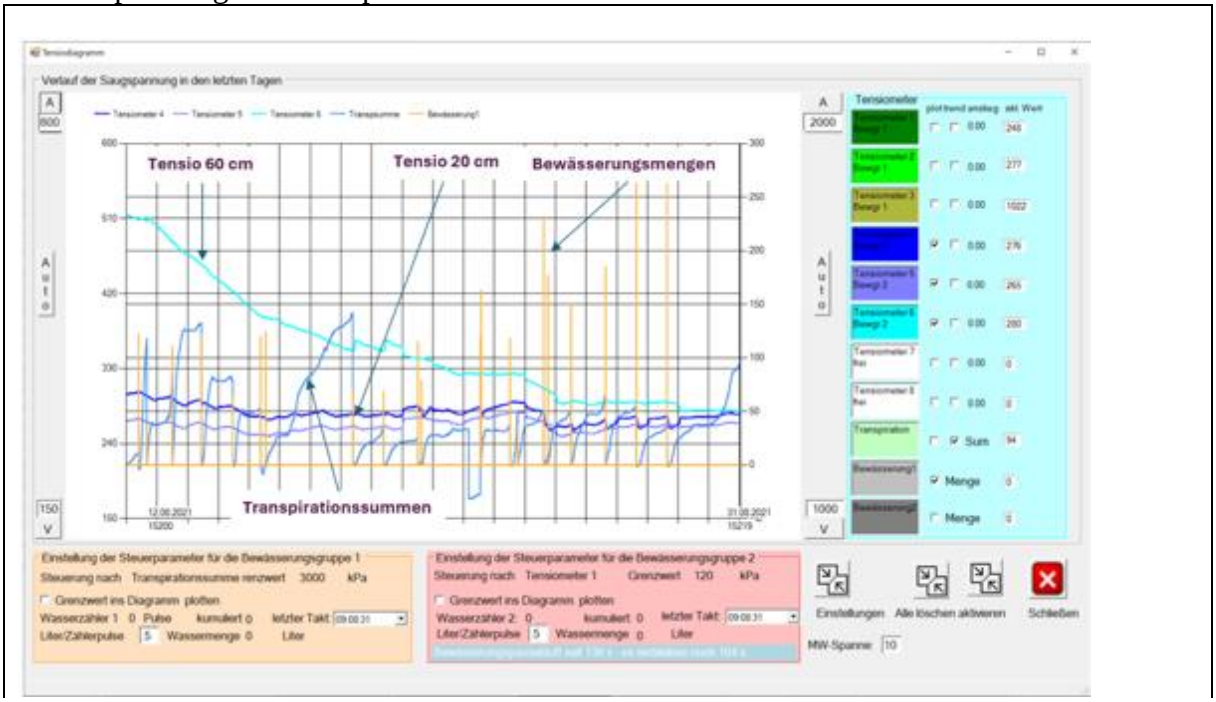

Fig. 3 Snapshot of the BERMONIS irrigation control dashboard

For the Regace partner in Watzkendorf, the Humboldt University developed measurement technology and software to control the irrigation under the PV modules using leaf transpiration sensors and soil moisture sensors. This system will be used to create water balances.

two of ten leaf cuvettes

This project has received funding from the European Commission's Horizon Europe programme under grant agreement number 101096056.

Fig. 4 The BERMONIS-plant monitoring system, developed on Humboldt University, installed in a Greenhouse in the Watzkendorf organic farm

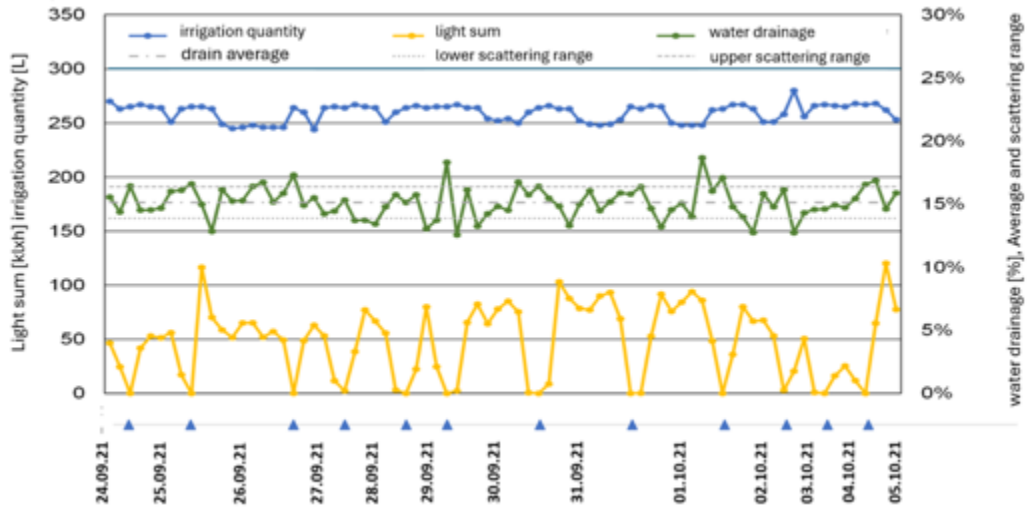

Fig. 5 Irrigation control according to transpiration sums and their effects on the drain

With this system, irrigation can be controlled with high precision. In a hydroponic system for tomato production in the greenhouse where the solar collector system was installed, irrigation was controlled by adding up the leaf transpiration. The controlled drainage of 15% could be maintained over several days with a small range of variation.

A climate chamber experiment was started in 2020 to investigate the influence of CO2 concentration in the air on water use by plants. It was investigated whether an increased CO2 level in the air can compensate for the reduction in light and how this changes water use efficiency. Experiments were carried out with tomatoes in a hydroponic system.

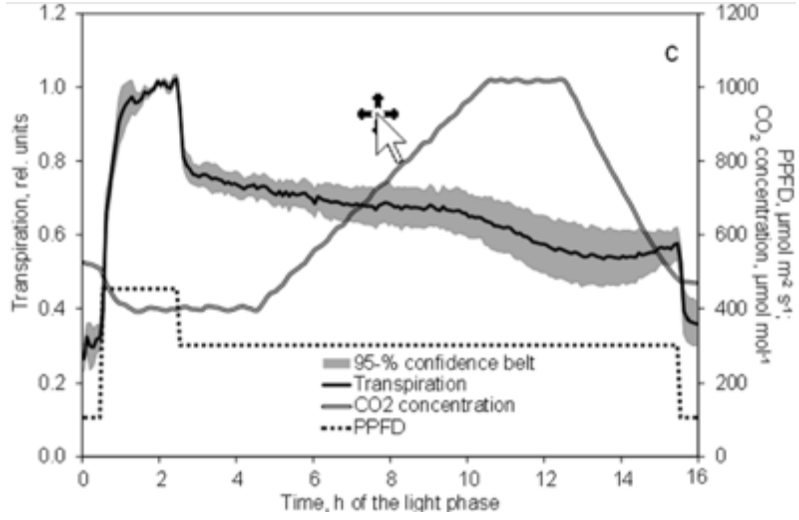

This project has received funding from the European Commission's Horizon Europe programme under grant agreement number 101096056.

Fig. 6 Decrease of leaf transpiration with increasing CO2-Level of the ambient air in a climate chamber under constant light conditions.

In the climate chamber, the light produced by LED lamps was increased during the first three hours of the day to measure the effect of light on photosynthesis. After reducing the light from the third hour, the CO2 concentration was slowly increased. The progress of photosynthesis and transpiration of the plants was measured with a Phytomonitor and recorded every 5 minutes. Analysis of the experiments showed a reduction in transpiration at higher CO2 levels (Fig. 6).

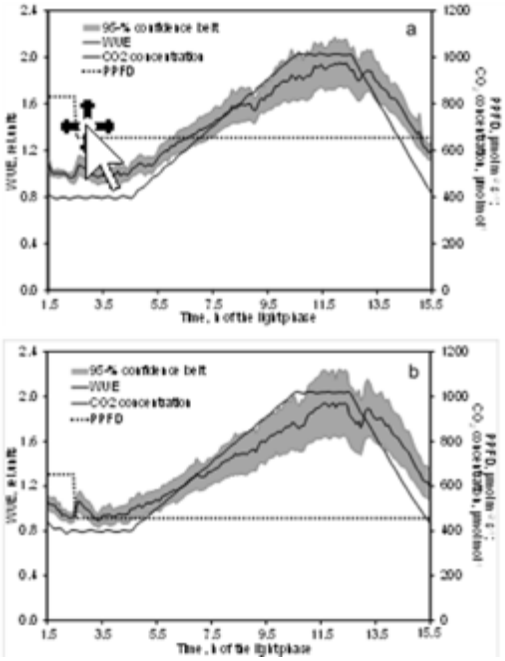

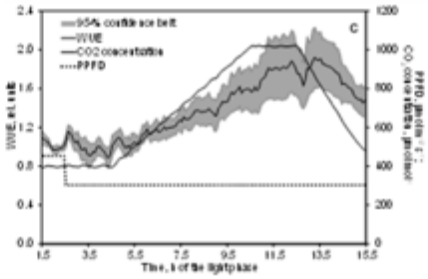

Figure 9. Effect of decreased PPFD followed by first increasing and later decreasing CO_2 concentration on water use efficiency (WUE, mmol CO_2 per mol H_2O) at high (a), moderate (b) and low (c) basic light intensities. Photosynthesis data of each day and chamber are related to the average of the second hour at increased PPFD (time 1.5 to 2.5). WUE data show the mean and 95-% confidence belt of 10 (a and b) and 9 (c) replications. CO_2 concentration data depict the corresponding mean of these replications.

Fig. 7 Increase of water use efficiency with higher CO2-concentration in the climate chambers at three different light levels

This showed that increased CO2 levels can not only compensate for the reduction in light but can also significantly increase water use efficiency (Fig. 7).[1]

[1] Dannehl, D.; Kläring, H.-P.; Schmidt, U. Light-Mediated Reduction in Photosynthesis in Closed Greenhouses Can Be Compensated for by CO2 Enrichment in Tomato Production. Plants 2021, 10, 2808. https://doi.org/10.3390/plants10122808

This project has received funding from the European Commission's Horizon Europe programme under grant agreement number 101096056.

Task 4.5 Digital Twins

Introduction

This deliverable marks the halfway point of Task 4.5 within Work Package 4, which focuses on the development of Digital Twins for PV greenhouses. Led by Universita Degli Studi di Roma Tor Vergata (UR), Task 4.5 aims to integrate the outputs from the previous tasks into a comprehensive empirical model based on machine learning (ML). This task aims at creating a generalized model that can describe both internal and external processes involved in PV greenhouse systems, from solar radiation input to crop production, including internal environment control.

The processes involved in PV and crop production encompass a multitude of physical and biological interactions, requiring complex models, extensive measurements, and diverse expertise. Task 4.5 leverages the knowledge and experience gained from Tasks 4.1 to 4.4 to build novel ML models that synthesize these outputs into a cohesive framework. This integration is essential for predicting the general behaviour of the PV/greenhouse system with an appropriate level of uncertainty, providing actionable insights for final users and stakeholders.

The work done so far aligns well with the project timeline and includes significant advancements in integrating different model outputs. The task employs advanced deep learning methods, particularly focusing on Recurrent Neural Networks (RNNs) and exploring the potential of Graph Neural Networks (GNNs).

Key accomplishments at this stage include:

- Data Collection and Preprocessing: Extensive data was collected from a PV greenhouse in Volos, Greece, spanning from January 9, 2020, to December 21, 2020. The dataset consists of 33,446 data points recorded at 15-minute intervals, capturing both external and internal environmental factors such as temperature, relative humidity, radiation level, and wind speed.
- Exploratory Analysis and Baseline Models: Initial models using Random Forest (RF) provided a baseline for predicting greenhouse temperature and humidity based on external environmental features. This exploratory analysis helped establish benchmark results into the data's behaviour.
- Development of RNN Models: Given the sequential nature of greenhouse microclimate data, RNNs were employed to capture temporal dependencies more effectively. The RNN models demonstrated strong predictive capabilities, particularly for greenhouse temperature.
- Future Exploration with GNNs: Recognizing the complex interactions within the PV greenhouse system, future work will explore the application of GNNs. GNNs offer a generalized approach to modelling energy fluxes and understanding the associated processes, enhancing the model's capabilities.

As we move forward, the focus will be on refining these models, conducting additional validations, and integrating the results into a robust Digital Twin ecosystem. This comprehensive modelling approach aims to support and optimize greenhouse design, crop production

This project has received funding from the European Commission's Horizon Europe programme under grant agreement number 101096056.

management, energy saving, and microclimate control, contributing significantly to the project's overall objectives.

In this deliverable, Recurrent Neural Networks (RNNs) are employed to recognize patterns in time-series data, such as greenhouse microclimate data. RNNs, with their capability to handle sequences, are particularly effective for predicting greenhouse conditions based on historical data.

RNNs have already successfully been applied for predicting microclimate conditions inside greenhouse. The use of RNNs in greenhouses dates back to 2007. In their study, (Fourati & Chtourou, 2007) trained a RNN to simulate the direct dynamics of a greenhouse, discovering that neural networks strategies perform well in controlling complex process like those found in greenhouses. (Dae-Hyun, Hyoung, Changho, Hak-Jin, & Soo, 2020) applied three neural network models to predict greenhouse microclimate. They found that the best results are achieved with RNNs, getting results very similar to ours in predicting temperature and relative humidity. Similar results are got by (Wang, et al., 2018), which employed RNNs to predict the temperature and humidity of a solar greenhouse in the north of China. Even if they used data recorded in only eight days, the achieved similar values of R^2.

Looking ahead, the task will explore the potential of Graph Neural Networks (GNNs) to handle the complex interactions within the PV greenhouse system, offering a more generalized and introspective approach to modelling energy fluxes and understanding the interconnected processes within PV greenhouses.

This report outlines the data collection, preprocessing, and analysis methods used in Task 4.5, as well as the development and performance of machine learning models, including Random Forests (RF) and Recurrent Neural Networks (RNNs), applied to greenhouse microclimate data. It also discusses the results, their implications for greenhouse management, and future directions, including the potential application of Graph Neural Networks (GNNs) to further enhance the model's capabilities.

Data

The data used in this study originates from a PV greenhouse located in Volos, Greece, for the year 2020. The dataset consists of measurements recorded at 15-minute intervals, resulting in 33,446 data points.

Data Description

Timeframe: The dataset spans from January 9, 2020, to December 21, 2020.

Greenhouse Focus: The study specifically focuses on Greenhouse 1 of 6.

Features:

- **External Environmental Factors**:

This project has received funding from the European Commission's Horizon Europe programme under grant agreement number 101096056.

  - **External Temperature (OUT_temp)**: The ambient temperature outside the greenhouse.
  - **External Relative Humidity (OUT_RH)**: The relative humidity of the air outside the greenhouse.
  - **Radiation Level (OUT_rad)**: The amount of solar radiation received.
  - **Wind Speed (OUT_wind_speed)**: The speed of the wind outside the greenhouse.
- **Internal Environmental Factors**:
  - **Greenhouse Temperature (G1_temp)**: The internal temperature within Greenhouse 1.
  - **Greenhouse Relative Humidity (G1_RH)**: The internal relative humidity within Greenhouse 1.

Data Handling and Missing Values

The dataset was divided into three seasons to analyze the seasonal variations in the greenhouse microclimate:

- **Summer**: June 1 to August 30
- **Winter**: January 9 to March 30
- **Autumn**: October 1 to December 12

We used seasonal names for these periods even though the dates don't perfectly correspond to the actual seasons. This discrepancy is due to a significant number of missing values.

Spring data was excluded from the analysis due to many missing values recorded between April 23 and April 27.

Missing Values:

The number of missing values for each variable in each season is as follows:

Season	*G1_temp*	*G1_RH*	*OUT_temp*	*OUT_RH*	*OUT_rad*	*wind_speed*
Summer	73	73	7	7	7	7
Winter	138	138	71	71	71	71
Autumn	153	153	152	152	152	152

To address missing data, we employed a combination of linear interpolation and rolling mean techniques. This approach ensured that the imputed values maintained the integrity of the time series without causing significant flattening of the data trends.

The graphs of the temperature inside and outside the greenhouse, for the three considered periods follow.

This project has received funding from the European Commission's Horizon Europe programme under grant agreement number 101096056.

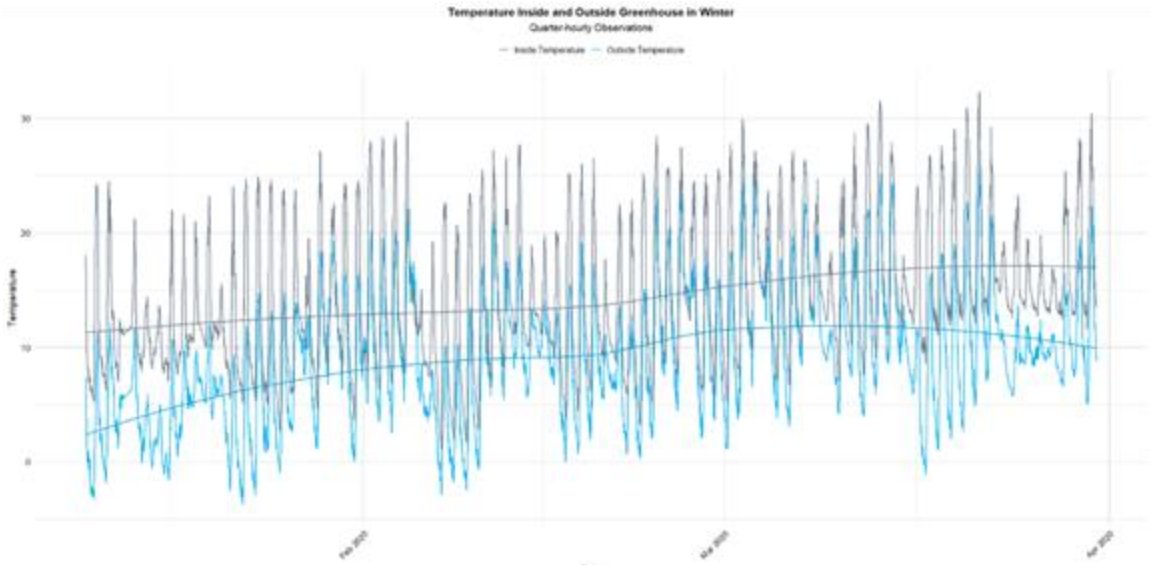

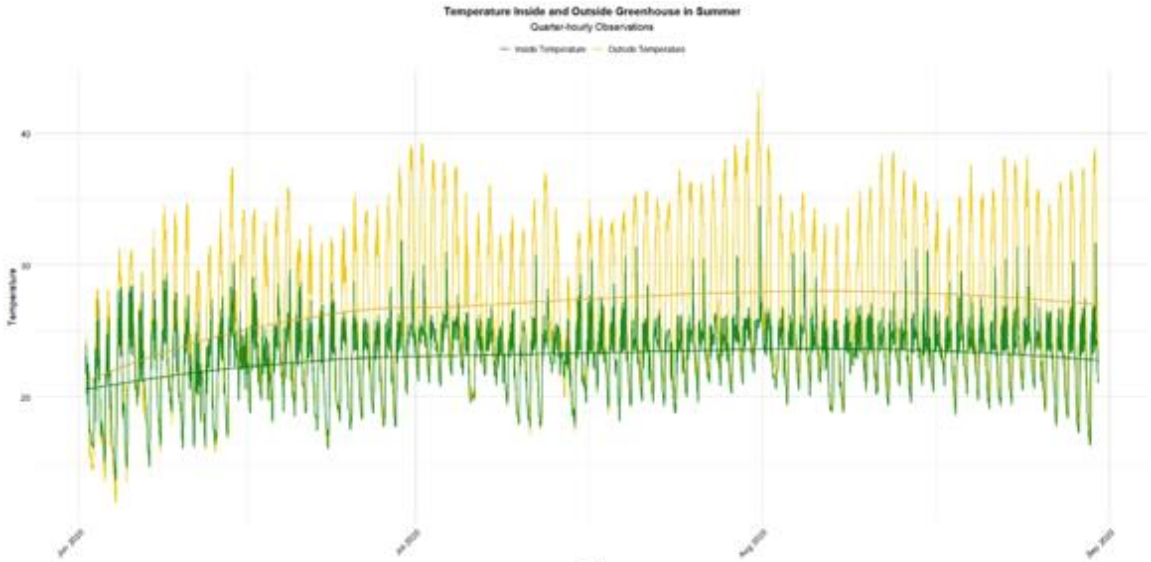

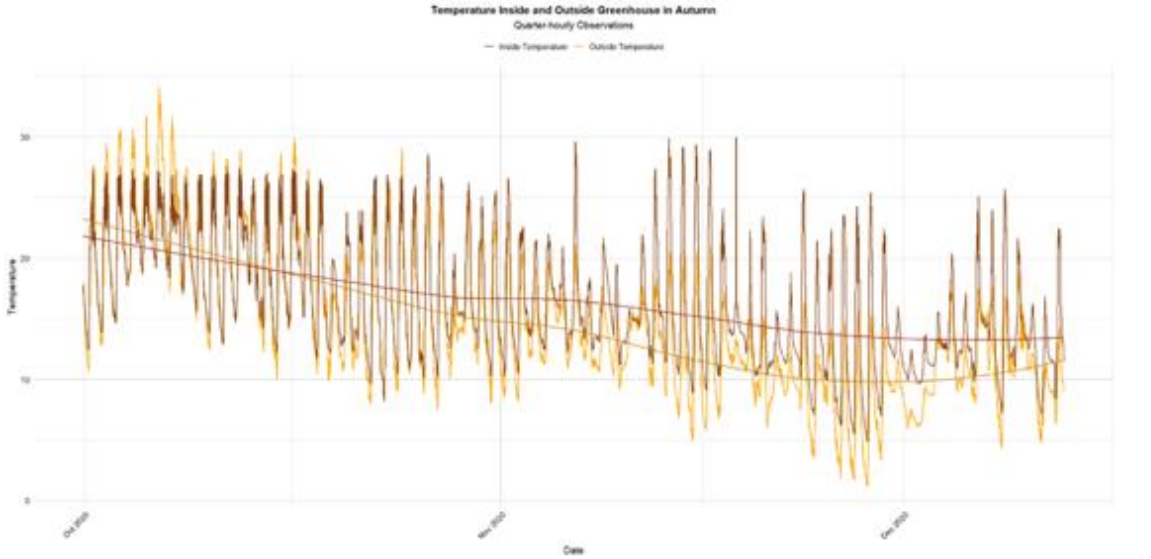

This project has received funding from the European Commission's Horizon Europe programme under grant agreement number 101096056.

Data Pre-processing

Prior to model development, the data underwent several preprocessing steps:

- **Normalization**: All features were normalized using the min-max method to scale the values between 0 and 1, ensuring comparability across different features (Alaimo & Seri, 2021).
- **Train-Test Split**: The dataset was split into training and testing sets. The training set comprised the first 80% of observations for each month, while the testing set included the last 20%. This split preserved the temporal sequence of the data, which is crucial for time-series analysis.

Stationarity

For effective time series analysis, it is essential to ensure that the data is stationary. Stationarity means that the statistical properties of the time series, such as mean and variance, remain consistent over time. This consistency is crucial because it ensures that the patterns observed in the past data are applicable to the future. A time series is stationary if it meets two conditions:

1. The mean (average value) of the series is constant over time.
2. The covariance between two points depends only on the time interval between them, not on their specific positions in time

In practice, stationarity implies that the series fluctuates around a constant level with consistent variation. This property is essential for making reliable inferences and predictions based on the data (Tsay, 2005).

To ensure our data met these criteria, we applied the Augmented Dickey-Fuller (ADF) test (Yin-Wong & Lai, 1995).

Hypotheses:

- **H0**: The series has a unit root (non-stationary).
- **H1**: The series is stationary.

The results for the summer period follow.

Variable	***Dickey-Fuller Statistic***	***p-value***	***Conclusion***
G1_temp	-15.855	< 0.01	Stationary
G1_RH	-11.471	< 0.01	Stationary
OUT_temp	-21.311	< 0.01	Stationary
OUT_RH	-16.621	< 0.01	Stationary
OUT_rad	-21.836	< 0.01	Stationary
OUT_wind_speed	-15.131	< 0.01	Stationary

This project has received funding from the European Commission's Horizon Europe programme under grant agreement number 101096056.

The ADF test results indicate that for all variables, the null hypothesis of non-stationarity is rejected, confirming that the series are stationary. For the winter and autumn period, the results are that all the variables are stationary like for the summer.

Methodology

This section provides a detailed overview of the machine learning techniques used to develop predictive models for the PV greenhouse microclimate, with a focus on Random Forest (RF) and Recurrent Neural Networks (RNN). We will discuss the theoretical foundations of these models, their interpretability, and why RNNs are particularly well-suited for this study.

Random forest

Random Forest is an ensemble learning method that enhances the predictive performance and robustness of decision trees. A decision tree splits the data into subsets based on the value of input features, creating a tree-like model of decisions. Each internal node represents a feature, each branch a decision rule, and each leaf node a predicted outcome. However, individual decision trees often suffer from overfitting, meaning they may perform well on training data but poorly on unseen data. Random Forest addresses this issue by constructing a multitude of decision trees during training and outputting the average prediction (for regression) or majority vote (for classification) of the individual trees (Biau & Erwan, 2016). This technique involves bootstrapping, where each tree is trained on a random subset of the data (with replacement), and random feature selection, where at each split, a random subset of features is considered. The aggregation of predictions from multiple trees reduces the risk of overfitting and improves generalization (Gareth, Witten, Hastie, & Tibshirani, 2013).

In our study, Random Forest was applied as exploratory analysis, to establish a baseline model for predicting greenhouse temperature (G1_temp) and relative humidity (G1_RH) using external environmental features. Random forest has already been applied for the analysis of greenhouse environments, for instance in (Taewon, et al., 2019), (Tsai, et al., 2020) and (Abderrachid, Abdolhamid, & Chandra, 2020). Despite its robustness, the temporal nature of our data necessitates models more suitable to capture sequential dependencies, leading us to explore neural networks, particularly Recurrent Neural Networks (RNNs).

Recurrent neural networks

Neural Networks (NN) are computational models inspired by the neural structure of the human brain. They consist of interconnected neurons (or nodes) organized into layers: an input layer, one or more hidden layers, and an output layer. Each connection between neurons has an associated weight that is adjusted during training to minimize the prediction error. Deep Neural Networks (DNN) are an extension of NNs with multiple hidden layers, allowing them to model complex, non-linear relationships in the data. They use activation functions (such as ReLU, sigmoid, tanh) to introduce non-linearity and backpropagation for training, which adjusts weights based on the error rate obtained in the previous epoch (Nielsen, 2015).

This project has received funding from the European Commission's Horizon Europe programme under grant agreement number 101096056.

Figure 8 - NN graphical example

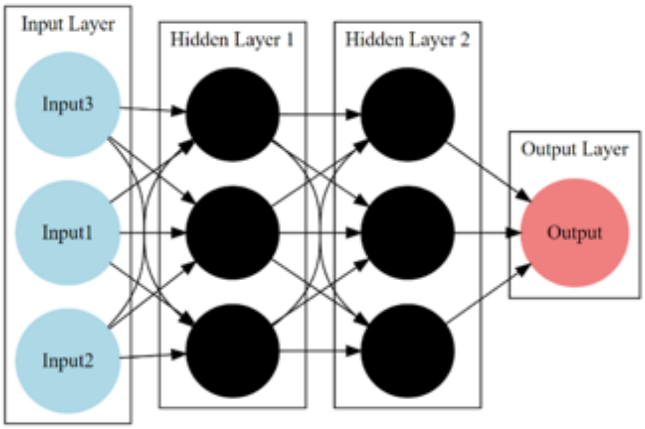

Recurrent Neural Networks (RNNs) are a specialized class of neural networks designed for sequential data, making them highly suitable for time-series analysis like ours (Medsker & Jain, 2001). Unlike traditional neural networks, RNNs have connections that loop back, allowing information to persist. This architecture enables RNNs to maintain context and capture dependencies in sequential data, which is essential for predicting time series. RNNs process sequences of data one element at a time while maintaining a hidden state that captures information about previous elements. This hidden state is updated at each time step based on the current input and the previous hidden state, enabling the network to learn temporal dependencies. The core RNN unit can be described by the following equations: the hidden state update and the output generation, where the hidden state at time step t is updated based on the input at time step t and the previous hidden state. Deep RNNs stack multiple RNN layers on top of each other, where each layer's hidden state serves as the input for the next layer. This deep architecture allows for capturing more complex temporal patterns and dependencies in the data (Nketiah, Chenlong, Yingchuan, & Aram, 2023).

RNNs are particularly well-suited for meteorological data forecasting (Balluff, Bendfeld, & Krauter, 2020) and for predicting features behaviour of complex systems with sequential nature, like greenhouse microclimate data (Rodriguez, Wiles, & Elman, 1999). They can effectively model how current and past environmental conditions influence future states, making them ideal for predicting variables like greenhouse temperature and humidity. In this study, we implemented a Simple RNN model with 48 timesteps (equivalent to 12 hours of data, considering each timestep as a 15-minute interval) and a batch size of 96 samples per batch, balancing computational efficiency and stable convergence. The model consisted of two layers of Simple RNN units, each with 50 units followed by dropout (rate = 0.2) to prevent overfitting, and a dense output layer with one unit for the final prediction. The layer structure and the choices of the number of timesteps and batch size, are coherent with the ones of similar works, such as (Salah & Fourati, 2021) and (Dae-Hyun, Hyoung, Changho, Hak-Jin, & Soo, 2020). However, as future development we aim to perform multiple experiments to verify the optimal choices of values.

This project has received funding from the European Commission's Horizon Europe programme under grant agreement number 101096056.

The RNN model was trained using the Mean Squared Error (MSE) loss function and optimized through backpropagation through time. A 10% subset of the training data was used as a validation set to monitor the model's performance on unseen data and prevent overfitting. By capturing the temporal dependencies in the greenhouse microclimate data, RNNs provide a powerful tool for predictive modeling in this context.

Analysis and results

Exploratory analysis: Random Forest results

The Random Forest model was used as a first exploration for the prediction of G1_temp and G1_RH. We trained the model on the first 80% data of each month and tested it on the remaining 20%.

Model Performance:

- **Temperature Prediction (G1_temp)**. **Formula:**
  G1_temp ~ G1_RH + OUT_temp + OUT_RH + OUT_rad + OUT_wind_speed
  - Percentage of Variance Explained: 91.46%
  - Test Error (MSE): 0.000851
  - R-squared: 0.9475

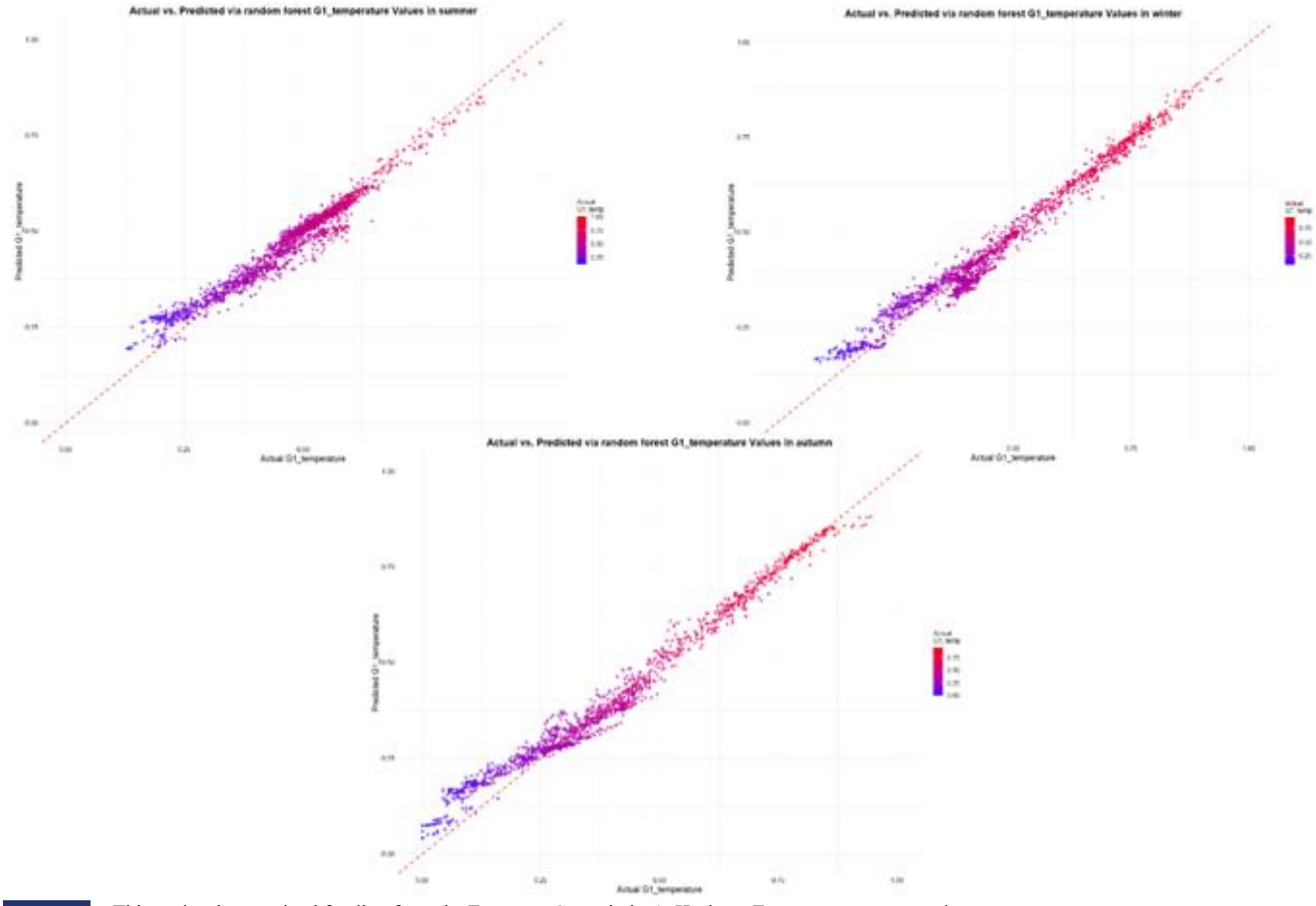

This project has received funding from the European Commission's Horizon Europe programme under grant agreement number 101096056.

- **Humidity Prediction (G1_RH)**. **Formula:**
  G1_RH ~ G1_temp + OUT_temp + OUT_RH + OUT_rad + OUT_wind_speed
  - Percentage of Variance Explained: 83.41%
  - Test Error (MSE): 0.00183
  - R-squared: 0.9005

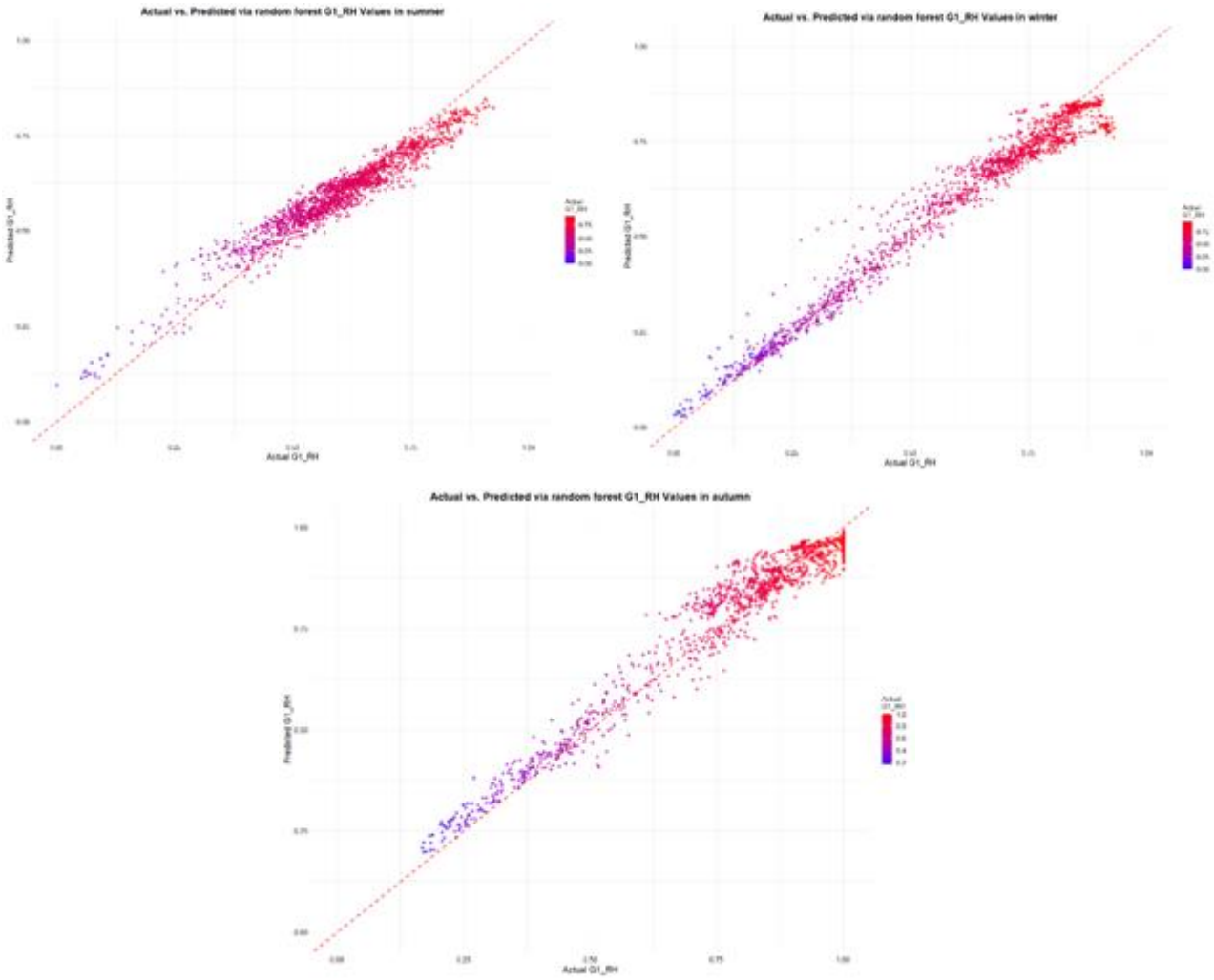

These results indicate that the Random Forest model performs well in predicting both temperature and humidity, explaining a significant portion of the variance in the data and achieving high R^2 values.

RNN results

Given the sequential nature of the data, the RNN model was expected to capture temporal dependencies more effectively than Random Forest. The RNN model was trained using 48 timesteps (equivalent to 12 hours of data) and a batch size of 96.

Model Performance:

This project has received funding from the European Commission's Horizon Europe programme under grant agreement number 101096056.

- **Temperature Prediction (G1_temp)**:
  - Training Loss: 0.002101
  - Validation Loss: 0.001048
  - R-squared: 0.9151

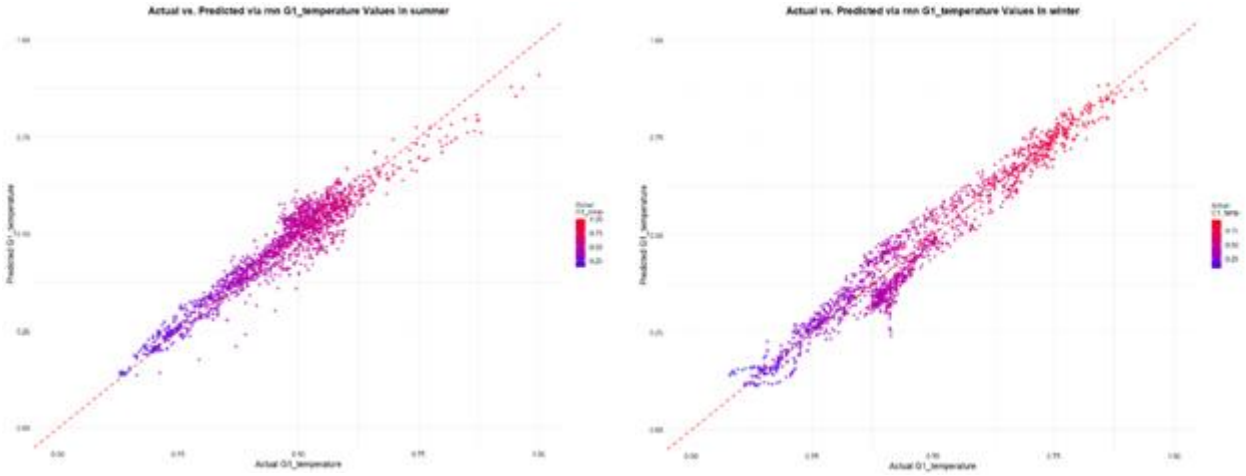

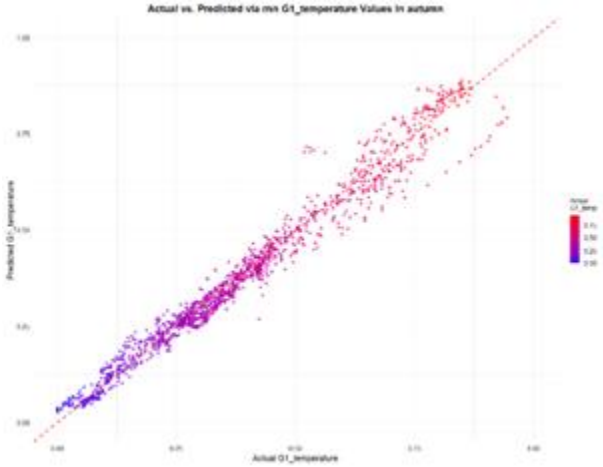

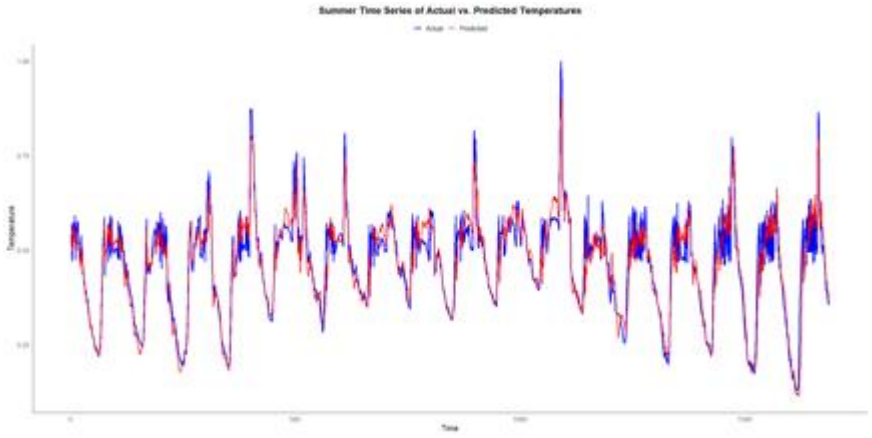

This project has received funding from the European Commission's Horizon Europe programme under grant agreement number 101096056.

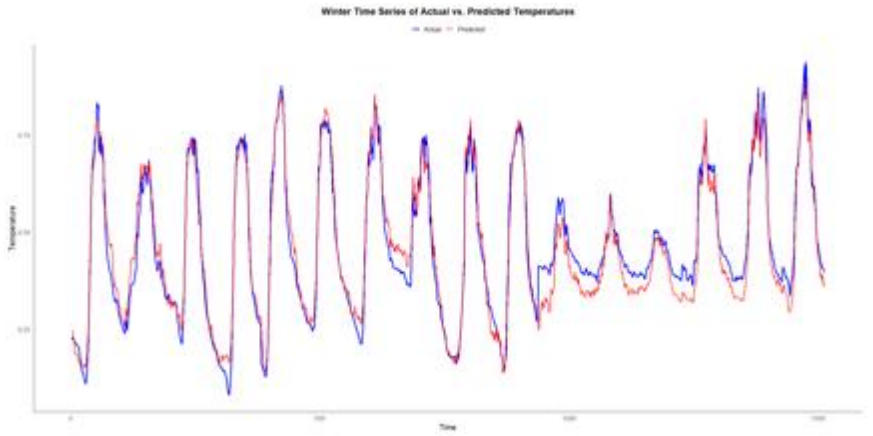

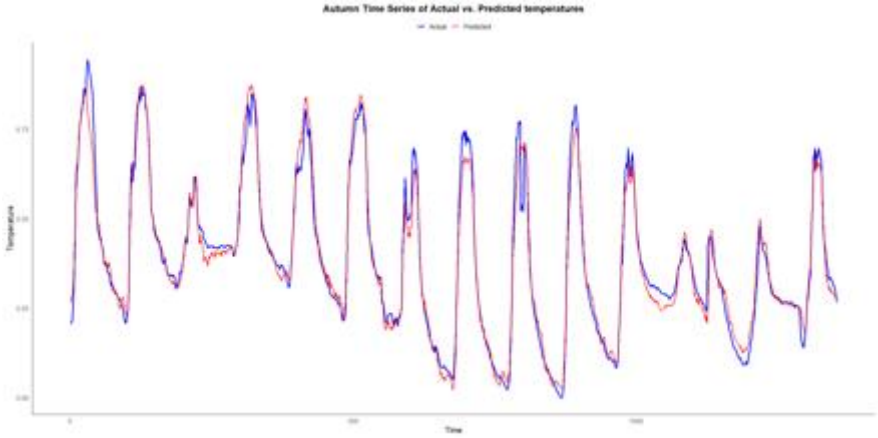

- **Humidity Prediction (G1_RH)**:
  - Training Loss: 0.004887
  - Validation Loss: 0.002688
  - R-squared: 0.7982

This project has received funding from the European Commission's Horizon Europe programme under grant agreement number 101096056.

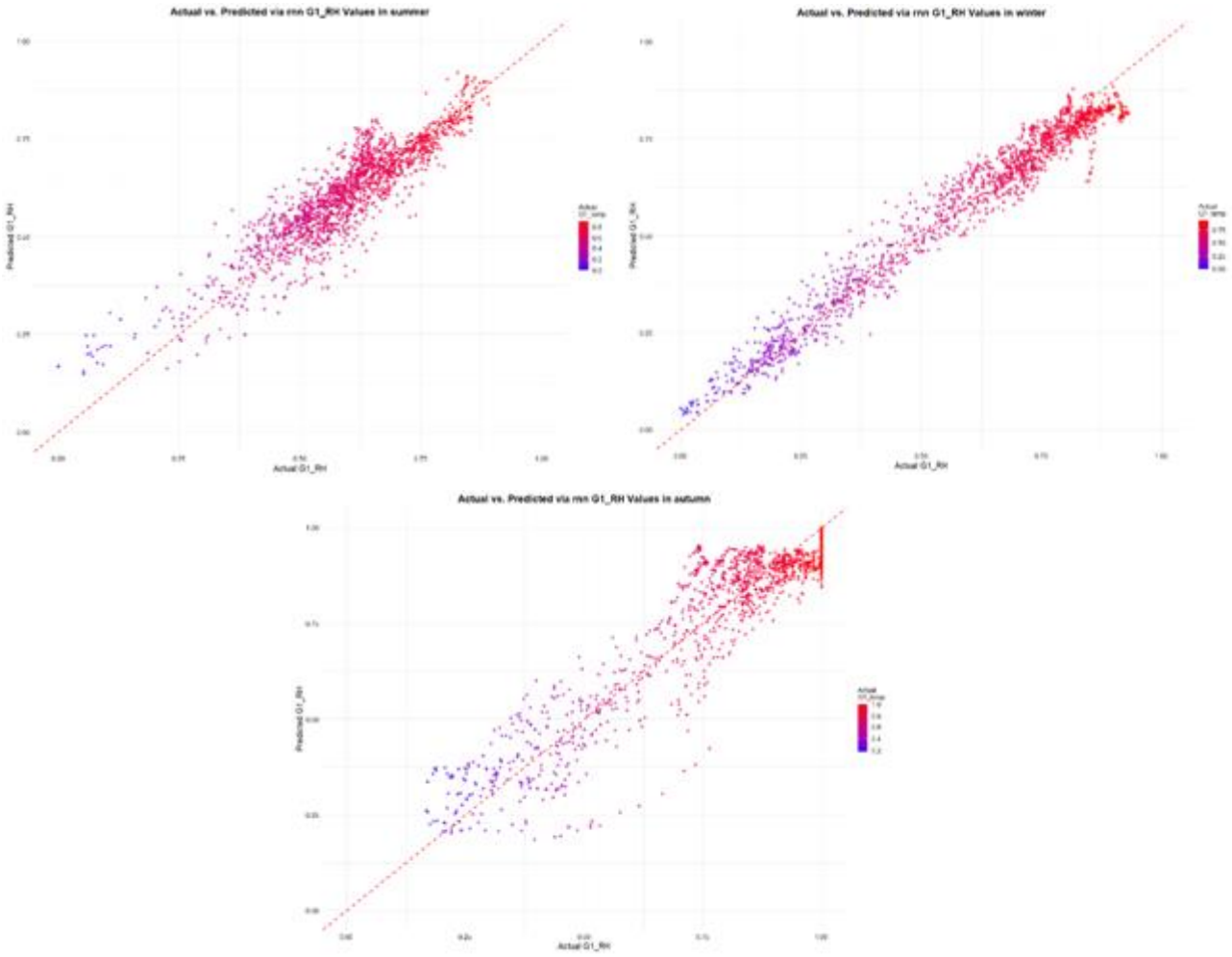

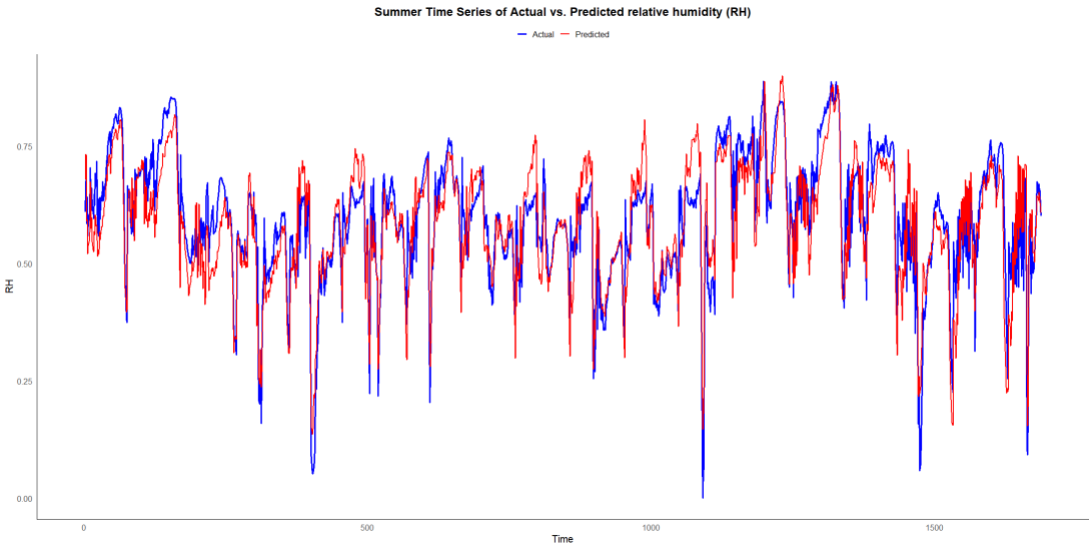

This project has received funding from the European Commission's Horizon Europe programme under grant agreement number 101096056.

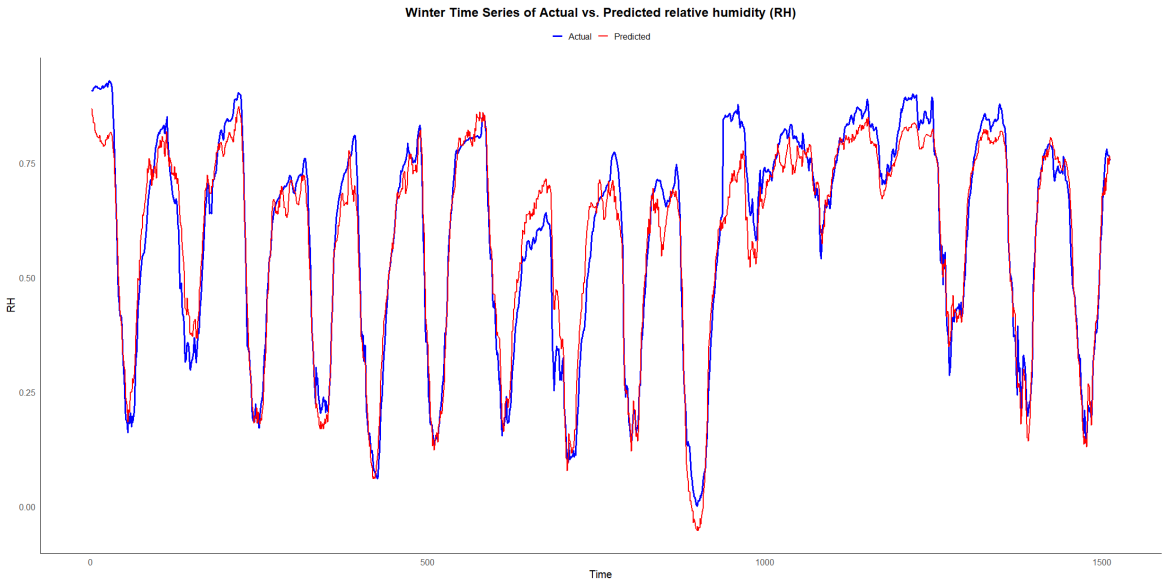

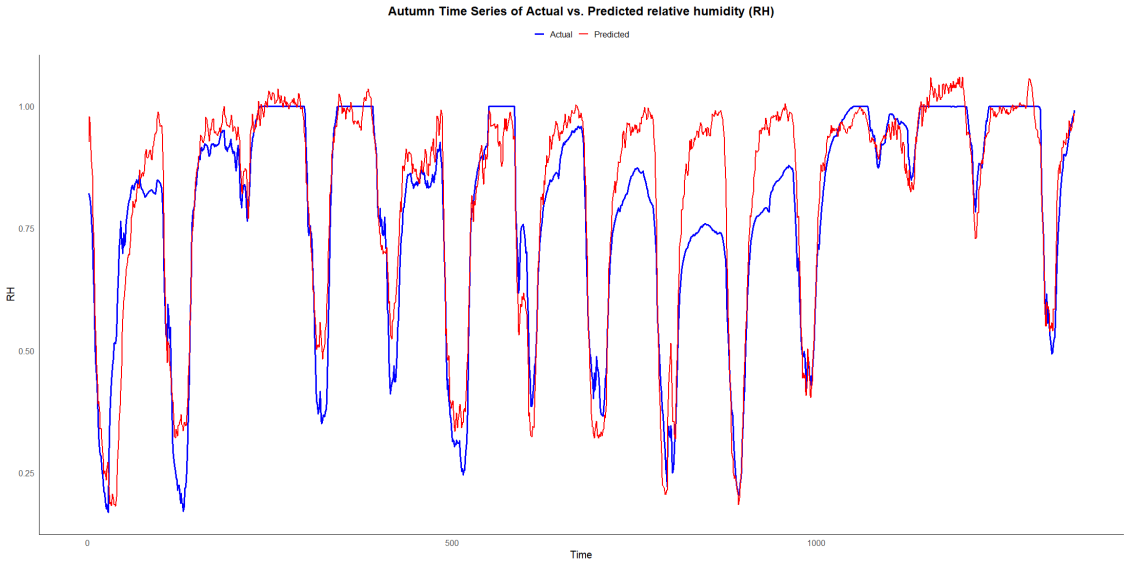

The RNN model demonstrated a strong ability to predict greenhouse temperature, with a high R^2 value indicating that it effectively captures the temporal patterns in the data. The performance in predicting relative humidity was slightly lower but still respectable, suggesting that the model could be further refined to improve accuracy.

Discussion

The analysis of model performance reveals several key insights. The Random Forest model serves as a robust baseline, providing strong predictive performance for both temperature and humidity. However, the sequential nature of greenhouse microclimate data makes RNNs a more suitable choice for capturing temporal dependencies. The RNN model achieved higher accuracy in predicting temperature, reflecting its ability to leverage past observations to inform future predictions. For humidity, while the RNN model's performance was good, it was not as strong as

This project has received funding from the European Commission's Horizon Europe programme under grant agreement number 101096056.

for temperature. This discrepancy may be due to the more complex nature of humidity dynamics, which could benefit from additional features or more sophisticated neural network architectures.

The results indicate that incorporating temporal dependencies through RNNs provides a significant advantage over traditional ensemble methods like Random Forest.

Conclusions

This study aimed to develop predictive models for the microclimate within a PV greenhouse system using advanced machine and deep learning techniques. The primary goal was to accurately predict key environmental variables such as greenhouse temperature (G1_temp) and relative humidity (G1_RH) based on external environmental factors. To do so, we employed Random Forest (RF) as exploratory analysis and Recurrent Neural Networks (RNN). The Random Forest model served as a robust baseline, demonstrating strong predictive capabilities for both temperature and humidity. The model achieved high R-squared values, explaining a significant portion of the variance in the data and handling the complexities of greenhouse environmental factors effectively. Given the sequential nature of the microclimate data, Recurrent Neural Networks were particularly well-suited for this study. The RNN model showed a notable ability to capture temporal dependencies, leading to accurate predictions of greenhouse temperature and relative.

Future work will deeply dig into RNNs, exploring its prediction performance in the different periods, by considering different numbers of time steps. Also, we aim to explore Graph Neural Networks (GNNs) to model the interactions between internal and external factors, considering PV production and plant growth data as it becomes available. Additionally, generalizing the models to various greenhouse designs and geographic locations would increase their applicability and robustness.

Outlook and future developments

Building on the promising results of this study, several future developments can enhance the modeling and optimization of PV greenhouse systems. These advancements will further leverage deep learning and advanced computational techniques to improve predictive accuracy and operational efficiency. One significant area for future work involves incorporating additional features into the models. By integrating PV production and plant growth data we can provide a more comprehensive understanding of the greenhouse.

Exploring advanced neural network architectures is another crucial direction. Recurrent Neural Networks (RNNs) have already shown their effectiveness; however, we aim to enhance its predictive performance at its best by performing it for a range of time steps.

Moreover, employing Graph Neural Networks (GNNs) present an exciting frontier for future research. GNNs graph structure fits particularly well the intricate relationships between various components of the PV greenhouse system, including internal and external environmental factors, PV production, and plant growth. By capturing these interactions more precisely, GNNs can provide deeper insights into the system's behaviour and enhance predictive capabilities.

This project has received funding from the European Commission's Horizon Europe programme under grant agreement number 101096056.

Expanding the scope of our models to include various greenhouse typologies and geographic locations is another important step. By generalizing the models to different designs and environmental conditions, we can increase their robustness and applicability. This expansion will involve collecting and integrating data from diverse greenhouse setups and regions, which will contribute to a more versatile and comprehensive predictive tool.

References

Nketiah, A. E., Chenlong, L., Yingchuan, J., & Aram, S. A. (2023). *Recurrent neural network modeling of multivariate time series and its application in temperature forecasting.* San Francisco: Plos one.

Abderrachid, H., Abdolhamid, A., & Chandra, A. (2020). Machine learning for predicting greenhouse gas emissions from agricultural soils. *Science of The Total Environment, 741*, 140338.

Alaimo, L. S., & Seri, E. (2021). Monitoring the main aspects of social and economic life using composite indicators. a literature review. *Research Group Economics, Policy Analysis and Language (REAL) series*.

Balluff, S., Bendfeld, J., & Krauter, S. (2020). Meteorological data forecast using RNN. In *Deep Learning and Neural Networks: Concepts, Methodologies, Tools, and Applications* (pp. 905--920). IGI global.

Biau, G., & Erwan, S. (2016). A random forest guided tour. *Test, 25*, 197-227.

Dae-Hyun, J., Hyoung, S., Changho, J., Hak-Jin, K., & Soo, H. (2020). Time-serial analysis of deep neural network models for prediction of climatic conditions inside a greenhouse. *Computers and Electronics in Agriculture, 173*.

Fourati, F., & Chtourou, M. (2007). A greenhouse control with feed-forward and recurrent neural networks. *Simulation Modelling Practice and Theory, 15*(8), 1016-1028.

Gareth, J., Witten, D., Hastie, T., & Tibshirani, R. (2013). *An introduction to statistical learning .* New York: Springer.

Medsker, L., & Jain, L. (2001). Recurrent neural networks. *Design and Applications, 5*(2), 64-67.

Nielsen, M. (2015). *Neural networks and deep learning* (Vol. 25). USA: Determination press San Francisco.

Rizwan, M. (2011). Augmented dickey fuller test. *SSRN*.

Rodriguez, P., Wiles, J., & Elman, J. (1999). A recurrent neural network that learns to count. *Connection Science, 11*(1), 5-40.

Salah, L. B., & Fourati, F. (2021). A greenhouse modeling and control using deep neural networks. *Applied Artificial Intelligence, 35*(15), 1905--1929.

This project has received funding from the European Commission's Horizon Europe programme under grant agreement number 101096056.

Taewon, M., Seojung, H., Ha, Y. C., Dae, H. J., Se, H. C., & Jung, E. S. (2019). Interpolation of greenhouse environment data using multilayer perceptron. *Computers and Electronics in Agriculture, 166*.

Tsai, Y.-Z., Hsu, K.-S., Wu, H.-Y., Lin, S.-I., Yu, H.-L., Huang, K.-T., . . . Hsu, S.-Y. (2020). Application of random forest and ICON models combined with weather forecasts to predict soil temperature and water content in a greenhouse. *Water, 12*(4), 1176.

Tsay, R. S. (2005). *Analysis of financial time series.* Wiley.

Wang, H., Li, L., Wu, Y., Meng, F., Wang, H., & N.A., S. (2018). Recurrent Neural Network Model for Prediction of Microclimate in Solar Greenhouse. *FAC-PapersOnLine*, 790-795.

Yin-Wong, C., & Lai, K. (1995). Lag Order and Critical Values of the Augmented Dickey–Fuller Test. *Journal of Business & Economic Statistics, 13*(3), 277--280.

This project has received funding from the European Commission's Horizon Europe programme under grant agreement number 101096056.

Overall Conclusion

The activities carried out in Work Package 4 (WP4) have demonstrated substantial progress toward the development of advanced modeling techniques for photovoltaic (PV) greenhouse systems. This deliverable, representing the midpoint of the project, showcases the integration of various modeling efforts that collectively enhance our understanding and optimization of PV greenhouse operations. The work completed to date lays a solid foundation for the continued advancement and eventual deployment of these innovative systems.

Dynamic Modelling of the Greenhouse Microclimate and Energy Demand (Task 4.1)

Task 4.1 has successfully developed a dynamic model that accurately simulates the microclimate and energy demand within PV greenhouses. The use of advanced Dynamic Building Simulation (DBS) software has allowed for detailed modeling that includes crucial physical processes such as plant growth and water use. The calibration and validation of the model using real-world data from WP3 have provided critical insights into the thermo-hygrometric behavior of the greenhouse system. These insights are invaluable for optimizing microclimate control and energy management, ensuring that the greenhouse operates efficiently and sustainably.

CFD Modelling of the Greenhouse Microclimate (Task 4.2)

Task 4.2 has defined the role of in Computational Fluid Dynamics (CFD) modeling within the project's activities, which is essential for understanding and optimizing the internal environment of PV greenhouses. The two-level approach, which includes radiation transport and internal microclimate modeling, has yielded comprehensive 2D and 3D models. These models have been validated and enhanced through extensive parametric studies, providing detailed simulations of heat exchange processes. This task's accomplishments contribute significantly to the overall Digital Twin model, ensuring that all aspects of the greenhouse microclimate are accurately represented and optimized.

Modelling of the PV Modules Performance (Task 4.3)

In Task 4.3, the development of a semi-empirical performance model for bifacial PV modules has been a critical achievement. This model takes into account various environmental factors that influence the performance of bifacial PV modules, such as temperature, irradiance, spectral effects, and reflection. Owing to lack of data from the pilot greenhouses and from the performance monitoring at ESTER lab (WP3, Task 3.1) due to delay in delivery of PV panels we could test and validate the model using other dataset coming from other test sites……. This task's outputs are crucial for predicting and optimizing the energy production of PV greenhouses, thereby enhancing their overall efficiency and sustainability.

Digital Twins (Task 4.5)

Task 4.5 has focused on the integration of outputs from previous tasks into a cohesive empirical model using advanced machine learning (ML) techniques. The development of Digital Twins has

This project has received funding from the European Commission's Horizon Europe programme under grant agreement number 101096056.

provided a generalized model that comprehensively describes the PV greenhouse system, from solar radiation input to crop production. By leveraging Recurrent Neural Networks (RNNs) for time-series data and exploring the potential of Graph Neural Networks (GNNs) for modeling complex interactions, Task 4.5 has made significant advancements in predictive modeling and system optimization. These models offer a powerful tool for stakeholders, providing actionable insights that support decision-making and enhance operational efficiency.

The progress made in WP4 highlights the importance of interdisciplinary collaboration and the application of advanced computational techniques in modern agricultural practices. Moving forward, the focus will be on refining these models, conducting further validations, and expanding their applicability to different greenhouse designs and geographic locations. The continued development and enhancement of these models will ensure their robustness and versatility, providing a reliable tool for optimizing PV greenhouse operations.

The work carried out in WP4 has profound implications for sustainable agriculture. By integrating PV technology with greenhouse operations, we can achieve a dual benefit of renewable energy production and optimized agricultural practices. The models developed in this work package provide a detailed understanding of the interactions between various environmental factors and their impact on crop yield and energy efficiency. This knowledge is crucial for designing and operating PV greenhouses that are both environmentally sustainable and economically viable.

Concluding Remarks

The successful integration of dynamic modeling, CFD simulations, performance modeling of bifacial PV modules, and the creation of Digital Twins has provided a comprehensive framework for optimizing PV greenhouse operations. These efforts align with the project's overarching goals of promoting sustainability, enhancing resource efficiency, and supporting innovative agricultural practices. As we move into the next phases of the project, the continued refinement and validation of these models will ensure their successful implementation and contribute to the broader adoption of PV greenhouse systems in sustainable agriculture.

This project has received funding from the European Commission's Horizon Europe programme under grant agreement number 101096056.